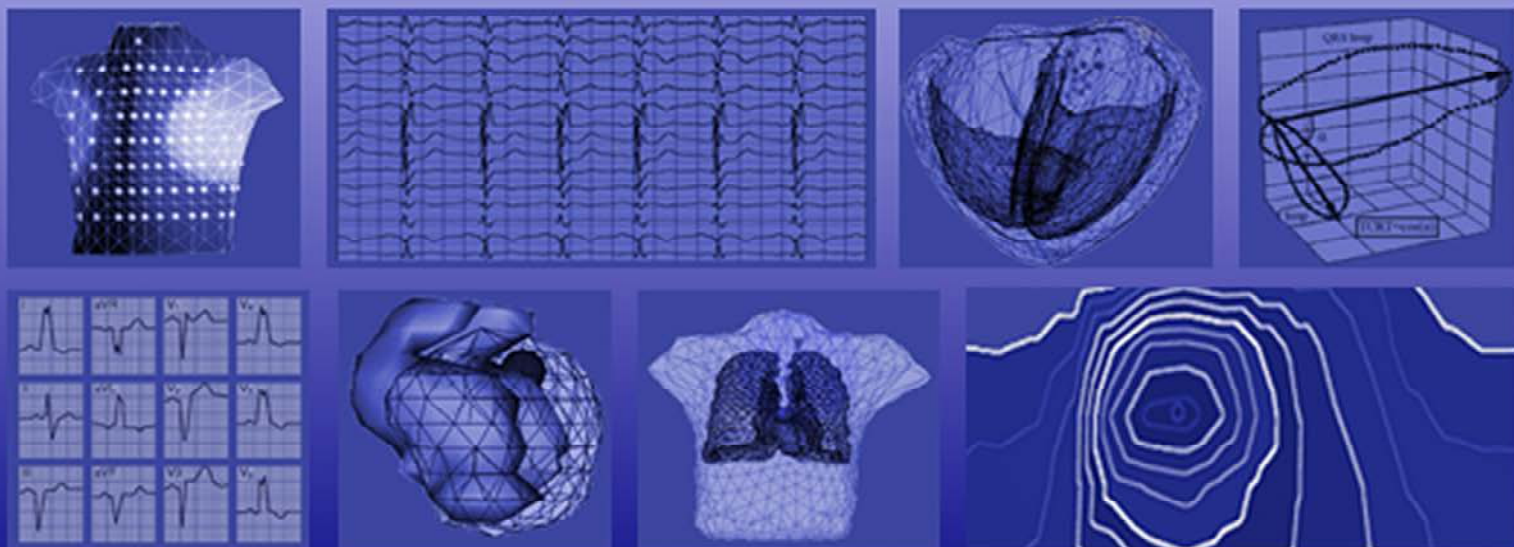


41st International Congress on Electrocardiology
June 4 -7, 2014, Bratislava, Slovakia

ELECTROCARDIOLOGY

2014

Abstracts





ELECTROCARDIOLOGY

2014

ABSTRACTS

of the 41st International Congress on Electrocardiology

June 4 - 7, 2014, Bratislava, Slovakia

ELECTROCARDIOLOGY 2014
Abstracts of the 41st International Congress on Electrocardiology

Copyright © 2014 by International Society of Electrocardiology

Publisher: Institute of Measurement Science
Slovak Academy of Sciences
Dúbravská cesta 9, 841 04 Bratislava
Slovakia

ISBN 978-80-969672-6-1

Printed in Slovakia
by VEDA, Publishing House of the Slovak Academy of Sciences



Congress organisers:

International Society of Electrocardiology

Slovak Heart Rhythm Association

Slovak Society of Cardiology

Institute of Measurement Science, Slovak Academy of Sciences

International Society of Electrophysiology

President:	C. Pastore (Brazil)
Past President:	M. Hiraoka (Japan)
President-Elect:	W. Zareba (USA)
Secretary:	L. Bacharova (Slovakia)
Treasurer:	P. W. Macfarlane (UK)
Council members:	A. Baranchuk (Canada) L. De Ambroggi (Italy) P. Dorostkar (USA) B. Gorenek (Turkey) T. Ikeda (Japan) G. Kozmann (Hungary) J. Liebman (USA) R. MacLeod (USA) P. Platonov (Sweden) M. Potse (The Netherlands) A. Ribeiro (Brazil) M. Roshchevsky (Russia) M. Sobieszczanska (Poland) M. Tysler (Slovakia) A. van Oosterom (The Netherlands) G. S. Wagner, ex officio (USA)
Founding Members:	I. Ruttkay-Nedecky (Slovakia) E. Schubert (Germany)
Honorary Members:	H. Abel (Germany) R. Selvester (USA)
Executive Committee:	C. Pastore, M. Hiraoka, W. Zareba, P.W. Macfarlane, L. De Ambroggi, J. Liebman
Membership Board:	M. Hiraoka, R. MacLeod, M. Sobieszczanska

Congress President: M. Tysler

Scientific Secretary: L. Bacharova

Program Committee: K. Kozlikova
V. Szathmary
R. Hatala
S. Filipova
I. Simkova
N. Tribulova
T. Ravingerova
L. Gaspar

Local Organising Committee: J. Svehlikova
E. Bukovenova
P. Kalavsky

CONTENTS

PRE-CONGRESS WORKSHOP ON QRST MORPHOLOGY	9
Classical Concepts of Electrocardiographic Diagnoses Extended.....	10
<i>L. Bacharova</i>	
QRS Morphology and Optimal CRT Response: QRS Pattern and Arrhythmias.....	11
<i>W. Zareba</i>	
Lessons Learned from Computer Modeling.....	12
<i>M. Potse</i>	
THE RIJLANT PAPER.....	13
The Role of Electrocardiography Today.....	14
<i>L. De Ambroggi</i>	
ECG IN HYPERTENSION, ISCHEMIA AND MI	15
Global Ischemia ECG Pattern for Diagnosis of Left Main Occlusion: Diagnostic Properties and Associated Mortality in Patients with Suspected Acute Myocardial Infarction.....	16
<i>C. Stengaard, Ch.J. Terkelsen</i>	
Suboptimal Diagnosis and Interventional Treatment of Patients with Bundle Branch Block and Acute Myocardial Infarction.....	17
<i>J.T. Sørensen, C. Stengaard, Ch.A. Sorensen, K. Thygesen, H.E. Botker, L. Thuesen, Ch.J. Terkelsen</i>	
Electrocardiographic Abnormalities in Patients with Hypertension: Study in a Large Primary Care Database.....	18
<i>M.S. Marcolino, B.C.A. Marino, M.B.M. Alkmim, A.L. Ribeiro</i>	
Defining QT/QTc Prolongation during ST-Elevation Myocardial Infarction and Reperfusion.....	19
<i>C. Green, W. Kuijt, D. Hegland, B. Atwater, M. Krucoff</i>	
ADVANCED METHODS FOR ECG EVALUATION	21
Discordant and Concordant Decomposition Model for Repolarisation Alternans in the ECG.....	22
<i>J. Coll-Font, B. Erem, C. Rees, A. Karma, R.S. MacLeod, D.H. Brooks</i>	
Excitation Specificity of Repolarization Parameters.....	23
<i>J. Halamek, P. Jurak, P. Leinveber, P. Vesely</i>	
Chaos Theory and Non-Linear Dynamics in Hypertensive Cardiopathy and Heart Failure.....	24
<i>V.D. Moga, I. Kurcalte, M. Moga, F. Vidu, C. Rezus, I. Cotet, R. Avram</i>	
Fractal Dimension of In-Vivo and Ex-Vivo Rabbit HRV Series.....	25
<i>O. Janoušek, M. Ronzhina, J. Kolářová, I. Provazník, M. Nováková, T. Stračina, V. Olejníčková</i>	

ARRHYTHMIAS AND CARDIAC RESYNCHRONIZATION

THERAPY..... 27

Significance of Ventricular Arrhythmia and Heart Rate Variability in Patients with CRT 28

W. Zareba - INVITED PAPER

Electrocardiographic Risk Factors for Sudden Cardiac Death. Usefulness and Limitations of ECG Screening 29

B. Gorenek

Postoperative Arrhythmias and Conduction Abnormalities in Patients with Heterotaxy 30

P. Dorostkar, S. Sivanandam, L. Kochilas

Left bundle branch block – renaissance of an old biomarker 31

R. Hatala

T-wave Area as an Additional Predictor of Response to Cardiac Resynchronization Therapy 32

E.B. Engels, E.M. Vegh, C.J.M. van Deursen, J.P. Singh, F.W. Prinzen

Difference Between Native and Right-Ventricular-Paced QRS Duration Predicts QRS Shortening by Cardiac Resynchronization Therapy: A Novel Marker of True Complete Left Bundle Branch Block..... 33

D. Wichterle, K. Sedláček, V. Vančura, H. Jansová, J. Kautzner

ECG METHODS AND TECHNOLOGIES 35

Selected Aspects of Racial Differences in the ECG 36

P.W. Macfarlane, E. Clark, B.G. Francq, S. Lloyd

Gender Differences in Novel Repolarization Parameters 37

K. Piotrowicz, M. Vaglio, J.P. Couderc, J. Xio, W. Zareba

Lead Selection for Maximal QT Interval Duration Measurement in Patients With Heart Failure And Stroke 38

I. Mozos

Body Surface T-wave Amplitude Dispersion in Diabetic Rabbits and Epicardial Repolarization Pattern 39

M.A. Vaykshnorayte, K.A. Sedova, O.G. Bernikova, A.O. Ovechkin, J.E. Azarov

Diagnostic Performance and System Delay Using Telemedicine for PreHospital Diagnosis in Triaging and Treatment of STEMI 40

A.M.B. Rasmussen, B.Ch.J. Terkelsen

YIA SESSION I:

NEW ECG METHODS AND ANIMAL EXPERIMENTS 41

Removing Ventricular Far Field Artifacts in Intracardiac Electrograms During Stable Atrial Flutter Using the Periodic Component Analysis – Proof of Concept Study 42

T.G. Oesterlein, G. Lenis, A. Luik, B. Verma, C. Schmitt, O. Dössel

An Iterative Method for Solving the Inverse Problem in Electrocardiography in Normal and Fibrillation Conditions: A Simulation Study..... 43

N. Zenzemi

Respiratory Rate Simultaneous Estimation from Two ECG-Derived Respiratory Waveforms Using an Adaptive Frequency Tracking Algorithm 44

L. Mirmohamadsadeghi, J.-M. Vesin

Novel Method for Deriving Vectorcardiographic Leads Based on Artificial Neural Network.....	45
<i>M. Vozda, T. Peterek, M. Cerny</i>	
Modified Lewis ECG Lead System for Ambulatory Monitoring of Atrial Arrhythmias	46
<i>A. Petrėnas, V. Marozas, L. Sörnmo, G. Jarušėvičius, D. Gogolinskaitė</i>	
Body Surface Potential Mapping During Heart Hypertrophy Development in Infant Rats.....	47
<i>A. Rasputina, I. Roshchevskaya</i>	
Effect of the Repeated Global Ischemia and Reperfusion on the RR and QT Interval in Isolated Rabbit Heart.....	48
<i>P. Veselý, J. Halánek, M. Ronzhina, O. Janoušek, J. Kolářová, M. Nováková</i>	

YIA SESSION II:

ECG MARKERS FOR CARDIAC DIAGNOSTICS 49

Vectorcardiographic Predictors of Ventricular Arrhythmia Inducibility in Patients with Tetralogy of Fallot.....	50
<i>D. Cortez, E. Ruckdeschel, A.C. McCanta, K. Collins, W. Sauer, J. Kay, D. Nguyen</i>	
Advanced Interatrial Block Predicts Atrial Fibrillation Post Cavotricuspid Isthmus Ablation for Typical Atrial Flutter.....	51
<i>A. Enriquez, J. Caldwell, F. Sadiq Ali, D. Conde, W. Hopman, D.P. Redfearn, K. Michael, H. Abdollah, Ch. Simpson, A. Bayés de Luna, A. Baranchuk</i>	
Interatrial Block is Associated with New-Onset Atrial Fibrillation in Patients with Chagas Cardiomyopathy and Implantable Cardioverter-Defibrillators	52
<i>A. Enriquez, D. Conde, F. Femenia, A. Bayés de Luna, A. Ribeiro, C. Muratore, M. Valentino, E. Retyk, N. Galizio, W.M. Hopman, A. Baranchuk</i>	
Dynamics of Heart Rate and Blood Pressure in Hypertensive Patients.....	53
<i>I. Cotet, I. Kurcalte, C. Rezus, V.D. Moga, R. Avram, A. Szekely, M. Moga, F. Vidu</i>	

ECG DIAGNOSTICS OF CARDIAC DISEASES 55

Computer Simulation of the Electric Activity of the Heart. A Multi-Scale Approach.....	56
<i>J.F. Rodriguez - INVITED PAPER</i>	
Brugada or Early Repolarization in V ₁ V ₂ V ₃ . Can VCG Aspects Differentiate the Localization of ECG Manifestations ?	57
<i>C.A. Pastore, N. Samesima, E. Kaiser, H.G. Pereira Filho</i>	
CT Angiography Ellucidates Venous Anatomy Supporting Electrophysiologic Substrate Ablation in Patients with Congenital Heart Disease.....	58
<i>Ch.W. Shepard, H. Roukoz, P. Dorostkar</i>	
ECG Patterns and Genotypes in Pediatric Patients with Channelopathies. 7-Year Experience in Slovakia.....	59
<i>V. Illikova, P. Hlivak, E. Balazova, R. Hatala</i>	
Brugada Phenocopy: Update 2014.....	60
<i>A. Baranchuk, B. Gottshalk, D. D. Anselm</i>	

CARDIAC ELECTROPHYSIOLOGY 61

Effects of Echinochrome on Ventricular Repolarization in Acute Ischemia.....	62
<i>K. Sedova, O. Bernikova, S. Kharin, D. Shmakov</i>	

Antiarrhythmic Potential of Hypolipidemic Drugs in Acute Ischemia/Reperfusion: Molecular Mechanisms of Pleotropic Lipid-Independent Effects	63
<i>T. Ravingerová, S. Čarnická, V. Ledvényiová, M. Nemčeková, T. Rajtík, E. Barlaka, I. Gablovský, A. Adameová, A. Lazou</i>	
Can We Prevent Malignant Arrhythmias by Targeting of Cardiac Connexin-43 ?	64
<i>N. Tribulova, B. Bacova, T. Benova, C. Viczenczova, J. Radosinska, V. Knezl, J. Slezak</i>	
The Influence of Omega-3 Fatty Acids on Permanent Light-induced Myocardial Alterations and Decrease of Ventricular Fibrillation Threshold in Hypertensive Rats	65
<i>T. Benova, J. Radosinska, C. Viczenczova, B. Bacova, J. Zurmanova, V. Knezl, M. Zeman, B. Obsitnik, N. Tribulova</i>	
MODELING IN ELECTROCARDIOLOGY	67
Computer Modeling to Understand the Failing Heart.....	68
<i>M. Potse - INVITED PAPER</i>	
The Impact of Action Potential and Conduction Velocity Distribution Changes on Markers of Repolarization Dispersion	69
<i>G. Kozmann, G. Tuboly, V. Szathmáry, J. Švehlíková, M. Tyšler</i>	
Constraints in the Inverse Problem of Electrocardiography	70
<i>A. van Oosterom</i>	
Inverse Localization of Pacing Sites on Heart Surface from 12 Lead Measurements and CT Imaging of Partial Torso	71
<i>J. Coll-Font, B. Erem, P. Stovicek, D.H. Brooks</i>	
Noninvasive Localization of Ectopic Activation Using BSPM and CT-Based Torso Model	72
<i>M. Tysler, J. Svehlikova, O. Punshchykova, P. Kneppo, V. Maksymenko</i>	
HEART RATE VARIABILITY.....	73
Circadian Variation of Holter-Based T-wave Alternans and Association with Autonomic Nerve System in Normal Heart Subjects.....	74
<i>K. Hashimoto, Y. Kasamaki, Y. Okumura, T. Nakai, S. Kunimoto, I. Watanabe, A. Hirayama, Y. Ozawa, M. Soma</i>	
Extrapolation of the QT/RR Relation: Individualized vs Universal Formulae.....	75
<i>V. Jacquemet, B. Dubé, A. Vinet, M. Sturmer, G. Becker, T. Kus, R. Nadeau</i>	
Does Vagus Nerve Make Mistake ? Vasovagal Reaction in Young Healthy Persons - Benign or Severe	76
<i>A. Stanczyk</i>	
Dynamic Beat-to-Beat Changes of the Cardiac Electric Field in Response to Situations with Increased Sympathetic Activity	77
<i>E. Kellerová, V. Szathmáry, G. Kozmann</i>	
BODY SURFACE POTENTIAL MAPPING.....	79
Body Surface Potential Mapping in Rats with Experimental Pulmonary Hypertension	80
<i>O. Suslonova, I. Roshchevskaya</i>	
The Extrema of Isopotential P-wave Maps in Young Adult Controls	81
<i>K. Kozlíková, M. Trnka</i>	
Impact of Heart Rate on Normal STT Integral Body Surface Potential Maps	82
<i>J. Svehlikova, M.Kania, R. Maniewski, M. Tysler</i>	

ATRIAL FIBRILLATIONS..... 83

Rate-Control Drugs Affect Variability and Irregularity Measures of RR Intervals in Permanent Atrial Fibrillation 84
V.D.A. Corino, S.R. Ulmoen, S. Enger, A. Tveit, P.G. Platonov

Analysis of Electrocardiographic Predictors of Atrial Fibrillation in Patients with Ischemic Stroke without Known History of Atrial Fibrillation 85
M.A.Baturova, S.H.Sheldon, J.Carlson, P.A.Brady, G.Lin, A.A.Rabinstein, P.A.Friedman, P.G.Platonov

Circadian Heart Rate Variability in Permanent Atrial Fibrillation Patients 86
I. Kurcalte, O. Kalejs, R. Erts, I. Konrade, A. Lejniaks

POSTERS:

EXPERIMENTAL AND CLINICAL ELECTROCARDIOLOGY 87

Alterations in Cardiac Cell-to-Cell Coupling Can Facilitate AF in Old Guinea Pig 88
N. Tribulova, V. Nagibin, T. Benova, C. Viczenczova, J. Radosinska, V. Knezl, I. Dovinova, M. Barancik

Hyper- and Hypothyroidism Affect Myocardial Connexin-43 Expression and Susceptibility of the Rat Heart to Malignant Arrhythmias 89
B. Bacova, C. Viczenczova, T. Benova, J. Radosinska, J. Zurmanova, S. Pavelka, T. Soukup, N. Tribulova

The Effect of Single-Dose Chest Irradiation on the Expression of Connexin-43 and PKC Signaling Pathway in the Heart of Rats 90
C. Viczenczova, B. Bacova, J. Radosinska, T. Benova, C. Yin, R. Kukreja, J. Slezak, N. Tribulova

Borderline and Spontaneously Hypertensive Male and Female Rats Exhibit Different Tolerance to Ischemia/Reperfusion 91
V. Ledvényiová, D. Pancza, S. Čarnická, M. Nemčeková, I. Bernátová, T. Ravingerová

Evaluation of Repeated Global Ischemia in Isolated Rabbit Heart 92
M. Ronzhina, V. Olejníčková, T. Stračina, T. Potočník, O. Janoušek, P. Veselý, J. Kolářová, M. Nováková, I. Provazník

Electrocardiographic Predictors of Response to Vasoreactivity Testing in Patients with Pulmonary Arterial Hypertension 93
E. Blinova, T. Sakhnova, O. Arkhipova, N. Danilov, T. Martynyuk, I. Chazova, V. Trunov, E. Aidu

QRS Complex Changes after Pulmonary Endarterectomy in Patients with Chronic Thromboembolic Pulmonary Hypertension 94
M. Boháčeková, T. Valkovičová, L. Bachárová, M. Kaldarárová, I. Šímková

Application of SFHAM Model for Diagnostics of Ischemic Heart Disease 95
J.S. Janicki, A. Teresińska, W. Leoński, M. Chapiński, M. Sobieszkańska, R. Piotrowicz

Comparative Assessment of ECG Dynamics in Myocardial Infarction According to Reperfusion Therapy (Primary or Facilitated Coronary Angioplasty) and Timing of the Procedure 96
G.V. Ryabykina, A.V. Sozykin, E.N. Dyuzheva

Myocardial Ischemia in Genesis of Microvolt T-wave Alternans 97
E.N. Dyuzheva, G.V. Ryabikina, A.V. Sobolev, A.E. Vlasova

Does Synthesized Lead V9 Reflect Left Atrial Activity During Atrial Fibrillation? 98
X. Zhu, Y. Yoshida, D. Wei, K. Fukuda, H. Shimokawa

Acute Effect of Caffeine on Heart Rate Variability in Young Healthy Subjects 99
T. Princi, K. Cankar, V. Starc, V. Grill

Electrocardiographic Abnormalities in the Elderly: A Study in a Large in Primary Care Database 100
M.S. Marcolino, B.C.A. Marino, A.M. Ribeiro, T.G.P. Assis, M.B.M. Alkmim, A.L. Ribeiro

QRS Complex Patterns in Patients with Obstructive Sleep Apnea.....	101
<i>L. Bacharova, E. Triantafyllou, Ch. Vazaios, R. Tisko, I. Paranicova, R. Tkacova</i>	
QRS Complex Characteristics in Patients with Eisenmenger Syndrome with Pre- and Post-Tricuspid Defects	102
<i>T. Valkovičová, M. Kaldararová, M. Boháčeková, L. Bachárová, I. Šimková</i>	
Holter ECG Findings in Patients with Medial Arterial Calcinosi s	103
<i>L. Gaspar, I. Gasparova, M. Makovnik, P. Gavornik, A. Dukat</i>	
Repolarization in Chronic Kidney Disease: Experimental Study	104
<i>S. Kharin, M. Strelkova, V. Krandycheva, A. Tsvetkova, K. Shumikhin, D. Shmakov</i>	

POSTERS: NEW METHODS AND TECHNOLOGIES IN ELECTROCARDIOLOGY 105

The Lead Fields of the Standard 12-Lead ECG	106
<i>M. Potse</i>	
Assesment of AF Capture during Antitachycardia Pacing by Using Largest Lyapunov Exponent. Insights from a Biophysical Model.....	107
<i>A. Luca, J-M. Vesin, A. Vlad</i>	
Derivation of McFee-Parungao Orthogonal Leads from Standard Electrocardiogram	108
<i>V. Trunov, E. Aidu, V. Fedorova, E. Blinova, T. Sakhnova</i>	
Prognostic Value of the QRS-T Angle Measured during Exercise Test.....	109
<i>M. Kania, R. Zaczek, M. Kobylecka, R. Maniewski</i>	
Comparison of Dubois and Base-Apex Lead Methods to Calculate QRS Angle (Mean Electrical Axis) in Thoroughbreds	110
<i>C. Fré da Costa, N. Samesima, C. A. Pastore</i>	
Heart Rate Variability Expressed by Poincaré Plot in Metabolic Syndrome.....	111
<i>A. Drkošová, J. Kozumplík</i>	
Assessment of the Number of Ischemic Lesions from Body Surface Potential Maps.....	112
<i>M. Teplan, J. Švehlíková, M. Tyšler</i>	
BSPM Band Patterns for Diagnosing Intraventricular Conduction Disturbances in Young Adults with Chronic Kidney Disease Treated with Hemodialysis.....	113
<i>K. Laszki-Szcząchor, M. Sobieszczkańska, D. Zwolińska, H. Filipowski, M. Tabin, D. Polak-Jonkisz</i>	
Analysis of the Ventricular Depolarisation Using Autocorrelation Maps.....	114
<i>M. Trnka, K. Kozlíková</i>	
Quantitative VCG and BSPM Repolarization Parameters Evidence Increased Sympathetic Activation of the Ventricular Myocardium in Different Adrenergic Situations	115
<i>V. Regecová, E. Kellerová</i>	
Comparison of Propagation of Atrial Excitation with the Cardiopotential Distribution on the Body Surface of Fish.....	116
<i>S. Smirnova, I. Roshchevskaya, M. Roshchevsky</i>	
First <i>In Vivo</i> Application of Tungsten Dotted Tubing in Cardiac Cryoablation.....	117
<i>M. Stöger, G. Fischer, C.N. Nowak, F. Hintringer</i>	
Tpeak-Tend Interval and Arteriography Variables	118
<i>I. Mozos, S. Gligor</i>	
Decartographic and Echocardiographic Correlations in Patients with Pulmonary Arterial Hypertension.....	119
<i>T. Sakhnova, E. Blinova, M. Saidova, A. Loskutova, O. Arkhipova, E. Yurasova, T. Martynyuk, I. Chazova</i>	

Synthesized Posterior Right Sided Chest Lead Electrocardiograms Are Useful for Detecting Right Ventricular Myocardial Infarction.....	120
<i>S. Fukunaga, T. Kinoshita, K. Akitsu, H. Koike, A. Abe, H. Yuzawa, T. Suzuki, H. Sato, T. Fujino, K. Kobayashi, Y. Okano, T. Ikeda</i>	
Relation of Sex and ECG Variables on Cardiovascular Mortality Risk in 10 Years Follow-Up	121
<i>G. Muromtseva, A. Deev, S. Shalnova</i>	
Automated ECG Delineation Using Machine Learning Algorithms	122
<i>I. Saini, D. Singh, A. Khosla</i>	
Heart Asynchrony in Time-Frequency Interpretation Up to 1000 Hz	123
<i>P. Jurak, J Halamek, P. Leinveber, T. Reichlova, F. Plesinger, P. Vesely, V. Vondra, P. Klimes, J. Sumbera, K. Zeman, M. Novak</i>	
QRS Power in Frequency Ranges up to 1000 Hz	124
<i>P. Leinveber, P. Jurak, J Halamek, T. Reichlova, F. Plesinger, P. Vesely, V. Vondra, P. Klimes, J. Sumbera, K. Zeman, M. Novak</i>	
Detection of Time Intervals in Biomedical Signals Using Template Matched Filter.....	125
<i>A. Sarwan Kumar, B. Sneh Anand, C. Amit Sengupta</i>	
Electrocardiographic Diagnosis of Emergency Conditions in Rural Areas by the System of Remote ECG Transmission and Analysis.....	126
<i>N.A. Vishnyakova, G.V. Ryabykina, V.E. Volkov, E.N. Dyuzheva, E.V.Blinova</i>	
Design of Very Precise and Miniature Low Power ECG Holter	127
<i>E. Vavrinsky, M. Daricek, M. Donoval, F. Horinek, D. Moskalova</i>	
Mechanical chest compressions and quality of CPR in out-of-hospital cardiac arrest evaluated by trans-thoracic impedance measurements	128
<i>T. Tranberg, CJ. Terkelsen</i>	
AUTHORS INDEX	129

**PRE-CONGRESS WORKSHOP
ON QRST MORPHOLOGY**

Classical Concepts of Electrocardiographic Diagnoses Extended

L. Bacharova

International Laser Center, Bratislava, Slovak Republic

Email: bacharova@ilc.sk

Keywords: slowed conduction velocity; reduced intercellular coupling; QRS pattern in ECG.

The classical concepts of ECG interpretation are based on considerable simplifications, some of them developed about one century ago. However, the current level of knowledge, new diagnostic imaging methods and computer simulations creates a solid basis for their re-evaluation.

The presentation summarizes the results of simulation studies on the effect of slowed conduction velocity and reduced intercellular coupling on the QRS pattern. These results suggest that reduced myocardial conduction velocity, either diffuse or regional, as well as reduced intracellular coupling, account at least in part for the changes in the QRS patterns observed in patients with left ventricular hypertrophy, myocardial ischemia and infarction, and with conduction system blocks. The changes in electrical properties could explain a wide spectrum of QRS changes observed in patients with left ventricular hypertrophy as well as in patients with myocardial ischemia and infarction. The changes observed in LVH patients includes increased QRS complex amplitude in limb and/or chest leads, increased QRS complex duration, deviation of the electrical axis in the frontal plane to the left and increased intrinsinoid deflection. Additionally, LVH is frequently associated with QRS patterns of intraventricular conduction defects: left bundle branch block (LBBB) and left anterior fascicular block (LAFB) and there are also ECG findings that are apparently normal. In myocardial ischemia and infarction, the changes that can be attributed to slowed conduction velocity include pathological Q waves, ST segment deviations, prolonged QRS and QT duration, electrical axis deviation, increased QRS voltage, terminal notching of QRS complex, and patterns of fascicular blocks.

Conclusions. Both conduction velocity and reduced intercellular coupling have been documented in variety of cardiac pathology as a possible arrhythmogenic substrate, however their impact on the QRS pattern is not taken into consideration in the practical ECG diagnosis. Discrepancies between anatomical LVH and ECG findings represent the added information value.

QRS Morphology and Optimal CRT Response: QRS Pattern and Arrhythmias

W. Zareba

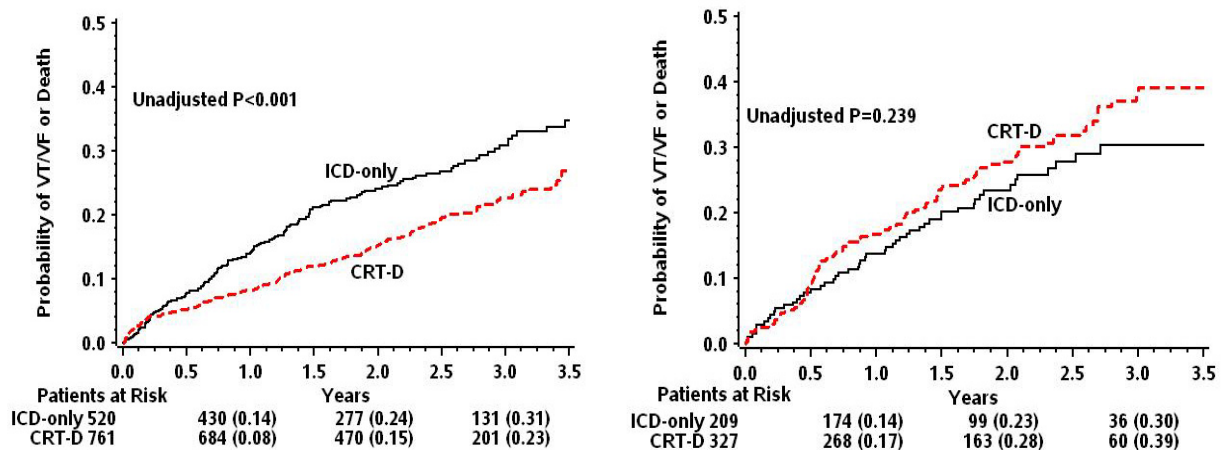
University of Rochester, Rochester, USA
Email: wojciech_zareba@urmc.rochester.edu

Keywords: QRS morphology, cardiac resynchronization therapy, heart failure

Introduction. Cardiac resynchronization therapy (CRT) is the most effective treatment reducing risk of heart failure progression and death. MADIT-CRT trial demonstrated a 30% reduction in the risk of heart failure hospitalization or death in overall patient population but a 50% reduction in patients with QRS of LBBB morphology whereas Non-LBBB patients did not derive benefit.

Methods and Materials. We analysed the association between risk of ventricular tachycardia (VT) or ventricular fibrillation (VF) requiring ICD therapy in relationship to QRS morphology in 1,817 patients enrolled in MADIT-CRT.

Results. Similarly to findings for the primary endpoint, there was a significant reduction in the risk of VT/VF/Death (Figure) in LBBB patients: HR=0.69 (p=0.002) but not in Non-LBBB patients (HR=1.21 (p=0.254); p for interaction = 0.006. When analysing VT/VF alone< LBBB patients showed HR=0.67 (p=0.002) whereas Non-LBBB patients showed HR=1.11 (p=0.574); p for interaction = 0.028. Reduction in VF was even more pronounced in LBBB patients: HR= 0.54 (p=0.011) but not in Non-LBBB patients HR= 1.24 (p=0.585); p for interaction = 0.070. Patients who at 12-month follow-up ECHO showed EF increased >35% demonstrated very significant reduction in VT/VF.



Conclusions. QRS morphology identifies patients who benefit from CRT by reducing not only the risk of HF/death but also by reducing arrhythmic events. LBBB patients treated with CRT show 33-46% reduction in VT/VF or VF alone. CRT in LBBB patients could be considered as the most effective antiarrhythmic therapy in heart failure patients.

Lessons Learned from Computer Modeling

^{1,2,3}M. Potse

¹Center for Computational Medicine in Cardiology, Università della Svizzera italiana,
Lugano, Switzerland

²Carmen Team, Inria Bordeaux Sud-Ouest, Bordeaux, France

³LIRYC-Institute of Cardiac Rhythmology and Modeling, Bordeaux, France
Email: mark.potse@usi.ch

Keywords: Myocardial ischemia; ventricular conduction disorders; computer models.

Introduction. Our knowledge of the ECG relies mostly on observation alone; i.e. ECG features are related to physiological conditions that have been diagnosed by other means or have been created in animal models. However, the interpretation of some ECG features has escaped the rigor of empiricism and has become established based solely on theoretical grounds. The development of these theories often involved gross simplifications of the physics of the heart. Using modern, realistic computer models of the heart these interpretations can be tested more accurately. I present two cases where well-established theories can no longer be supported: ST depression in subendocardial ischemia and QRS-complex enlargement in ventricular hypertrophy.

Methods and Materials. Computer simulations of cardiac activation and recovery were conducted using a monodomain reaction-diffusion model at 0.2 mm resolution. Cardiac and thoracic anatomy were adapted to individual patients. The surface ECG was simulated by injecting transmembrane current from the heart model in a bidomain model of the torso at 1 mm resolution. Regions of ischemic tissue were created in four quadrants of the ventricles, at various levels of transmural. A hypertrophic model was created by expanding the patient-tailored model artificially, and variations in tissue conductivity were tested.

Results. Surface ECG effects of transmural ischemia corresponded to the classical view, and were largely indicative of the affected regions. However, ST elevation due to ischemia of the inferior wall was most prominently seen on the abdomen, not on the back of the model. Subendocardial ischemia generated the mirror images of the transmural ischemic regions, but with such small amplitude that they would not be measurable in patients, even when the electrodes were placed exactly at the location of the voltage minimum. Left ventricular hypertrophy (LVH) caused a minor increase in QRS amplitude. However, a reduction in conductivity, which often accompanies LVH, more than compensated this increase and led to a decreased QRS amplitude.

Conclusions. When theories are based on simplifying assumptions, they need to be tested anew when technology allows removal of such assumptions. In particular, textbook explanations of ST depression and hypertrophy-induced amplitude changes need to be revised.

THE RIJLANT PAPER

The Role of Electrocardiography Today

L. De Ambroggi

Arrhythmias and Electrophysiology Center, IRCCS Policlinico San Donato,
Milan, Italy

Email: luigi.deambroggi@unimi.it

Keywords: Electrocardiography; Electrophysiology; Cardiac arrhythmias.

The electrocardiography is an old technique born more than one hundred years ago. During the past century the ECG has become an indispensable tool for diagnosis and management of patients with varying heart diseases. Despite the widespread clinical use, in the last decades the ECG has lost some of its diagnostic importance with the growing use of newer sophisticated imaging techniques, which can provide precise anatomic and functional information on several heart conditions (e.g., hypertrophy, location and extension of myocardial infarction, and so on), that in the past were obtained almost exclusively by means of ECG. Nevertheless, still today the ECG provides useful diagnostic and prognostic information in every type of heart disease. It maintains a unique, primary role not only in the field of arrhythmias and conduction disturbances, in which no other technique can provide relevant insights, but also in other clinical settings such as in the ischemic heart disease, particularly during the acute phase.

In addition to the use of ECG for the diagnosis of specific arrhythmias and conduction disturbances, the ECG has gained an important role in the identification of subjects prone to malignant ventricular arrhythmias and sudden cardiac death. Various methods of analysis of short or long periods of electrocardiographic recordings have been proposed in order to detect information not deducible by the traditional analysis of the standard 12-lead ECG, specifically, signal averaging ECG (ventricular late potentials), T wave alternans, RR/QT relation variations, heart rate variability, heart rate turbulence and others.

Beyond the traditional clinical use of 12-lead ECG, it is worth mentioning the ECG-imaging (ECG-I), a new modality of electrocardiology which has been developed and applied in humans in the last decade. From potential recordings over the entire thoracic surface and the geometries of the heart and torso surface, obtained by a computed tomography, electrograms, potential distributions, activation sequences (isochrones) and repolarization patterns are reconstructed on the heart surface. The ECG-I has been successfully applied in humans in different situations including the normal heart, hearts with conduction disorders, ventricular pre-excitation, ventricular tachycardias, focal atrial tachycardia, flutter and atrial fibrillation.

Conclusion. The ECG, in its second century of life, is still quite “vital”. In fact, the continuing research in the field of electrocardiology has provided new knowledge that gives the possibility, in clinical setting, to gain from the analysis of the 12-lead ECG more information than in the past for the diagnosis and prognosis of various heart diseases. Moreover the tremendous advance in technology allows to merge electrical information from ECG with anatomic, functional and metabolic information provided by other imaging modalities, enabling new clinical applications, particularly in the field of cardiac arrhythmias.

ECG IN HYPERTENSION, ISCHEMIA AND MI

Global Ischemia ECG Pattern for Diagnosis of Left Main Occlusion: Diagnostic Properties and Associated Mortality in Patients with Suspected Acute Myocardial Infarction

C. Stengaard, Ch.J. Terkelsen

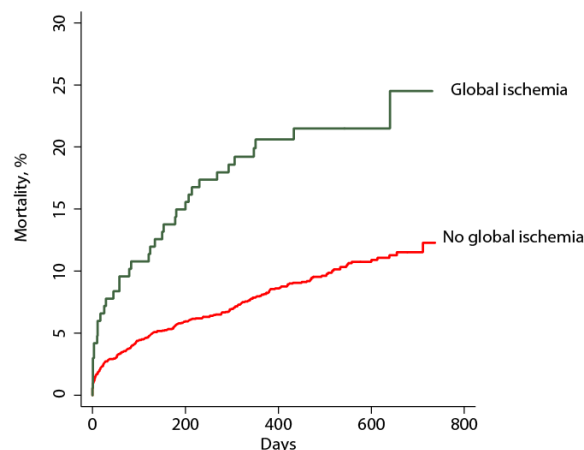
Department of Cardiology, Aarhus University Hospital, Aarhus, Denmark
Email: carsten.stengaard@ki.au.dk

Keywords: left main stenosis; electrocardiography; diagnosis; acute myocardial infarction.

Introduction. A global ischemia ECG pattern (GIP) has been proposed for diagnosis of acute left main stem (LM) occlusion. The GIP is defined by ST-elevation of 1mm in lead aVR and ST-depression of 0.5mm in seven or more ECG leads. We investigated the diagnostic and prognostic properties of GIP in a large cohort of patients with suspected acute myocardial infarction (AMI).

Methods and Materials. We analyzed the prehospital recorded ECG's from 4905 consecutive patients suspected of AMI using the automatic Marquette 12SL algorithm for determination of GIP or no GIP. Mortality and angiography data were obtained from the Danish cause of death registry and the Western Denmark Heart Registry. Patients with left bundle branch block were excluded. We identified patient with significant LM lesions and LM-equivalent lesions in both proximal LAD and Cx. Lesions were significant if they were more than 75% of the cross-sectional area. Protected lesions were not included. The Diagnostic performance of GIP for identification of LM and LM equivalent lesions was calculated. Kaplan Meier plots for patients with and without GIP were constructed and mortality compared using log rank statistics.

Results. ECG's from 2709 patients qualified for analysis and 167 patients (6%) had GIP. AMI was diagnosed in 561 patients (21%) and 55 (10%) of these had GIP. Coronary angiography was performed in 617 patients (23%). Of 43 patients with LM or LM-equivalent lesions 14% had GIP and 4% of those with GIP had significant LM or LM-equivalent lesions. Mortality in patients with GIP was significantly higher compared to patients without GIP ($p<0,001$).



Conclusions. The sensitivity and positive predictive value of GIP for identification of LM occlusions in unselected patients with suspected of AMI is very low. However GIP is an independent predictor of poor outcome. Special attention should be given to these patients to provide optimal treatment.

Suboptimal Diagnosis and Interventional Treatment of Patients with Bundle Branch Block and Acute Myocardial Infarction

**J.T. Sørensen, C. Stengaard, Ch.A. Sorensen, K. Thygesen, H.E. Botker,
L. Thuesen, Ch.J. Terkelsen**

Aarhus University Hospital, Department of Cardiology, Aarhus, Denmark
Email: jacobthorsted@gmail.com

Introduction. International guidelines recommend immediate revascularization in patients with presumed new-onset bundle branch block myocardial infarction (BBBMI). It is a major challenge to determine the age of the bundle branch block (BBB) and triage accordingly in the acute setting..

Methods. Prehospital ECGs, final diagnosis and mortality were assessed in 4905 consecutive patients with suspected AMI. BBB was defined as QRS duration >120 ms in the absence of pace-rhythm, AV-block or ventricular rhythm. Mortality and angiography data were obtained from the Danish Cause of Death Registry and the Western Denmark Heart Registry. Final diagnosis of AMI and the onset of BBB were determined by expert consensus. Patients were divided into 4 groups +/-AMI and +/- BBB. Mortality was evaluated by Kaplan-Meier plots using Log rank statistics.

Results. AMI was diagnosed in 954 patients, of whom 118 had BBBMI. In the 3951 patients without AMI, 436 had BBB. Coronary angiography (CAG) was performed in significantly fewer patients with BBBMI compared to patients with AMI without BBB (41% vs. 68%, $p<0.001$). In patients undergoing CAG, revascularization was more frequent in AMI patients without BBB (59% vs. 79%, $p=0.002$).

Conclusions. Patients with new-onset BBBMI seem to be difficult to diagnose based on ECG and symptoms, leading to low rates of invasive procedures. To improve outcome we recommend a more aggressive approach to diagnosing and triaging patients with BBB and chest pain.

Electrocardiographic Abnormalities in Patients with Hypertension: Study in a Large Primary Care Database

¹M.S. Marcolino, ¹B.C.A. Marino, ²M.B.M. Alkmim, ¹A.L. Ribeiro

¹Medical School and Telehealth Center, University Hospital Universidade Federal de Minas Gerais, Belo Horizonte, Brazil; Telehealth Network of Minas Gerais, Brazil

²Telehealth Center, University Hospital Universidade Federal de Minas Gerais, Belo Horizonte, Brazil; Telehealth Network of Minas Gerais, Brazil

Email: milenamarc@gmail.com

Keywords: electrocardiography; primary health care; telemedicine; hypertension.

Introduction. The 12-lead electrocardiogram (ECG) is the most readily available non-invasive test for the detection of cardiac disease in primary care. The detection of preclinical cardiac abnormalities is a key clinical step in hypertension management, and several guidelines for hypertension recommend an ECG in hypertensive patients to improve risk prediction. The objective of this study is to assess the prevalence of ECG abnormalities in patients with hypertension who were attended at primary care centres in Brazil.

Methods and Materials. Observational, retrospective study. All 12-lead standard digital ECGs analysed by cardiologists of the Telehealth Network of Minas Gerais, a public telemedicine service in Brazil, from January to December 2011, were assessed. This service attends primary care of 660 cities in the state of Minas Gerais. The prevalence of ECG abnormalities in patients with hypertension was assessed.

Results. During the study period, 82,125 primary care patients with hypertension underwent ECG (mean age 60.8 ± 13.5 years, 63.7% females). The most common comorbidities besides hypertension were diabetes (14.2%), smoking (11.4%), hyperlipidemia (7.0%) and Chagas disease (5.6%). Regarding the ECG analysis, 48.3% of them had no abnormalities, and the mean number of abnormalities per patient was 0.9 ± 1.1 (range 0-9). Regarding the rhythm, 2.9% had atrial fibrillation or flutter, 3.2% ventricular premature beats, 2.4% supraventricular premature beats and 0.6% were pacemaker users. Left bundle branch block (LBBB) was observed in 2.4% of the ECGs, incomplete LBBB in 1.8%, right bundle branch block (RBBB) in 4.6% and left anterior hemiblock in 8.7%. First degree atrioventricular block was found in 2.5%, second and third degree in less than 0.1% each. There was electrocardiographic evidence of left ventricular and atrial hypertrophy in 5.2% and 3.2% of patients, respectively, and pathological Q waves in 1.5%. Non-specific repolarization abnormalities were observed in 29.4% of the patients.

Conclusions. In this large sample of primary care patients with hypertension, ECG abnormalities were observed in more than 50% of patients. The most common abnormalities were non-specific repolarization abnormalities, RBBB, LBBB, left ventricular hypertrophy, premature beats and atrial fibrillation.

Defining QT/QTc Prolongation during ST-Elevation Myocardial Infarction and Reperfusion

¹C. Green, ²W. Kuijt, ¹D. Hegland, ¹B. Atwater, ¹M. Krucoff

¹Duke University Medical Center, Durham, NC, USA,

²Academic Medical Center, University of Amsterdam, Amsterdam, The Netherlands

Email: cindy.green@duke.edu

Keywords: ST-segment; QT interval; STEMI; reperfusion.

Introduction. Before novel drugs are approved, the US FDA mandates an adequate safety evaluation, including evaluation of measurable QT interval changes. Defining the safety profile of drugs for patients in disease states is a particular challenge, including patients suffering ST-elevation myocardial infarction (STEMI). Although STEMI therapies are effective in restoring perfusion at the epicardial level, ongoing cellular injury “downstream” can result in adverse arrhythmic events and remains an area of active research. To determine if therapies administered during STEMI create an increased safety risk, QT behavior from the disease itself needs to be quantified sufficiently to define boundary conditions evaluative of acute arrhythmic risk.

Methods and Materials. We conducted a feasibility study to define the expected QT range during STEMI and reperfusion. Four cardiologists each measured QT and RR in a random sample of 44 subjects selected from a larger database of 24-hour, continuously recorded, 12-lead electrocardiograms (ECG) previously analyzed for ST-segment deviation. Seven pre-specified time points related to ST deviation were utilized. QTcF mean estimates were computed at each time point using repeated measures analysis, demonstrating the range, accuracy, and variation across different periods of ST deviation and the consistency across readers.

Results. 1,413 ECGs were measured with mean QTcF estimates by decreasing ST deviation from 416 ± 5.2 to 431 ± 5.2 msec, demonstrating a significant negative correlation between ST-segment deviation and QTcF ($p=0.02$). Intra-observer correlation among each pair of readers ranged from 0.87 to 0.94 and 0.90 to 0.99 for QT and RR, respectively.

Conclusions. Study results could provide a global first-in-kind reference standard for patients in a disease state, complementing the existing standards utilized for thorough QT studies in normal volunteers. This STEMI ST-QT reference standard would further inform drug safety research and development paths in actual population of use STEMI studies. Boundaries around the mean QT for risk related to drugs given during STEMI would enable outliers to be characterized as safety concerns for proarrhythmic risk.

ADVANCED METHODS FOR ECG EVALUATION

Discordant and Concordant Decomposition Model for Repolarisation Alternans in the ECG

¹J. Coll-Font, ²B. Erem, ³C. Rees, ³A. Karma, ⁴Rob S. MacLeod, ¹D.H. Brooks

¹B-SPIRAL Group, ECE Dept. Northeastern University, Boston, USA,

²Boston Children's Hospital, Boston, USA,

³Physics Dept. Northeastern University, Boston, USA,

⁴SCI Institute, University of Utah, Salt Lake City, USA

Email: jcollfont@ece.neu.edu

Keywords: T-wave; repolarization; alternans; modelling.

Introduction. Repolarization alternans (Repol-TWA), generally defined as a regular beat-to-beat alternation in repolarization time of the transmembrane potentials (TMPs), can be manifested spatially as concordant (in-phase alternation throughout both ventricles) or discordant (inhomogeneous alternans pattern). Spatially discordant alternans has been reported to create a substrate for the initiation of re-entrant arrhythmias and ventricular fibrillation (VF), while spatially concordant alternans is believed to be less arrhythmogenic. This suggests that noninvasive distinction between them is of interest. Alternans detection usually depends on the appearance of alternating T-wave amplitudes —T-wave alternans (ECG-TWA) —but the connection between heterogeneity of Repol-TWA and characteristics of ECG-TWA is not well understood.

Methods and Materials. In this work we use a simple mathematical model to analyze the relationship between spatially concordant and discordant Repol-TWA in the ECG. Our model decomposes general Repol-TWA into a homogeneous repolarization delay that corresponds to the concordant component and a spatially varying delay corresponding to the discordant component. Using a model of propagation of excitation in the myocardium, we can show that the concordant component produces a delay in the ECG T-wave while the discordant component produces a change of shape. We use ECGSIM to validate the model by synthesizing Repol-TWA and comparing the resulting T-waves.

Results. We illustrate our method using three cases of Repol-TWA. The first is purely concordant, the second purely discordant, and the third a mixture (in effect, only one part of the heart showing Repol-TWA). Fig. 1 shows agreement between the theoretical decomposition and the three numerical experiments, producing T-waves that contained a simple delay, a change of shape, and a delay plus change of shape, respectively, compared to the original T-wave.

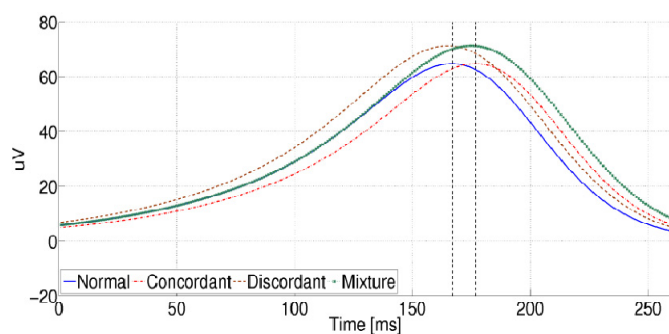


Fig. 1 T-waves from concordant, discordant and mixture TWA cases compared against normal T-wave.

Conclusions. We have shown that spatially concordant and discordant repolarisation alternans produce distinguishable features in the T-wave segment of the ECG — a shift in timing and a change of shape. The ability to distinguish these features provides a basis for improving risk stratification by TWA testing.

Excitation Specificity of Repolarization Parameters

^{1,2}J. Halamek, ^{1,2}P. Jurak, ²P. Leinveber, ²P. Vesely

¹Institute of Scientific Instruments, Brno, Czech Republic

²St. Anne's University Hospital, ICRC, Brno, Czech Republic

Email: josef@isibrno.cz

Keywords: repolarization analysis; QT/RR slope; QT restitution; excitation specificity.

Introduction. The analysis of QT/RR coupling is based on measurement with significant heart rate changes to preserve sufficient signal to noise ratio. The QT parameters are excitation specific and the type of used stress should not be neglected.

Methods. Two groups of subjects (healthy and hypertensive), measured during pedaling exercise and tilt test, were analyzed. The dynamic model with 3 optimized parameters that suppose restitution and memory of QT coupling was used to eliminate QT hysteresis. The QTc and QT/RR slope were analyzed by linear model (LM) and nonlinear model (NLM). The optimal model (OPM) was given by QTc reproducibility. .

Results. Comparing both excitations, QTc was significantly longer ($P<0.05$) during tilt test in both groups with NLM. The QTc was similar in both tests using LM or OPM. QT/RR slope was significantly steeper with LM or OPM ($P<0.01$) during exercise test, but not different during NLM. QT restitution (immediate change of QT) was higher during exercise test, but not significantly. The QT adaptation to RR changes was faster during tilt test, ($P<0.05$). The linear model was found the best during tilt test and the QTc reproducibility depends primarily on the level of heart rate change. The QT-RR nonlinearity exists in about 50 % of subjects during exercise test.

Conclusions. The measurement with defined heart rate stress and the analysis of QT/RR linearity-nonlinearity should be used to achieve reproducible QT parameters. Excitation specificity of QT parameters and linearity/nonlinearity of QT/RR coupling may explain the specific triggers of arrhythmias, such as genetic dependent triggers in LQT subjects.

Chaos Theory and Non-Linear Dynamics in Hypertensive Cardiopathy and Heart Failure

¹V.D. Moga, ²I. Kurcalte, ³M. Moga, ³F. Vidu, ⁴C. Rezus, ⁵I. Cotet, ¹R. Avram

¹University of Medicine and Pharmacy “V.Babes” Cardiology Clinic Emergency
County Hospital Timisoara, Romania

²Riga Stradins University, Riga Eastern Clinical University Hospital, Latvia

³IT Department of the Emergency County Hospital Timisoara, Romania

⁴University of Medicine and Pharmacy “Gr.T.Popa” Iasi, Romania

⁵Emergency County Hospital Arad, Romania

Email: moga.victor@gmail.com

Purpose. Hypertension is a risk factor for the development of heart failure (HF), both because hypertension increases cardiac work, which leads to the development of left ventricular hypertrophy, and because hypertension is a risk factor for the development of coronary heart disease. Knowing the role of the autonomic nervous system (ANS) in the mechanism of hypertension, the challenge is to evaluate the arrhythmic risk of hypertensive patients. Disturbances in the activity of the autonomic nervous system (ANS) also significantly influence the outcome of patients with chronic heart failure (CHF). A subject open to debate is to compare heart rate variability (HRV) parameters and the chaos theory methods for the assessment of the clinical status and the outcome in hypertensive cardiopathy.

Method. In this study we evaluate the level of the autonomic dysfunction in hypertension (n: 26, mean age: 53.6 yrs) compared to the more well-known autonomic disturbances in heart failure (n: 39, mean age: 58.5 yrs) using non-linear dynamics methods compared with heart rate variability.

Results. Hypertensive patients have a high sympathetic tone, expressed as the power spectral density (PSD, s²/Hz, ms²) of heart rate variability parameters and the low to high frequency ratio (LF/HF) compared with the control group (LF/HF ratio:1.16 vs. 0.94 p<0,01). A significant difference was found between patients with heart failure and healthy controls in short time scales (DFA α_1 : 0.72 vs. 0.87 p < 0.05). The DFA α_1 showed higher values in the hypertensive group compared with the heart failure group (0.84 vs 0.72 p: ns). It was found that the short-term fractal scaling exponent alpha (1) is significantly lower in arrhythmic hypertensive patients (0.75 vs. 0.84; p < 0.03). Left ventricular ejection fraction (LVEF %), SDNN (ms), LF/HF ratio, and the baroreflex sensitivity (BRS) parameters had been proved to be independent risk factors for ventricular arrhythmia. BRS is correlate with QT/RR ratio (r: 0.48) and with DFA α_1 (r: 0.40).

Conclusions. The nonlinear dynamic methods could have clinical and prognostic applicability also in short-time ECG series. Dynamic analysis based on chaos theory point out the multi-fractal time series in patients who loss normal fractal characteristics and regularity in HRV. Nonlinear analysis technique may complement traditional ECG analysis. It seems possible to conclude that patients with hypertensive cardiopathy are vulnerable to arrhythmias like in patients with heart failure and it is necessary to improve ventricular arrhythmia prophylaxis in hypertensive patients.

Fractal Dimension of In-Vivo and Ex-Vivo Rabbit HRV Series

¹O. Janoušek, ¹M. Ronzhina, ¹J. Kolářová, ¹I. Provazník, ¹M. Nováková,
²T. Stračina, ²V. Olejníčková

¹Brno University of Technology, Brno, Czech Republic,

²Masaryk University, Brno, Czech Republic

Email: janouseko@feec.vutbr.cz

Keywords: fractal dimension, box-counting.

Introduction. In recent years, non-linear methods for heart rate variability (HRV) assessment have been utilized, including those based on fractal dimension quantification. Hypothesis exists, that fractal dimension computed from large sets of RR intervals, may be associated with autonomous nervous system impact on HRV. We investigated differences of fractal dimension between in-vivo and isolated rabbit HRV series with aim to discover, whereas fractal dimension may servers as an indicator of autonomic nervous system activity elimination.

Methods and Materials. Five New Zealand white rabbits and five isolated New Zealand rabbit hearts in Langendorff setup were studied. The R-peaks from five-minute long ECG records have been manually detected. Fractal dimension values were computed by custom made box-counting algorithm in Matlab.

Results. The fractal dimension values of in-vivo HRV series do not statistically differ ($\alpha = 0.05$) from the isolated heart ones. In-vivo HRV series fractal dimension value is equal to 1.49 ± 0.03 , whereas isolated hearts HRV series has fractal dimension equal to 1.45 ± 0.14 . On the other hand, mean of RR intervals computed from the same data series, statistically differs between in-vivo ($\text{meanRR} = 0.25 \pm 0.02$) and isolated ($\text{meanRR} = 0.38 \pm 0.07$) HRV series.

Conclusions. We conclude, that fractal dimension of HRV does not provide a tool for assessment of autonomous nervous system impact on heart rhythm. In-vivo RR series have a negligible amount of self-similarity, which persist even after heart isolation. Heart isolation cause prolongation of the RR interval, however stochastic character of RR series is not influenced by autonomous nervous system effect elimination.

**ARRHYTHMIAS
AND CARDIAC RESYNCHRONIZATION THERAPY**

Significance of Ventricular Arrhythmia and Heart Rate Variability in Patients with CRT

W. Zareba

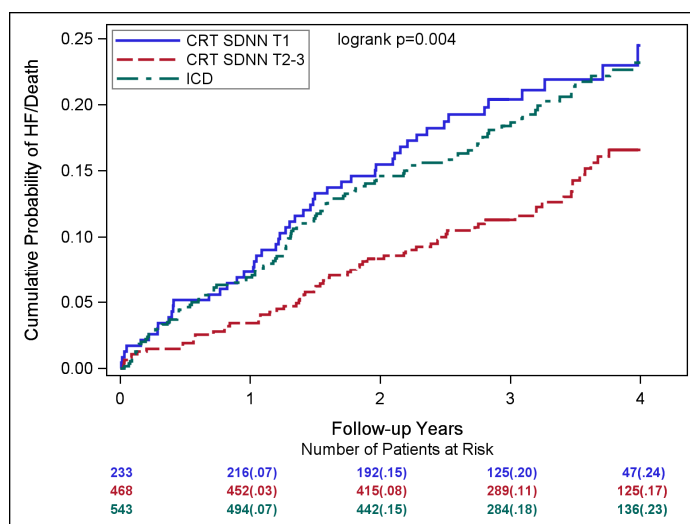
University of Rochester, Rochester, USA
 Email: wojciech_zareba@urmc.rochester.edu

Keywords: Ventricular Arrhythmias, Cardiac Resynchronization Therapy, Heart Rate Variability.

Introduction. Patients with heart failure frequently present on 24-hour Holter recording with ventricular arrhythmias and with impaired heart rate variability. There are limited data regarding the prognostic significance of Holter-documented ventricular arrhythmias and heart rate variability in patients with cardiac resynchronization therapy (CRT).

Methods and Materials. In the MADIT-CRT trial, we conducted Holter substudy with 950 CRT-D patients undergoing 24-hour Holter recordings. Time-domain HRV parameters were analysed from 24-hour recording whereas frequency-domain HRV parameters were derived from a 5-minute supine recording. Presence of NSVT was evaluated in association with the primary endpoint of heart failure hospitalization or death and in association with VT/VF requiring ICD therapy

Results. Among HRV parameters SDNN derived from time-domain analysis and VLF from frequency-domain analysis were found to be best predictors of heart failure hospitalization or death. Figure shows that LBBB patients with SDNN in first tertile (≤ 93 ms) did not benefit from CRT with their event risk similar to that of ICD patients, however patients with $SDNN > 93$ ms had a 39% reduction in the risk of HF/Death when comparing to patients with $SDNN \leq 93$ ms (HR=0.61; $p=0.10$). Similar results were observed when evaluating $VLF \leq 179$ ms² vs. > 179 ms². NSVT observed on baseline Holter monitoring were associated with significant increase in the risk of rapid VT/VF > 180 bpm or death with HR = 2.17; $p < 0.0001$. The 2-year event rate in patients with an ischemic cardiomyopathy and NSVT was 21% as compared to 10% in patients without NSVT; the same relationship was observed in patients with a non-ischemic cardiomyopathy (20% with vs. 8% without NSVT, $p < 0.01$). NSVT were associated with HF or death in nonischemic cardiomyopathy patients (HR=2.59; $p=0.01$) but not in ischemic cardiomyopathy patients (HR=0.83; $p=0.42$).



Conclusions. LBBB patients with depressed HRV ($SDNN \leq 93$ ms) do not benefit from CRT. HRV analysis available in every holter recording could help optimizing use of CRT in heart failure patients. NSVT remain predictive for the endpoint of rapid VT/VF or death in CRT-treated patients.

Electrocardiographic Risk Factors for Sudden Cardiac Death. Usefulness and Limitations of ECG Screening

B. Gorenek

Eskisehir Osmangazi University, Eskisehir, Turkey

Email: bulent@gorenek.com

Introduction. Sudden cardiac death (SCD) is a leading cause of death among adults over the age of 40 in the US and other countries. Much effort has been focused on the problem of risk stratification for SCD over a period of decades. Risk is a challenging concept for both physicians and patients.

In the Framingham Study, electrocardiographic abnormalities were associated with an increased risk of all clinical manifestations of coronary artery disease, including SCD. Long-term electrocardiographic monitoring indicated that left ventricular hypertrophy and intraventricular block are associated with frequent ventricular premature beats. However some studies didn't ECG screening in the general population is unproven and is only performed in specific groups and for specific purposes, such as employment, health insurance or participation in competitive sports. The major objective of ECG screening is to detect potentially lethal cardiovascular diseases likely to manifest with SCD in youth.

Preparticipation cardiovascular screening focuses in general on a young population group (aged less than 30 y), among whom most anomalies will be congenital, although some might be acquired disorders. SCD in the young often occurs without warning or recognition of warning symptoms. SCD in young athletes is uncommon. The resting ECG has been shown to be crucial for cardiac screening, having a high sensitivity for detecting underlying diseases associated with SCD in athletes.

Patients with hypertrophic cardiomyopathy and with arrhythmogenic right ventricular cardiomyopathy (ARVC) frequently presents with ECG abnormalities. Electrophysiological abnormalities such as long and short QT syndrome, Brugada syndrome, high-grade AV block and the delta-wave characteristic of WPW syndrome are also usually detected by ECG. Unfortunately, some underlying disorders, such as early ARVC and coronary artery anomaly, may not show any ECG changes.

We should know what is normal and what is abnormal in athletes' ECG. Abnormal ECG screening findings lead to disqualification of up to 2% of athletes from competitive sports. Normal cardiac adaptation to training may also include ECG changes, such as sinus bradycardia, sinus arrhythmia, AV block I (and possibly IIa), as well as repolarization changes and isolated voltage criteria of left ventricular hypertrophy, which all may be considered abnormal in a nonathlete population. This has led to the assumption that the ECG in athletes is 'often or always abnormal'. The ESC recommends the inclusion of the resting ECG, in addition to family/personal history and physical examination, whereas the AHA advocates only personal/family history and physical examination..

Conclusions. ECG screening in the general population is unproven and is only performed in specific groups and for specific purposes. A 12 lead basal ECG is a non-expensive, largely available in practice test for a mass screening of SCD especially in athletes. The sensitivity, specificity, and predictive value of ECG screening by itself, or as an adjunct to other forms of screening, remain largely unknown. Misinterpretation of 12 lead ECG is not uncommon, especially if physicians interpreting the ECG do not have special expertise in sports cardiology. Some cardiovascular disorders at risk of SCD are not associated with ECG changes. As a consequence of the high number of false-positive results, the proportion of unnecessary tests ordered is high and accounts for the high cost and low cost effectiveness of ECG screening programs. The future for prevention of SCD in the athlete by large-scale ECG screening program lies in continuing efforts to better understand the scientific basis for ECG interpretation and to define standards of ECG criteria for differentiation between athlete's heart and true heart diseases. Further studies are needed to test the accuracy of ECG screening, in relation to gender, age, ethnicity, and different level of training and/or type of sports.

Postoperative Arrhythmias and Conduction Abnormalities in Patients with Heterotaxy

P. Dorostkar, S. Sivanandam, L. Kochilas

University of Minnesota, Minneapolis, MN, USA,

Email: pcd@umn.edu

Keywords: Heterotaxy syndromes, Pediatric, Arrhythmias

Introduction. Cardiovascular laterality defects of left and right atrial isomerism (LAI, RAI) are associated with high surgical mortality and poor prognosis, even after accounting for severity of the cardiac phenotype. Arrhythmias and conduction abnormalities are frequently encountered, but their association with surgical interventions is not well understood.

Methods and Materials. A retrospective study of patients with heterotaxy and cardiac surgery (1979-2013) was performed. Arrhythmia manifestations and treatment were compared with regard to the type of isomerism and surgical interventions.

Results. There were 23 patients with heterotaxy. Fourteen out of 15 with RAI underwent single ventricle (SV) palliation. Seven of them had postoperative arrhythmias (1-4 days post surgery): Three had junctional ectopic tachycardia after total anomalous venous return repair (one in association with Norwood and one with Glenn operation), two had atrial tachycardia post Fontan palliation and two had atrial tachycardia remotely, 14 and 19 years postoperatively. Pacing was instituted in 4 RAI patients post-operatively: three due to inadequate chronotropy and one 34 years later for complete heart block (CHB), while one received a defibrillator as a bridge to cardiac transplantation. The RAI patient who underwent 2-ventricle repair had no arrhythmias or conduction abnormalities. Three RAI patients died after surgical intervention, but none from an arrhythmia. Six out of 8 LAI patients required pacing due to inadequate chronotropy and/or atrioventricular conduction disease [relative risk (RR) for pacing in LAI vs. RAI = 2.8, $p < 0.039$]. Five out of 8 LAI patients underwent SV palliation (RR for SV palliation in RAI vs. LAI = 1.5, $p = 0.1$) with 3 of them receiving pacing due to inadequate chronotropy. Three LAI patients with 2-ventricle repair received pacing in association with ASD/VSD repair, two for inadequate chronotropy and one for CHB. One LAI patient died intra-operatively in association with CHB.

Conclusions. In our series, LAI patients have a much higher risk of electrical abnormalities requiring pacing, mostly due to inadequate chronotropy; this finding seems to be independent of the type of surgical intervention.

Left Bundle Branch Block – Renaissance of an Old Biomarker

R. Hatala

Dept. of Cardiology and Angiology, National Cardiovascular Institute and Slovak
Medical University School of Medicine, Bratislava, Slovakia
Email: hatala@nusch.sk

Keywords: left bundle branch block; heart failure; cardiac resynchronization therapy

With the widespread implementation of electrocardiography as the key diagnostic method in cardiology during the first half of the last century ventricular conduction defects got in focus of clinical research. It soon became evident that left bundle branch block (LBBB) – in contrast to RBBB – was usually associated with severe structural heart disease, often in the clinical context of chronic heart failure (HF). The clinical significance of LBBB revived with the introduction of cardiac resynchronization therapy (CRT) for chronic heart failure. About 1/3 of patients with HF with severely depressed left ventricular (LV) systolic function have a prolonged QRS complex due to intraventricular conduction defect with “LBBB like” pattern. According to the most recent (2013) European ESC guideline CRT is highly indicated (class I) in HF patients (pts) with NYHA class II - ambulatory class IV in sinus rhythm with QRS complex of LBBB morphology lasting >120 ms. Up to 10% of all HF patients may fulfil these criteria. However, multiple clinical trials have shown that at least 30% of patients fulfilling criteria for CRT do not benefit from this therapy (“non-responders”). One of the reasons for such therapeutic failure might be a “loose” definition of LBBB, based mostly on prolonged QRS duration (>120 ms) and QRS morphology with QS or dominant S in lead V1 and with R wave in V6 (absent Q waves). Furthermore, in clinical practice the mere presence of prolonged QRS with dominant S waves in leads V1-V3 is considered as LBBB. Detailed ECG analyses have demonstrated that such conduction abnormalities do not represent “genuine” LBBB but rather reflect the presence of left anterior fascicular block in the context of LV hypertrophy.

Recent computer simulations, in accordance with original clinical studies, emphasize the importance of applying strict ECG criteria for diagnosing LBBB when selecting HF patients for CRT. These should include:

1. QRS duration of 140 and 130 ms in men and women, respectively
2. Distinctive mid-QRS slurring and notching in leads I, aVL, V5-V6
3. Absent septal q waves in leads I, V5, and V6

However, presence of concomitant structural abnormalities further complicates exact ECG interpretation. Large anteroseptal infarction scar may account for rS configuration in V1 even in the presence of complete LBBB. Nevertheless, residual conduction via the left bundle should be expected in patients with LBBB like patterns with presence of q waves in aVL and/or an r wave ≥ 1 mm in lead V1. Preliminary reports suggest that residual LB conduction significantly reduces the benefit of CRT and contributes to “non-responding” phenomenon.

Conclusions. Meticulous individual ECG evaluation focused on identification of “genuine” LBBB should be mandatory for appropriate indication of CRT in HF pts. This should be emphasized also in future practice guidelines for CRT in order to optimize patient selection for CRT and avoid iatrogenic complications in suboptimal candidates.

T-wave Area as an Additional Predictor of Response to Cardiac Resynchronization Therapy

¹E.B. Engels, ²E.M. Vegh, ¹C.J.M. van Deursen, ²J.P. Singh, ¹F.W. Prinzen

¹Department of Physiology, CARIM School for Cardiovascular Diseases, Maastricht University, Maastricht, The Netherlands.

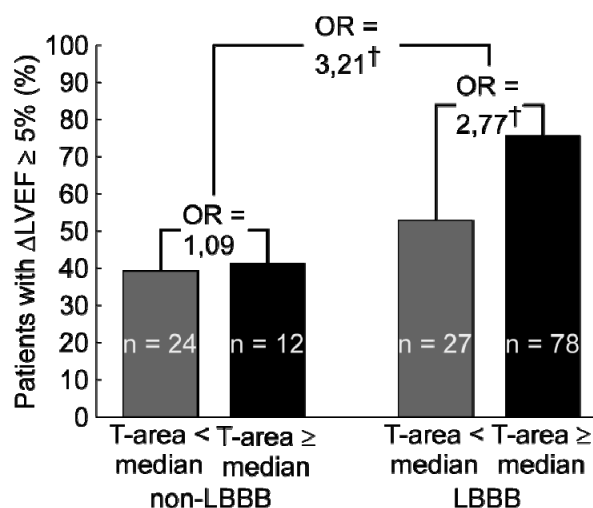
²Cardiac Arrhythmia Service, Massachusetts General Hospital, Harvard Medical School, Boston, USA
Email: e.engels@maastrichtuniversity.nl

Keywords: Cardiac Resynchronization Therapy; ECG analysis; Vectorcardiography

Introduction. Chronic heart failure patients with a left ventricular (LV) conduction delay, mostly due to left bundle branch block (LBBB), generally derive benefit from cardiac resynchronization therapy (CRT). However, approximately 30% of patients do not improve clinically after CRT. We investigated whether T-wave analysis can improve patient selection.

Methods and Materials. Baseline 12-lead electrocardiograms (ECGs) and baseline and follow-up echocardiograms were recorded in 258 CRT recipients. CRT response was defined as absolute increase in LV ejection fraction (LVEF) of $\geq 5\%$ after 6 months of CRT. Vectorcardiograms (VCGs) were constructed from the measured 12-lead ECGs using an adapted Kors method.

Results. Logistic regression models indicated repolarization variables as good predictors of CRT response. The VCG-derived T-wave area had the best ability to predict CRT response, even better than QRS-wave area (odds ratio (OR) per 10 μ Vs increase 1.172 ($p < 0.001$) vs. 1.116 ($p = 0.001$) respectively). The figure indicates that after dividing the study cohort in LBBB and non-LBBB patients, T-wave area had especially predictive value in the LBBB patient group. The ORs remained the same after adjustment of multiple covariates, such as gender, ischemia, age, hypertension, coronary artery bypass graft and the usage of diuretics and beta blockers.



Conclusions. In patients with LBBB morphology of the QRS complex, a larger baseline T-wave area is an important additional predictor of LVEF increase upon CRT.

Difference Between Native and Right-Ventricular-Paced QRS Duration Predicts QRS Shortening by Cardiac Resynchronization Therapy: A Novel Marker of True Complete Left Bundle Branch Block

D. Wichterle, K. Sedláček, V. Vančura, H. Jansová, J. Kautzner

Department of Cardiology, Institute for Clinical and Experimental Medicine, Prague, Czech Republic

Email: wichterle@hotmail.com

Keywords: left bundle branch block; right-ventricular pacing; cardiac resynchronization therapy

Introduction. True complete left bundle branch block (cLBBB) predicts greater response to cardiac resynchronization therapy (CRT). Right-ventricular (RV) midseptum pacing approximates a true cLBBB QRS complex morphology. We investigated whether the difference between native and right-ventricular-paced QRS duration (QRSd) predicts QRSd shortening by CRT.

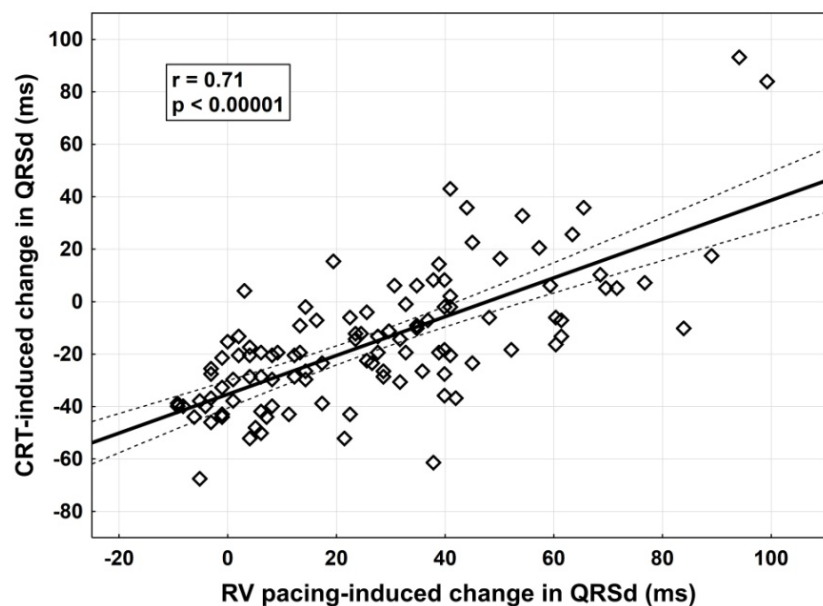
Methods and Materials. We prospectively collected ECGs and EGMs in 110 consecutive patients (aged 66 ± 9 yrs; 72% males; 59% non-ischemic cardiomyopathy; LVEF $26 \pm 5\%$) with native non-RBBB QRS morphology undergoing CRT implant. Recordings of spontaneous rhythm, RV and CRT pacing were carefully edited, signal-averaged and manually measured by electronic calipers.

Results. Native QRS width was 181 ± 21 ms. Left ventricular (LV) pacing lead was implanted at the position with Q-LV /QRSd ratio of 0.73 ± 0.11 . QRSd was prolonged by 27 ± 25 ms during RV pacing ($\Delta\text{QRS}_{\text{RVP}}$) and shortened by -15 ± 26 ms during CRT pacing ($\Delta\text{QRS}_{\text{CRT}}$).

$\Delta\text{QRS}_{\text{CRT}}$ correlated with $\Delta\text{QRS}_{\text{RVP}}$ ($r = 0.71$, Figure), with native QRSd ($r = -0.65$), and with Q-LV ratio ($r = -0.43$); all $p < 0.00001$. In multivariate

analysis, $\Delta\text{QRS}_{\text{CRT}}$ was most strongly associated with $\Delta\text{QRS}_{\text{RVP}}$ ($r^2 = 0.33$, $p < 0.00001$), followed by native QRSd ($r^2 = 0.27$, $p < 0.00001$), and Q-LV ratio ($r^2 = 0.15$, $p = 0.02$).

Conclusions. The QRSd prolongation by RV midseptum pacing is a surrogate of residual left bundle conduction. The difference between native and RV-paced QRSd is the strongest predictor of CRT-induced QRSd change independent of native QRSd. Whether this is also independent of pre-implant surface ECG markers of true cLBBB remains to be investigated.



ECG METHODS AND TECHNOLOGIES

Selected Aspects of Racial Differences in the ECG

¹P.W. Macfarlane, ¹E. Clark, ²B.G. Francq, ²S. Lloyd

¹Institute of Cardiovascular and Medical Sciences, University of Glasgow, Scotland,

²Institute of Health and Wellbeing, University of Glasgow, Scotland

Email: Peter.Macfarlane@glasgow.ac.uk

Keywords: ECG; Racial Variation; Automated Analysis.

Introduction. There has been little work done in assessing the effects of ethnic variation in ECG appearances. This study set out to address this shortcoming in a limited way by analysing ECGs from different racial groups using the same measurement techniques for each cohort.

Methods and Materials. Four different populations were available for study, namely 1496 white Caucasians living in the West of Scotland, 503 Chinese individuals living in Taiwan, 963 individuals from three different areas in India and 1261 Africans living in and around Ilorin in Nigeria.

12 lead ECGs were recorded in digital form on different machines at a sampling rate of 500 samples/sec. The digital data were returned to Glasgow and analysed using the same version of the Glasgow program. Regression analysis was undertaken along with tests of significance on the effect of race and age in males and females separately.

Results. There were 4223 individuals recruited into the study, with approximately two thirds being male. The mean age of each of the four different populations in the order listed above was 37±13, 43±14, 36±14 and 43±14 years.

QRS voltages were significantly linked with race though not in a consistent way. There was a significant effect of race on the ST amplitude in V1-V2, particularly V2 which was higher in Chinese and Nigerian individuals, male and female, compared to the Caucasian groups.

With respect to time intervals, mean QRS duration was always shorter in females. Interesting data for the mean QTc (Hodges correction) are shown in the Table.

	Caucasian	Chinese	Indian	Black
MALE	402.83	401.28	388.77	392.81
FEMALE	409.63	418.55	404.99	406.19

Conclusion. These and other data indicate that race is a factor which should indeed be taken into consideration when interpreting the ECG.

Gender Differences in Novel Repolarization Parameters

¹K. Piotrowicz, ²M. Vaglio, ²J.P.Couderc, ²J. Xio, ²W. Zareba

¹Military Institute of Medicine, Warsaw, Poland,

²Heart Research Follow-Up, Rochester, NT, USA

Email: kpiotrowicz@wim.mil.pl

Background. The complex nature of the transmural dispersion of repolarization requires more detailed assessment than QT interval duration. The new computer-based parameters might be useful for evaluation of repolarization; however, there are limited data regarding the normal values.

Objectives. The aim of this study was to assess normal standards and their gender dependent variability of various new computer-based repolarization parameters.

Methods. Twenty-minute high-resolution ECGs were recorded in healthy volunteers and the comprehensive analysis of the repolarization signal was employed. The following scalar parameters were studied: repolarization duration (QT, TpTe), length (Tl), amplitude, ascending and descending slope of the T wave (Tamp, α_L , α_R). Principal Component Analysis was applied to obtain multidimensional view of repolarization and two groups of novel parameters were computed: based on T-loop preferential plan- repolarization duration (QT, QTa), complexity (λ_2/λ_1 , λ_3 , MV) and early/late repolarization duration (ERD, LRD, TRD) and based on eigenvector 1 – T wave duration and morphology (LST, RST).

Results. Results are shown in the Table.

Skalar Parameters	Male n=95	Female n=97	P- value
RR (ms)	941 ±144	870 ±129	<0.001
QT (ms)	398 ± 28	396 ± 28	0.578
QTa (ms)	310 ± 25	313 ± 24	0.444
T _L (ms)	214 ± 26	197 ±31	<0.001
TpTe (ms)	88 ±12	83 ±11	0.003
T amp (μV)	560 ± 171	389 ± 159	<0.001
α_L (μV/ms)	4.8 ±1.7	3.7 ± 1.7	<0.001
α_R (μV/msec)	-8.4 ± 2.9	-6.1 ± 2.8	<0.001
Novel parameters			
λ_2 / λ_1	18.5 ± 8.5	23.0 ± 1.2	0.003
λ_3	2.7 ± 1.7	3.9 ± 2.1	<0.001
MV (ms)	0.97 ± 0.29	0.67 ± 0.27	<0.001
QT (ms)	401 ± 28	399 ± 26	0.563
ERD	41.3 ± 6.7	35.4 ± 7.5	<0.001
LRD	29.0 ± 4.6	26.7 ± 4.9	0.001
TRD	75.4 ± 10.4	75.4 ± 10.4	<0.001
LST (μV/ms)	8.5 ± 3	6.8 ± 3	<0.001
RST (μV/ms)	14 ± 5	11 ± 5	<0.001
QRST angle	65 ± 30	50 ± 25	<0.001

Conclusions. In present study, gender-related norms of the new computer-based repolarization parameters were recommended. There were statistically significant differences in repolarization by gender thus male and female should be evaluated independently.

Lead Selection for Maximal QT Interval Duration Measurement in Patients with Heart Failure and Stroke

I.Mozos

”Victor Babes” University of Medicine and Pharmacy, Department
of Functional Sciences, Timisoara, Romania
Email: ioanamozos@yahoo.de

Keywords: Electrocardiography; QT interval; Heart failure; Stroke.

Introduction. A prolonged QT interval is a predictor of sudden cardiac death. QT interval is prolonged in several diseases, including heart failure and stroke. Interlead variability of the QT interval is considerable, but its measurement is laborious in all 12 standard ECG leads. The objective of the present study was to find the leads with the longest QT interval duration.

Methods and Materials. A total of 122 patients, 43 with heart failure, 61 with stroke and 18 healthy controls, underwent standard 12-lead ECG. QT interval was measured in each lead, corrected for heart rate using the Bazett formula (QTc) and compared in the different leads.

Results. Maximal QT interval duration (QTmax) was measured most often in the precordial leads, especially: V2 (18%), V4 (15%), V3 (14%). Considering limb leads, QTmax was measured most often in DII. Considering only patients with a prolonged QTc, QTmax was measured most often in V3 (16%), DI, aVL and V2 (14%) and DII, aVF, V4 and V5 (12%). The leads proving the closest approximation to QTmax were: V3, V6, V2 and DII. The leads with the highest deviation from QTmax were: DIII and V1, followed by leads DI and aVR. The highest QTc (494±69 ms) and QTmax (434±57 ms) values were recorded in stroke and heart failure patients, respectively. QT interval duration and QTc in different leads was further compared in 30 participants with measurable QT intervals in all leads, showing no statistically significant differences (p by ANOVA = 0.232 and 0.355 for QT and QTc, respectively).

Conclusions. The precordial leads are the most reliable leads for assessment of QT interval duration, especially V3, V2 and V4. DII, the inferolateral lead, is the most reliable limb lead for QT interval measurements.

Body Surface T-wave Amplitude Dispersion in Diabetic Rabbits and Epicardial Repolarization Pattern

**¹M.A. Vaykshnorayte, ^{1,2}K.A. Sedova, ^{1,3}O.G. Bernikova, ^{1,3}A.O. Ovechkin,
^{1,3}J.E. Azarov**

¹Institute of Physiology, Komi Science Center, Ural Branch, Russian Academy of Sciences, Syktyvkar, Russia,

²Czech Technical University, Kladno, Czech Republic,

³Komi Branch of Kirov State Medical Academy, Syktyvkar, Russia.

Email: m.vaykshnorayte@mail.ru

Keywords: T-wave; diabetes.

Introduction. In spite of the accepted concept that the *T*-wave results from ventricular repolarization gradients, there is still a great deal of controversy concerning the major gradient. In the present experimental study we investigated the influence of diabetes mellitus on epicardial repolarization pattern and ECG T wave amplitude dispersion (TWAD).

Methods and Materials. The diabetes mellitus was induced in 11 rabbits and 9 animals served as healthy controls. In anaesthetized (zoletil 15mg/kg, i.m.) animals the T wave amplitude was measured in unipolar precordial basal and apical ECG leads. TWAD was determined as the difference in the T wave amplitudes between basal and apical leads. Unipolar electrograms were then recorded from 64 ventricular epicardial leads in an open-chest preparation. In each epicardial lead, the end of repolarization time (RT) was determined. Apicobasal, interventricular and anteroposterior gradients of RTs were derived and RT global dispersion (GD) was assessed.

Results. Diabetic group showed less apicobasal, larger anteroposterior RT gradients and less TWAD as compared to controls ($p < 0.05$). However, multiple regression analysis of TWAD revealed only GD of RT gradient as an independent contributing factor (Beta=-0.71, $p = 0.01$), which in turn, depended on the anteroposterior RT gradient (Beta=0.52, $p = 0.038$).

Conclusions. The TWAD decrease in diabetic animals was related to the development of the predominant posterior-to-anterior RT sequence instead of normal apicobasal RT sequence, which flattened the precordial T waves.

The study was supported by the Ural Branch of the Russian Academy of Sciences (Projects No 12-I-4-2059 and 13-4-032-KSC).

Diagnostic Performance and System Delay Using Telemedicine for PreHospital Diagnosis in Triage and Treatment of STEMI

^{1,2}A.M.B. Rasmussen, ²B.Ch.J. Terkelsen

¹Department of Medicine, Silkeborg Regional Hospital and Cardiovascular Research Centre Viborg and Silkeborg Hospital & Institute of Clinical Medicine, Aarhus University Hospital, 8600 Silkeborg, Denmark,

²Department of Cardiology B, Aarhus University Hospital in Skejby, 8200 Aarhus N, Denmark

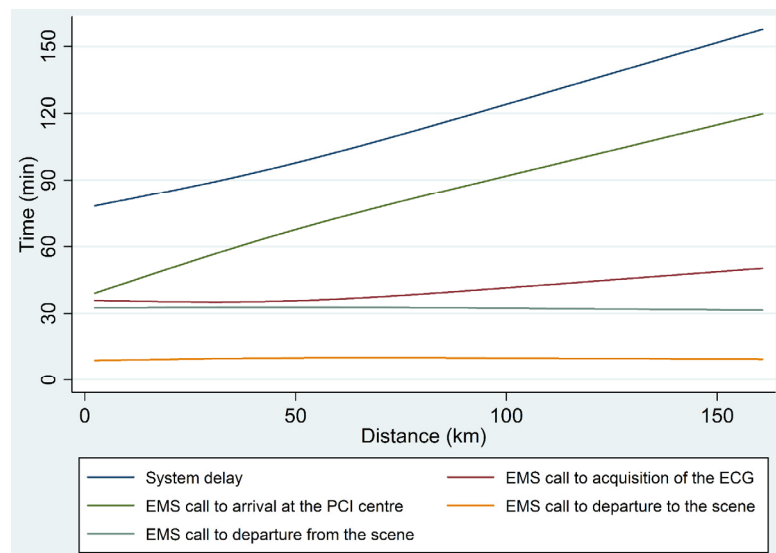
Email: martin.b.rasmussen@dadlnet.dk

Keywords: myocardial infarction; electrocardiography; triage/methods; emergency medical services; coronary angiography

Introduction. European ST-elevation myocardial infarction (STEMI) guidelines recommend pre-hospital diagnosis to facilitate early reperfusion in patients with STEMI and provide recommendations regarding optimal system delay (time from first medical contact (FMC) to primary percutaneous coronary intervention (PPCI)). There are limited data regarding achievable system delays in an optimal STEMI system of care using pre-hospital diagnosis to triage patients with STEMI directly to PCI centres. We examined the proportion of tentative pre-hospital STEMI diagnoses established by telemedicine confirmed at hospital arrival, and we determined system delay in patients diagnosed pre-hospitally and triaged directly to the catheterisation laboratory (cath. lab.).

Methods and Materials. A population-based follow-up study in Central Denmark Region with 15,992 patients diagnosed using telemedicine. Outcome measures was confirmation of STEMI diagnosis and determining the system delay.

Results. During the study period, a tentative diagnosis of STEMI was established in 1,061 patients, of whom 919 were triaged directly to the PCI centre. In 771 (84%) patients, a diagnosis of STEMI was confirmed. Patients transported less than 10 kilometres (km) had a mean system delay of 82 minutes. 553 (81%) were treated within 120 minutes of FMC, and a system delay of less than 120 minutes was achievable among 89% of patients living up to 95 km from the PCI centre.



Conclusions. The use of telemedicine for pre-hospital diagnosis and triage of patients directly to the cath. lab. is feasible and allows 89% of patients living up to 95 km from the invasive centre to be treated with PPCI within 120 minutes of the emergency medical service (EMS) call. The study confirms that a recommendation of a system delay less than 60 minutes is unachievable if FMC is EMS call.

**YIA SESSION I:
NEW ECG METHODS AND ANIMAL EXPERIMENTS**

Removing Ventricular Far Field Artifacts in Intracardiac Electrograms During Stable Atrial Flutter Using the Periodic Component Analysis – Proof of Concept Study

¹T.G. Oesterlein, ¹G. Lenis, ²A. Luik, ¹B. Verma, ²C. Schmitt, ¹O. Dössel

¹Institute of Biomedical Engineering, Karlsruhe Institute of Technology, Germany,

²Städtisches Klinikum Karlsruhe, Karlsruhe, Germany

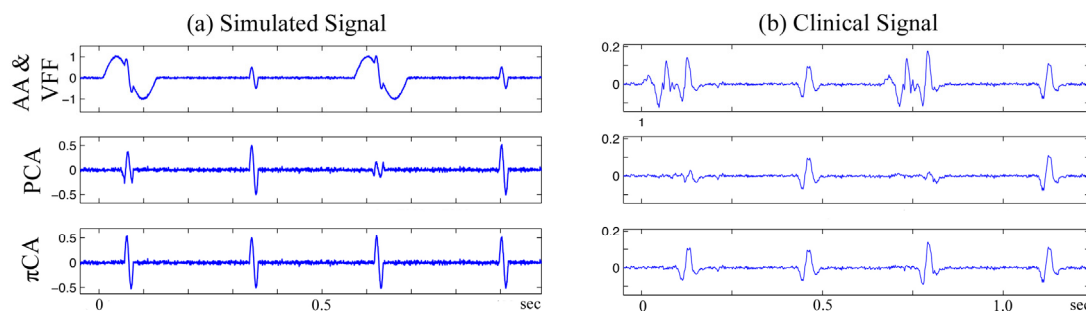
Email: publications@ibt.kit.edu

Keywords: intracardiac electrograms; ventricular far field; periodic component analysis; atrial flutter; signal processing.

Introduction. Intracardiac electrograms (EGM) provide useful information for diagnosing cardiac arrhythmias. However, even in bipolar EGM measured close to the mitral valve are frequently comprised by the ventricular far field (VFF) and thus atrial activity (AA) can be obscured. This work introduces the Periodic Component Analysis (π CA) for VFF removal in atrial flutter (AFlut). It is benchmarked against the common approach of Principal Component Analysis (PCA) using simulated data and demonstrated on a clinical case.

Methods and Materials. A total of 1200 AFlut signals with VFF and length 5 sec were simulated. Flutter cycle length was chosen 280 and 200 ms for 2:1 and 3:1 conduction, respectively. RR intervals were varied within the signals to mimic variability in AV conduction time. A time shift between VFF and AA was introduced to simulated recordings at different phases of the flutter circuit. White Gaussian noise was added to each signal. Measured clinical data was processed as proof of concept (65 year old female patient, AFlut after ablation for persistent AFib, bipolar filtered (30-250 Hz)). The concept of π CA was adapted to maximize the periodicity of the AA without the need of knowing its morphology and is robust against variability in RR.

Results. Initial average correlation coefficient (CC) between AA and the compromised signal was 0.3 ± 0.05 , and improved by π CA to 0.98 ± 0.003 . Applying PCA, average CC was 0.93 ± 0.05 (0.98 ± 0.003 to 0.90 ± 0.04 for non-/simultaneous AA and VFF, respectively). Power of VFF was reduced by π CA filtering by 99.6%. Application of PCA was shown to deform AA as depicted in the figure.



Removing VFF artifacts using PCA and π CA. Each signal contains four atrial activations with the first and third comprised by VFF. (a) Simulated signal. Filtering using PCA results in changes to AA morphology while it is retained when applying π CA. (b) Measured clinical signal with biphasic VFF preceding AA. Using PCA, every second AA complex is removed since it is synchronous to the VFF and thus violates the statistical independence assumed for PCA. π CA successfully retains AA morphology. Amplitudes given in mV, time in sec.

Conclusions. π CA was shown to successfully remove VFF artifacts (CC 0.98) by utilizing the stable dynamics of AFlut. PCA fails since the assumption of statistical independence of AA and VFF is violated. Recovering obscured AA using π CA was confirmed in a clinical case.

An Iterative Method for Solving the Inverse Problem in Electrocardiography in Normal and Fibrillation Conditions: A Simulation Study

N. Zemzemi

INRIA Bordeaux Sud-Ouest, Talence France

Email: nejib.zemzemi@inria.fr

Keywords: electrocardiography imaging; inverse problem; domain decomposition; bidomain model; ECG modelling.

Introduction. Electrocardiographic Imaging (ECGI) is a new imaging technique that noninvasively images cardiac electrical activity on the heart surface. In ECGI, a multi-electrode vest is used to record the body-surface potential maps (BSPMs). Then, using geometrical information from CT-scans and a mathematical algorithm we construct the electrical potentials on the heart surface. The reconstruction of cardiac activity from BSPMs is an ill-posed inverse problem. In this work, we present a new mathematical approach based on domain decomposition methods and test it on synthetically data generated using a human geometry.

Methods and Materials. The method splits the mathematical problem in two auxiliary problems: The first takes into account the measured potential and the second takes into account the non flux boundary condition on the torso surface. We use the finite element method obtained from a CT-scan of 43 year old women. The geometrical model takes into account, the heart, the lungs, the bones and the remaining tissue. In order to generate the potential data, we use our ECG simulator based on the bidomain model. We add 10% of noise to the generated BSPs and reconstruct the heart surface potential only from BSPs.

Results. In Figures A and B, we show two snapshots of reconstructed potential and compare them to the forward solution. Although, quantitatively, we obtain an error of 15% due to the fact that the noise does not satisfy the compatibility condition, we remark that the wave front is remarkably smoothed but correctly captured.

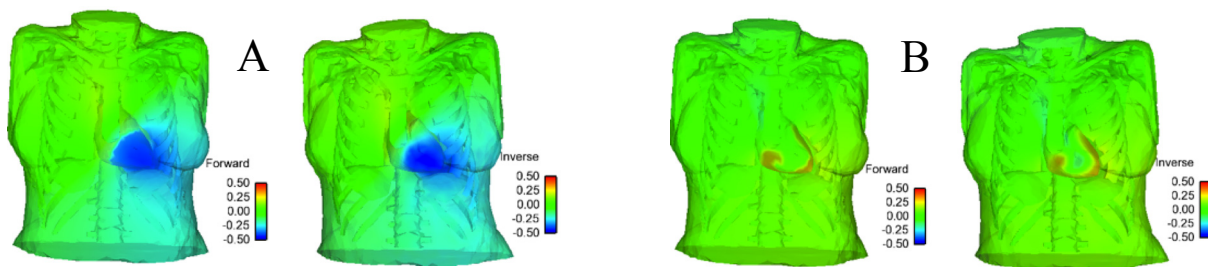


Figure: Comparison between the forward problem solution (first column) and the computed solution of the inverse problem (second column). A: a snapshot of the potential distribution in case of apex stimulations. B: a snapshot of potential distribution for re-entry case.

Conclusions. In this work we present a new approach for solving the ECGI problem based on domain decomposition techniques. The obtained results are very promising; the next step will be to test the accuracy of the method on real life measurements.

Respiratory Rate Simultaneous Estimation from Two ECG-Derived Respiratory Waveforms Using an Adaptive Frequency Tracking Algorithm

L. Mirmohamadsadeghi, J.-M. Vesin

Swiss Federal Institute of Technology Lausanne (EPFL), Lausanne, Switzerland,

Email: leila.mirmohamadsadeghi@epfl.ch

Keywords: Respiratory rate; adaptive frequency tracking, respiratory sinus arrhythmia.

Introduction. Monitoring the respiratory rate (RR) in a fast, inexpensive and continuous manner is of great interest as its direct measurement requires bulky, expensive and inconvenient equipment. In this study, the RR is estimated in an instantaneous manner from the electrocardiogram (ECG) using two ECG-derived respiratory waveforms and an adaptive frequency tracking algorithm.

Methods and Materials. Respiration influences cardiac signals and thus the ECG in several ways, two of which are of interest here: respiratory sinus arrhythmia (RSA), is the modulation of the ECG R-peak intervals by respiration, and R-peak amplitude modulation (RPA). In this study, a multi-signal oscillator-based band pass filter (W-OSC) is used to adaptively and simultaneously track the common instantaneous frequency component of the RSA and RPA waveforms, which is the RR. This frequency tracking algorithm is based on a band-pass filter whose central frequency is adaptively updated using signal-to-noise ratio weighting from the two inputs, the RSA and RPA waveforms.

Results. The algorithm is evaluated on the publicly available Physionet Fantasia dataset, which contains simultaneously recorded ECG and respiratory waveforms (2 hour recordings) from 20 young and 20 elderly subjects. The ECG-derived RR is compared to a reference computed from the respiratory signal. It was found that this algorithm is capable of estimating the RR with an average error of 8% and an average adaptation delay of 14s over the entire dataset. Furthermore, the combination of the RSA and RPA waveforms to estimate the RR outperformed using either one separately.

Conclusions. The presented algorithm tracks in real-time the instantaneous RR using two ECG-derived respiratory waveforms. It competes with the state-of-the-art in terms of accuracy, rapidity and convenience. It was shown that combining RSA and RPA waveforms is better than using either one alone.

Novel Method for Deriving Vectorcardiographic Leads Based on Artificial Neural Network

¹M. Vozda, ²T. Peterek, ¹M. Cerny

¹FEECS, Department of Cybernetics and Biomedical Engineering, VSB – Technical University of Ostrava, Ostrava - Poruba, Czech Republic

²IT4 Innovations, VSB – Technical University of Ostrava, Ostrava - Poruba, Czech Republic,

Email: michal.vozda@vsb.cz

Keywords: vectorcardiography; artificial neural network.

Introduction. Vectorcardiograms (VCG) are often used for features extraction and classification in electrocardiology. The VCGs are not usually directly measured in clinical practise but they are derived from a 12-lead electrocardiogram (ECG). There is usually used Kors regression-related transformation or inverse Dower transformation. This paper describes a new method of transformation of 12-lead ECG to VCG which is based on an artificial neural network (ANN). The Kors transformation, the inverse Dower transformation, and proposed transformation based on neural networks were compared and tested on 280 patients. Data were obtained from PTB Diagnostic ECG database.

Methods and Materials. Training and testing data were obtained as one averaged beat for each of the 280 patients in 15 leads (12 ECG and 3 VCG). Signals were normalized and all ECG signals were transformed by three independent neural feed-forward neural networks. Each neural network transforms 12 ECG leads to one VCG lead (X, Y or Z).

Accuracy of the transformation is determined by two parameters R2 and MSE. These two parameters were calculated between originally measured VCG signals and transformed signals for all methods and leads.

10-folds cross validation, which is commonly used for testing methods based on learning algorithms, was used for evaluating proposed method.

Results. The neural network has achieved the lowest error (MSE_x=0.0022; MSE_y=0.0022; MSE_z=0.0024) and the highest squared correlation (R_{2x}=0.884; R_{2y}=0.827; R_{2z}=0.890) compared with Kors transformation (MSE_x=0.0043; MSE_y=0.0034; MSE_z=0.0045; R_{2x}=0.869; R_{2y}=0.794; R_{2z}=0.880) and inverse Dower transformation (MSE_x=0.0052; MSE_y=0.0035; MSE_z=0.0056; R_{2x}=0.819; R_{2y}=0.788; R_{2z}=0.752).

Conclusions. In this paper we proposed new transformation method based on ANN. Proposed method achieved very good results in transformation of ECG to the VCG in comparison with standard approaches. We conclude that this improvement in accuracy of transformation may lead to more accurate features extracted from so-transformed VCGs in the future.

Modified Lewis ECG Lead System for Ambulatory Monitoring of Atrial Arrhythmias

¹A. Petrėnas, ¹V. Marozas, ²L. Sörnmo, ³G. Jaruševičius, ¹D. Gogolinskaitė

¹Biomedical Engineering Institute, Kaunas University of Technology,
Kaunas, Lithuania

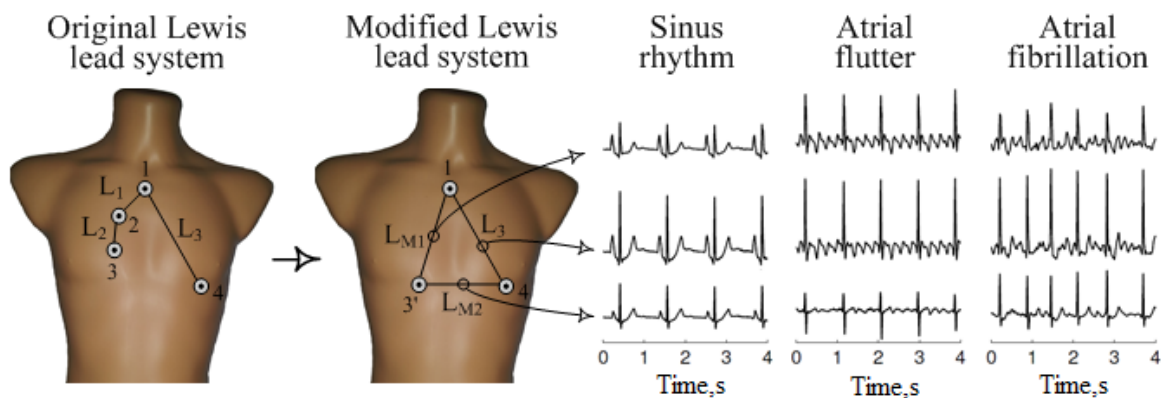
²Department of Biomedical Engineering, Lund University, Lund, Sweden

³Institute of Cardiology, Lithuanian University of Health Sciences, Kaunas, Lithuania
Email: andrius.petrenas@ktu.lt

Keywords: Atrial activity enhancement; ECG lead configuration; Lewis lead system.

Introduction. The analysis of atrial activity (AA) during atrial arrhythmias can be problematic when a reduced lead system is used due to low amplitude and susceptibility to noise. In such cases leads with larger AA amplitude is highly desirable. Despite that lead placement for AA enhancement was proposed many years ago by Sir Thomas Lewis, such placement requires that two electrodes are placed directly on the chest, and therefore hand movement artefacts may occur. Since such placement should be avoided in ambulatory applications, we propose a modified Lewis lead system with electrodes attached to areas with less muscles.

Methods. The modified Lewis lead system was designed by removing electrode 2 and moving electrode 3 one intercostal space downwards (from 4th to 5th) in order to increase the immunity to hand movements. The proposed configuration was compared to the original Lewis lead system in terms of the atrial-to-ventricular activity ratio (A_{AA}/A_{VA}) in each lead. Healthy volunteers and patients with atrial flutter and fibrillation participated in the study. The ratio A_{AA}/A_{VA} was computed for each subject by finding the mean peak-to-peak AA and VA amplitude in 10 consecutive ECG beats. The overall results are expressed as mean and two-sided confidence interval (95%).



Results. The results show that A_{AA}/A_{VA} increases in leads L₁, L₂ and L_{M1} regardless of rhythm type. The highest ratio A_{AA}/A_{VA} of 0.23 ± 0.07 was observed for the modified lead L_{M1}, while both leads of the original Lewis lead system (L₁ and L₂) showed similar performance of A_{AA}/A_{VA} (0.20 ± 0.05 and 0.21 ± 0.06), respectively.

Conclusions. This study suggests that the modified Lewis lead system produces higher A_{AA}/A_{VA} ratio than original Lewis system. This modification of lead system can be valuable in those cases of long term ambulatory monitoring when high atrial-to-ventricular activity ratio is required e.g. atria originating arrhythmias.

Body Surface Potential Mapping During Heart Hypertrophy Development in Infant Rats

A. Rasputina, I. Roshchevskaya

Laboratory of comparative cardiology, Komi Science Center, RAS, Syktyvkar, Russia

Email: nastyur@rambler.ru

Keywords: heart hypertrophy; depolarization; rats; ontogenesis.

Introduction. The goal of this work is to investigate age-specific alterations of heart ventricular depolarization in normotensive rats and in rats with inherited stress-induced arterial hypertension (ISIAH) to establish whether some signs of the ventricular hypertrophy caused by inherited arterial hypertension during postnatal ontogenesis are “visible” even at birth.

Methods and Materials. Body surface potential mapping (BSPM) was done in Wistar and ISIAH rats at the age of 1, 7, 17 and 30 days of postnatal ontogenesis.

Results. When analyzing BSPM maps of rats 3 phases of the ventricular depolarization were defined, and significant changes in durations of these phases in Wistar and ISIAH rats were determined. It was revealed that the duration of the ventricular depolarization in Wistar rats increased gradually from the 1st to the 30th day of postnatal ontogenesis and mostly on account of the middle phase. Duration of the ventricular depolarization in 1 day aged ISIAH rats was significantly larger than in Wistar rats of the same age, but it didn't change during the 1st month of postnatal ontogenesis and moreover it paradoxically decreased from the 1st to 17th day on account of the initial and terminal phases.

Conclusions. For the first time significant changes in the durations of the ventricular depolarization and its phases between normotensive and hypertensive rats of the same ages revealed by the using BSPM may be considered as initial markers of the ventricular hypertrophy that developed in ISIAH rats during the early postnatal ontogenesis.

The work is supported by the program of the basis investigations between UD and SD RAS.

Effect of the Repeated Global Ischemia and Reperfusion on the RR and QT Interval in Isolated Rabbit Heart

^{1,3}P. Veselý, ^{1,2}J. Halánek, ^{1,3}M. Ronzhina, ^{1,3}O. Janoušek,
^{1,3}J. Kolářová, ^{1,4}M. Nováková

¹International Clinical Research Center, St. Anne's University Hospital, Brno, Czech Republic,

²Institute of Scientific Instruments, Academy of Sciences, Brno, Czech Republic,

³Department of Biomedical Engineering, Brno University of Technology, Brno, Czech Republic

⁴Department of Physiology, Faculty of Medicine, Masaryk University, Brno, Czech Republic.

Email: p.vesely@fnusa.cz

Keywords: isolated rabbit heart; global ischemia; QT/RR coupling

Introduction. The experiments with isolated animal heart offer big advantage to create boundary conditions and monitor the heart response. This study was aimed to determine the QT/RR coupling during the repeated global ischemia and reperfusion.

Methods and Materials. The experiments were performed on 11 rabbits, divided into A (with voltage-sensitive dye di-4-anepss) and N (without di-4-anepss) groups. The experimental protocol consisted of preparatory stage (lasting 60 minutes) and experimental stage. The preparatory stage was dedicated to stabilization and voltage-sensitive dye application in case of group A. The experimental stage consisted of three phases of global ischemia (I) alternating with phases of reperfusion (R), each lasted 10 minutes. ECG in three orthogonal leads was continually recorded (2000 Hz, 16 bits) during the whole experiment. The position of R wave and the end of T wave were detected and manually corrected. The mean level of RR and QT intervals were computed from the window of 40 beats at the end of all phases. The absolute values of RR and QT intervals together with normalized values to the resting state (nRR, nQT) were analyzed.

Results. The mean±STD of RR and QT at the end of resting state over all experiments were 519±74, 204±18 and 345±23, 162±5 [ms] for group A and N respectively. The influence of ischemia or reperfusion on RR and QT intervals is described by the mean±STD of difference to the resting value (ΔnRR , ΔnQT) over all experiments.

	Group A		Group N	
	Ischemia	Reperfusion	Ischemia	Reperfusion
	mean ± std	mean ± std	mean ± std	mean ± std
ΔnRR	0,574 ± 0,371	0,062 ± 0,177	0,887 ± 0,282	0,008 ± 0,040
ΔnQT	-0,127 ± 0,094	-0,004 ± 0,064	-0,253 ± 0,117	-0,005 ± 0,053
$\Delta nQT/\Delta nRR$	-0,497 ± 0,540	0,644 ± 0,949	-0,305 ± 0,143	-0,213 ± 2,739

Conclusion. The relationship between RR and QT reverses with ischemia, i.e. QT intervals decrease with increasing RR. In addition, the heart response on the global ischemia is stronger for experiments without voltage-sensitive dye, as voltage-sensitive dye decreased the heart rate.

**YIA SESSION II:
ECG MARKERS FOR CARDIAC DIAGNOSTICS**

Vectorcardiographic Predictors of Ventricular Arrhythmia Inducibility in Patients with Tetralogy of Fallot

¹D. Cortez, ¹E. Ruckdeschel, ¹A.C. McCanta, ¹K. Collins, ²W. Sauer,
^{1,2}J. Kay, ²D. Nguyen

¹Children's Hospital of Colorado, Denver, USA

²University of Colorado Hospital, Denver, USA

Email: dr.danielcortez@gmail.com

Keywords: vectorcardiography; tetralogy of Fallot; ventricular tachycardia; inducibility.

Introduction. Vectorcardiographic (VCG) principles may provide additional clinical information to the 12-lead electrocardiogram (ECG). We hypothesize that some of these parameters may have predictive value on Tetralogy of Fallot (TOF) patients undergoing electrophysiology (EP) studies for ventricular arrhythmia (VA) inducibility.

Methods. A blinded retrospective analysis of 35 adult TOF patients undergoing EP studies prior to pulmonary valve replacements was performed (19 female patients, median age 37 years). VA inducibility and vectorcardiography were evaluated from electrophysiology studies and resting 12-lead electrocardiograms, respectively. Specifically, measurements of Q-T interval adjusted for heart rate (QTc), QRS duration, spatial QRS-T angle (peaks), principal T wave and principal QRS-complex component vectors (root mean square of the T-wave and QRS-complex vector components, respectively) were used to compare those with inducible VA versus those without inducible VA. A student t-test and Analysis of Variance were used to assess differences between those with and without sustained inducible VA and between the three groups, respectively (non-inducible vs monomorphic vs polymorphic VA patients). An odds ratio and relative risk were calculated for inducible VA.

Results. Of the 35 patients analyzed, 15 had inducible VA (>5 beat ventricular tachycardia) with 5 having monomorphic VA and 10 having polymorphic VA. 20 patients were not inducible. Principal QRS-complex vector components showed significant differences between those with and those without VA inducibility, $1.04 \pm 0.31 \text{ mV}$ vs. $1.45 \pm 0.48 \text{ mV}$ respectively ($p < 0.003$), with an Odds ratio of 19.44 (95% confidence interval (CI) 1.01 to 371.3) and relative risk of 1.51 (95% CI 1.09 to 2.10). No significant differences were found for the other parameters tested between these two groups. No inter-group variability existed between those with inducible monomorphic VT, as compared to those with inducible polymorphous VT and those without VA inducibility.

Conclusion. In this retrospective analysis of TOF patients undergoing EP studies, VCG evidence of depolarization differences was present between those TOF patients with and without inducible VA, while the QRS duration as well as all other parameters tested did not. This suggests that VCG may have a role in risk stratification for arrhythmias in TOF patients. Larger, prospective studies are needed to validate this method.

Advanced Interatrial Block Predicts Atrial Fibrillation Post Cavotricuspid Isthmus Ablation for Typical Atrial Flutter

**¹A. Enriquez, ¹J. Caldwell, ¹F. Sadiq Ali, ¹D. Conde, ¹W. Hopman,
¹D.P. Redfearn, ¹K. Michael, ¹H. Abdollah, ¹Ch. Simpson,
²A. Bayés de Luna, ¹A. Baranchuk**

¹Queen's University, Kingston, Canada

²Hospital de la Santa Creu i Sant Pau, Barcelona, Spain

Email: andresaep@gmail.com

Keywords: Interatrial block; atrial flutter; atrial fibrillation.

Introduction. A significant proportion of patients may develop atrial fibrillation (AF) following cavotricuspid isthmus ablation for typical atrial flutter (AFL). The aim of our study was to assess whether the presence of advanced interatrial block (IAB) is associated with a higher risk of AF after CTI ablation in patients with typical AFL and no prior history of AF.

Methods and Materials. We included patients with typical AFL and no prior history of AF referred to Kingston General Hospital for CTI ablation. Redo-ablations and patients without demonstration of bidirectional block were excluded. In all patients a post-ablation ECG in sinus rhythm was evaluated for the presence of advanced IAB, defined as a p-wave duration \geq 120 ms and biphasic morphology in the inferior leads. New-onset AF was identified from 12-lead ECGs, Holter monitoring and device interrogations.

Results. We included 122 patients. Mean age was 67 ± 10.6 years and 79.5% were male. Left atrial (LA) diameter was 42.8 ± 6 mm and ejection fraction was $55.8 \pm 11.2\%$. Advanced IAB was detected in 23% of the patients. Mean follow-up was 30.5 ± 15.3 months and 57 patients developed new onset AF (46.7%). In patients with advanced IAB the incidence of AF was 71.4% vs. 39.4% in those without advanced IAB (p 0.003). In a multivariate analysis, advanced IAB remained statistically significant (OR 2.9, 95% CI 1.02-8.6; p<0.04).

Conclusions. Advanced IAB is associated with a higher occurrence of AF after successful CTI ablation in patients with typical AFL and no prior history of AF.

**Interatrial Block is Associated with New-Onset Atrial Fibrillation
in Patients with Chagas Cardiomyopathy
and Implantable Cardioverter-Defibrillators**

**A. Enriquez, D. Conde, F. Femenia, A. Bayés de Luna, A. Ribeiro, C. Muratore,
M. Valentino, E. Retyk, N. Galizio, W.M. Hopman, A. Baranchuk**

Queen's University, Kingston, Canada
Email: andresaep@gmail.com

Keywords: Interatrial block; Chagas cardiomyopathy; atrial fibrillation.

Introduction. Chagas cardiomyopathy is an endemic disease in Latin America. A significant proportion of patients develop atrial fibrillation (AF), which may result in stroke and increased morbidity or mortality. Interatrial block (IAB) has been associated with the development of AF in different clinical scenarios. The aim of our study was to determine whether IAB can predict new onset AF in patients with Chagas cardiomyopathy and implantable cardioverter-defibrillators (ICDs).

Methods and Materials. We conducted a retrospective study of patients with Chagas cardiomyopathy and ICDs from 14 centers in Latin America. Demographics, clinical and device follow up were collected. Surface ECGs were scanned at 300 DPI and maximized x8. Semiautomatic calipers were used to determine P-wave onset and offset. Partial IAB was defined as a P-wave > 120 ms and advanced IAB as a P-wave > 120 ms with biphasic morphology (\pm) in inferior leads. AF events and ICD therapies were reviewed during follow-up by 2 independent investigators.

Results. A total of 80 patients were analyzed. Mean age was 54.6 ± 10.4 years, 52 (65%) were male. Mean left ventricular ejection fraction was $40 \pm 12\%$. IAB was detected in 15 patients (18.8%), with 8 (10.0%) partial and 7 (8.8%) advanced. During a follow up of 33 ± 20 months, 11 patients (13.8%) presented with new AF. IAB (partial + advanced) was strongly associated with new AF ($p < 0.0001$) and inappropriate therapy by the ICD ($p = 0.014$).

Conclusions. IAB (partial + advanced) predicted new onset AF in patients with Chagas cardiomyopathy and ICDs.

Dynamics of Heart Rate and Blood Pressure in Hypertensive Patients

¹I. Cotet, ²I. Kurcalte, ³C. Rezus, ⁴V.D. Moga, ⁴R. Avram, ⁵A. Szekely,
⁶M. Moga, ⁶F. Vidu

¹Emergency County Hospital Arad, Romania,

²Riga Stradins University, Riga Eastern Clinical University Hospital, Latvia

³University of Medicine and Pharmacy “Gr.T. Popa” Iasi, Romania,

⁴University of Medicine and Pharmacy “V. Babes” Cardiology Clinic Emergency
County Hospital Timisoara, Romania

⁵Emergency County Hospital Timisoara, Romania,

⁶IT Department of the of the Emergency County Hospital Timisoara, Romania

Email: moga.victor@gmail.com

Keywords: Hypertension; heart rate variability; nonlinear analysis; circadian rhythm.

Abstract. Hypertension represents an important condition that affects the adult population worldwide; it contributes significantly to morbidity and mortality from stroke, heart failure, coronary heart disease and renal failure. Although the pathogenesis of most hypertension is unclear, imbalance of the autonomic nervous system has been implicated in its development. Heart rate variability (HRV) has emerged as a practical, noninvasive tool to quantitatively investigate cardiac autonomic imbalance in hypertension. The aim of our study was to highlight the complex heart rate modulation in hypertension and to analyze the behaviour of RR intervals dynamics compared to normotensives subjects. Hypertensive patients have been monitored 24 hours using a combined ECG and ambulatory blood pressure monitoring system. ECG signals in sinus rhythm and blood pressure measurement have been recorded

Table 1. Alteration of the autonomic tone in hypertensive patients

	Hypertension + events	Control	p
Mean RR (ms)	827	741	0.005
SDNN (ms)	106	166	0.03
LF/HF	1.25	0.84	0.05
ApEn	0.98	1.20	Ns
DFA α 1	0.75	0.87	0.005

and analyzed. As expected essential hypertension is characterized by alteration of the autonomic tone, and probably those alterations are responsible for the arrhythmic events in relation with the worsening of the performance of the left ventricle (Table 1).

The most important aspect of this study is that even in the presence of early stages of essential hypertension, the autonomic tone mechanisms involved in the outcome and prognosis of those patients are detectable by noninvasive methods. Beside the now consecrated well known heart rate variability parameters, it seems that new parameters like Δ HR (b/min) and Δ SBP (mmHg) can offer data related to the involvement of the circadian rhythm in hypertension (Fig. 1).

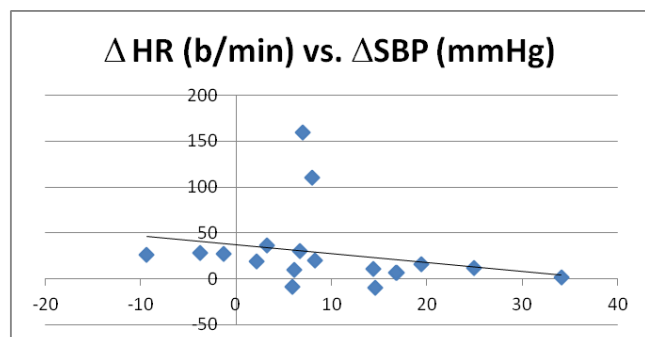


Fig.1. The relation between Δ HR (b/min) and Δ SBP (mmHg)

ECG DIAGNOSTICS OF CARDIAC DISEASES

Computer Simulation of the Electric Activity of the Heart. A Multi-Scale Approach

J.F. Rodriguez

Univeristy of Zaragoza, Zaragoza, Spain

Email: jfrodri@unizar.es

Introduction. The electrophysiology problem posses a big challenge, not only because of the structural complexities inherent to the heart tissue, but also because of the complex electric behavior of the cardiac cells. Solving the electric activity of the heart requires an enormous effort of data integration for generating a suitable model for simulation.

Methods and Materials. A suitable model incorporates substructures and specialized subsystems of the heart, namely the atria, the ventricles, the sino-atrial node, the atrio-ventricular node, the His bundle and the Purkinje fiber system, and will also include an anatomically accurate description of the human torso in which the heart is embedded. The resulting model will be of multi-scale nature (ranging from the microscopic ionic channels to the surface ECG). The multi-scale nature of the electrophysiology problem (time constants for the different kinetics ranging from 0.1 to 500ms) makes difficult its numerical solution, requiring temporal and spatial resolutions of 0.1ms and 0.2mm respectively for accurate simulations, leading to models with millions degrees of freedom that need to be solved for thousand time steps. Solution of this problem requires the use of algorithms with higher level of parallelism in multi-core platforms. In this regard the newer programmable graphic processing units (GPU) has become a highly parallel, multithreaded, many-core processor with tremendous computational horsepower.

Results and Conclusions. This paper presents results obtained with a novel electrophysiology simulation software entirely developed in CUDA. The software implements fully explicit and semi-implicit solvers for the mono-domain model, using operator splitting. Performance is compared against classical multi-core MPI based solvers operating on dedicated high-performance computer clusters. Results obtained with the GPU based solver show enormous potential for this technology not only for research but also for clinical application due to its efficiency and lower hardware cost. The versatility of in-silico simulations is demonstrated on two applications: simulation of acute regional ischemia in the human heart, and the study of heart variability.

**Brugada or Early Repolarization in V₁ V₂ V₃.
Can VCG Aspects Differentiate the Localization of ECG Manifestations ?**

C.A. Pastore, N. Samesima. E. Kaiser, H.G. Pereira Filho

Heart Institute (InCor) – Hospital das Clínicas da Faculdade de Medicina da USP,
São Paulo, Brazil

Email: ecg_pastore@incor.usp.br

Keywords: vectorcardiography; differential diagnosis; J-point; early repolarization syndrome; Brugada syndrome.

Introduction. Electrocardiographic aspects found in Brugada (BrS) and early repolarization (ERS) syndromes may hinder the diagnosis, especially when these findings are located in the anteroseptal region of the rest-ECG (V₁-V₃). Vectorcardiography (VCG) can be useful to differentiate between the two syndromes, both through visual characteristics of vector loops and quantification of certain measurements. The objective of this study was to define BrS and ERS characteristic and distinctive patterns, using aspects of the QRS complex loops and ST segments.

Methods. S[∧]J-point of vectorcardiographic loops, obtained in the horizontal plane (HP), of 29 BrS patients and 30 individuals with ERS were analyzed. The J-point resulting vector was obtained by the lack of coincidence between the QRS complex starting point and its end. We measured the angle of this resulting vector in PH and compared its value between groups. Nonpaired t-test and the ROC curve were used, with P ≤ 0.05 significance level.

Results. Men age was 47±15 vs 38±14 y.o. (p=0.02), 66% vs 90% male (p=0.03); QRS duration was 101.6±10.2 vs 94.9±12.5ms (p=0.03); mean S[∧]J-point was 103.4±18.9 vs 54.5±16.3° (p<0.0001), BrS vs ERS, respectively. S[∧]J-point>75° cut-off value as obtained by ROC curve better identified BrS, with 96.6% sensitivity and 93.3% specificity.

Conclusions. S[∧]J-point, as assessed by vectorcardiography can differentiate between the two syndromes with high sensitivity and specificity levels when above 75°.

CT Angiography Ellucidates Venous Anatomy Supporting Electrophysiologic Substrate Ablation in Patients with Congenital Heart Disease

Ch.W. Shepard, H. Roukoz, P. Dorostkar

University of Minnesota, Minneapolis, MN, USA

Email: pcd@umn.edu

Keywords: Congenital heart disease; ablation; CT angiography.

Introduction. Congenital venous anomalies or surgically redirected venous flow can predispose the development of substrates that cause tachycardia(s), which can be challenging to ablate. Anomalous venous drainage has been associated in patients with single ventricle physiology, Transposition of the great arteries, Heterotaxy syndromes or can be seen as isolated findings of the vena cavae or coronary sinus.

Methods and Materials. We describe a case series where CT angiography (CTA) defined detailed venous anatomy that was incompletely defined by echocardiography. More detailed definition of the anatomy and flow supported successful ablation. Prospective ECG-gated, breath-hold Flash CTA of the chest was performed with 80 – 100 KV care dosing to reduce patient radiation exposure. Images underwent post-processing on a Voxar 3D visualization system. Carto maps created during the electrophysiology study (EPS) were super-imposed over the 3D CT reconstruction of the heart during the study.

Results. Seven patients with congenital heart disease (ages 6-33 years) underwent EPS and ablation of the underlying substrate. A CTA was obtained to define the venous anatomy and its relationship to the atria prior to the electrophysiology study. Congenital heart disease diagnoses included: Transposition of the great arteries in 3 patients, Heterotaxy in one patient, double inlet left ventricle in one patient, left superior vena cava to coronary sinus one patient, and middle cardiac vein anomaly in one patient. The CT demonstrated abnormalities of the vena cavae in 5 of 7 and of the coronary sinus in 2 of 7 patients. In 2 of seven patients the clinical tachycardia consisted of an accessory pathway and in 5 patients there were one or more atrial tachycardias. The accessory pathway was ablated in 1 and modified in the other patient. Multiple atrial tachycardias were successfully ablated in 3 of 5 patients, modified in one patient and not ablated in one patient due to non-inducibility. The ablation approach with regards to type, energy delivery and duration of ablation was gated, incorporating data from the CT angiogram, facilitating successful ablation.

Conclusions. CTA of the heart in patients with congenital heart disease can delineate and define anatomical structures that support expression of tachycardia in the young. It can help guide altered or unusual ablation strategies due to improved understanding of unique anatomy and flow dynamics. This diagnostic test can be used as an adjunct for planning, reconstruction and subsequent successful ablation of the substrate(s) that support tachycardia in young patients with congenital heart disease.

ECG Patterns and Genotypes in Pediatric Patients with Channelopathies. 7-Year Experience in Slovakia

V. Illikova, P. Hlivak, E. Balazova, R. Hatala

Depts. of Arrhythmias and Pacing and ICU, Children's Cardiac Center and National
Cardiovascular Institute, Bratislava, Slovakia
Email: illikova@dkc-sr.sk

Keywords: channelopathy; genetic testing; children.

Introduction. Primary genetic arrhythmias or channelopathies are associated with mutations of genes encoding proteins creating or interacting with the specialized ion channels in the myocardial cell membranes. The resulting increased or decreased ion channel function forms the arrhythmogenic substrate predisposing the patient with structurally normal heart to sudden cardiac death (SCD) on the basis of ventricular tachycardia or fibrillation. The study focuses the clinical and ECG presentation and management of children with channelopathies in Slovakia.

Materials and Methods. 18 children (aged from neonatal to 18 years) with suspected primary genetic arrhythmia were admitted to Children's Cardiac Center Bratislava in the years 2007 - 2013. Twelve patients were symptomatic (chest pain, syncope, aborted SCD).

Results. In 10 of 18 children the underlying channelopathy was genetically proved: in 7 patients syndrome of long QT interval was found (KCNQ1 gene mutation in 3, KCNH2 in 2 and SCN5A in 4, 2 children had more than one mutation) and in 3 patients catecholaminergic polymorphic ventricular tachycardia (CPVT, RyR2 mutation). The remaining patients are in the process of genetic testing or haven't been tested yet, 4 of them with obvious symptoms of primary genetic arrhythmia. Sixteen children are treated with betablockers, 2 of them (with SCN5A gene mutation) in combination with mexiletine, 4 patients received implantable cardiac defibrillator (ICD) and one underwent left cardiac sympathetic denervation. None of the treated patient died, one girl died before treatment was initiated and 1 boy has neurologic disability after cardiopulmonary resuscitation. In 2 of 4 patients with ICD the appropriate shock was delivered.

Conclusions. Early diagnosis of channelopathies allows for the adequate treatment and lifestyle modification (avoidance of specific triggers of arrhythmic events). Genetic testing is important both for the optimal management of the patient and of the family.

Brugada Phenocopy: Update 2014

A. Baranchuk, B. Gottshalk, D. D. Anselm

Division of Cardiology, Electrophysiology and Pacing, Queen's University, Kingston
General Hospital, Kingston, Ontario, Canada
Email : barancha@kgh.kari.net

Keywords: Brugada Syndrome, Brugada Phenocopy, Genetics, Ion Channels

Brugada Phenocopies (BrP) continue to emerge as clinical entities that are distinct from true congenital Brugada Syndrome (BrS). BrP are characterized by type 1 and type 2 Brugada ECG patterns in leads V1-V3; however, BrP are elicited by various underlying associated conditions. The term Phenocopy was chosen because it was previously used to describe an environmental condition that imitates one produced by a gene; therefore, it served as a reasonable and succinct description for all acquired Brugada-like ECG manifestations

The diagnostic distinction between BrP and true congenital BrS focuses on a few key features. The first is that patients with BrP have a reversible underlying condition such as adrenal insufficiency, hypokalemia, or myocardial ischemia which elicits the Brugada ECG pattern. Once this underlying condition resolves, there is normalization of the ECG. Second, patients with BrP have a low clinical pretest probability of true BrS as opposed to a high pretest probability in patients with true BrS. Third, patients with BrP have a negative provocative challenge with a sodium channel blocker, while those with true BrS have a positive provocative challenge. It is also desirable that patients with BrP present with negative genetic alterations associated with BrS.

In this update, we review the progress made to-date regarding BrP, discuss areas of ongoing controversy, and identify opportunities for further investigation including the development of an international registry in order to evaluate the natural history of this entity.

CARDIAC ELECTROPHYSIOLOGY

Effects of Echinochrome on Ventricular Repolarization in Acute Ischemia

^{1,2}K. Sedova, ¹O. Bernikova, ¹S. Kharin, ¹D. Shmakov

¹Laboratory of Cardiac Physiology, Institute of Physiology of the Komi Science Centre of the Ural Branch of the Russian Academy of Sciences, Syktyvkar, Russian Federation,

²Department of Biomedical Engineering, Czech Technical University, Kladno, Czech Republic

Email: sedova.ks@gmail.com

Keywords: cardiac electrophysiology; repolarization; ischemia; antioxidant; animal model.

Introduction. Ischemia-related processes, including electrophysiological alterations, are associated with the generation of reactive oxygen species. Although the cardioprotective action of antioxidants against ischemic injury has been proposed, their electrophysiological effects are not clear. The aim of this study was to investigate the effects of the antioxidant Echinochrome on ischemia-induced alterations of ventricular repolarization in a feline model of coronary occlusion.

Methods and Materials. Experiments were performed on open-chest anesthetized adult cats. Activation-recovery intervals were measured from 64 ventricular epicardial unipolar electrograms recorded simultaneously before and during ligation of the left anterior descending coronary artery. Synthetic Echinochrome was infused five minutes before coronary occlusion in two different doses (1.0 mg/kg and 2.0 mg/kg, i.v.).

Results. Pre-occlusion administration of Echinochrome in a dose of 1.0 mg/kg resulted in the reduction of ischemia-induced shortening of activation-recovery intervals and the restricted increase in the repolarization dispersion during 30 minutes of ischemia. Echinochrome in a dose of 2.0 mg/kg demonstrated a more pronounced effect.

Conclusions. Ability of the antioxidant Echinochrome to decrease ischemia-induced alterations of ventricular repolarization was demonstrated in a feline model of coronary occlusion. A dose-dependent effect was suggested. This study was supported by the Ural Branch of the Russian Academy of Sciences (project No. 12-C-4-1009). Synthetic Echinochrome was provided by the G.B. Elyakov Pacific Institute of Bioorganic Chemistry of the Far Eastern Branch of the Russian Academy of Sciences (Vladivostok, Russian Federation).

**Antiarrhythmic Potential of Hypolipidemic Drugs
in Acute Ischemia/Reperfusion:
Molecular Mechanisms of Pleiotropic Lipid-Independent Effects**

¹T. Ravingerová, ¹S. Čarnická, ¹V. Ledvényiová, ¹M. Nemčeková, ²T. Rajtík,
³E. Barlaka, ¹I. Gablovský, ²A. Adameová, ³A. Lazou

¹Institute for Heart Research, Slovak Academy of Sciences, Centre of Excellence SAS
NOREG, Bratislava, Slovak republic

²Department of Pharmacology and Toxicology, Faculty of Pharmacy, Comenius
University, Bratislava, Slovak republic

³School of Biology, Aristotle University of Thessaloniki, Thessaloniki, Greece
Email: usrdravi@savba.sk

Keywords: ischemia/reperfusion injury; arrhythmias; hypolipidemic drugs; pleiotropic effects; preconditioning.

Introduction. Hypolipidemic drugs (statins and fibrates) confer preconditioning-like protection against cardiac ischemia/reperfusion (I/R) injury far beyond their lipid-lowering capacity. Molecular mechanisms of pleiotropic (non-lipid) effects are currently under investigation. We found that short-term pretreatment of rats with simvastatin rendered them more resistant to ischemia- and reperfusion-induced arrhythmias without decreasing lipid levels. Protection against I/R was associated with antiapoptotic effects and up-regulation of nuclear peroxisome proliferator-activated receptors (PPAR- α). To get further insight into molecular mechanisms that underlie PPAR- α -mediated cytoprotection, we aimed to explore the effects of PPAR- α activation and its potential downstream pathways, on the occurrence of malignant ventricular arrhythmias and infarction size (IS) in a setting simulating „delayed“ preconditioning.

Methods and Materials. Rats were given PPAR- α agonist WY-14643 (WY, 1 mg/kg, i.p.) with or without PPAR- α antagonist MKK-886, 24 hr prior to 30-min global ischemia/2-h reperfusion in Langendorff-perfused hearts. Sampling for PPAR- α expression, its target genes of fatty acids (FA) (MCAD, PDK-4, mCPT-1) and glucose (GLUT-4) metabolism, heme oxygenase-1 (HO-1) as a key antioxidative enzyme (real-time RT-PCR), as well as for determination of survival proteins (Akt, eNOS) and markers of apoptosis (Bax, Bcl-2, caspase-3) was performed before and after I/R (Westernblotting).

Results. WY suppressed ectopic activity, duration and severity of ventricular tachyarrhythmias, and reduced IS. Protection was reversed by MKK indicating a PPAR- α -dependent response, and blunted by NO synthase inhibitor L-NAME. Administration of WY up-regulated PPAR- α and its target FA genes, increased gene expression of HO-1 and protein levels of phospho-Akt and eNOS. Changes in pro/antiapoptotic markers (enhanced Bcl-2/Bax, reduced caspase-3 cleavage) were also observed in the WY-treated hearts.

Conclusions. Up-regulation of PPAR- α metabolic genes regulating FA oxidation may underlie delayed protection in the rat heart. Potential non-genomic effects of PPAR- α -mediated cardioprotection may involve activation of PI3K/Akt-eNOS-NO pathway and modulation of oxidative stress and apoptosis.

Grants APVV-LPP-0393-09, APVV-0102-11.

Can We Prevent Malignant Arrhythmias by Targeting of Cardiac Connexin-43 ?

¹N. Tribulova, ¹B. Bacova, ¹T. Benova, ¹C. Viczenczova, ^{1,2}J. Radosinska,
³V. Knezl, ¹J. Slezak

¹Institute for Heart Research, SAS, Bratislava, Slovakia,

^{1,2}Department of Physiology, Fac. Med., Comenius University, Bratislava, Slovakia,

³Institute of Experimental Pharmacology and Toxicology, SAS, Bratislava, Slovakia

Email: narcisa.tribulova@savba.sk

Keywords: Connexin-43, ventricular fibrillation prevention

Introduction: Rapid spreading of the electrical impulse throughout the heart is essential for synchronized contraction that is ensured by electrical coupling of cardiomyocytes at the connexin (Cx) channels. Heart disease-related abnormal myocardial Cx43 distribution, expression and/or phosphorylation impairs coupling and facilitates development of re-entry arrhythmias. We hypothesized that cardioprotective compounds such as atorvastatin (ATO), melatonin, omega-3 FA and red palm oil (RPO) may affect Cx43 and protect from malignant arrhythmias.

Methods and Materials: Experiments were conducted on male rats that were: 1/ spontaneously hypertensive (SHR) without or with intake of omega-3 FA (300mg/day/2month), melatonin (400µg/day/6 weeks) or RPO (200mg/day/6weeks); 2/ hereditary hypertriglyceridemic (HTG) without or with ATO (1.5mg/day/2mth) and omega-3 FA treatment; 3/ hyper- (TH) and hypo-thyroid (HY) without and with RPO intake, as well as age-matched Wistar rats. Basic characteristics of animals were registered and left ventricular tissue was examined for myocardial ultrastructure and Cx43 using immunofluorescence, immunoblotting and real-time PCR. El.-induced sustained ventricular fibrillation (sVF) was examined using isolated perfused heart.

Results: Compared to Wistar rats the incidence of sVF was significantly higher in SHR, HTG and TH rat hearts that exhibited abnormal distribution and down-regulation of Cx43, while sVF was not induced in HY rat hearts with up-regulation of Cx43. Treatment of SHR, HTG and TH rats with either compounds resulted in protection from sVF that was associated with attenuation of Cx43 abnormalities and improvement of integrity of cardiomyocytes.

Conclusions: Results point out antiarrhythmic effect of atorvastatin, omega-3 FA, melatonin and red palm oil due to, at least in part, modulation of myocardial Cx43. Further studies should elucidate pathways involved in Cx43 modulation by these compounds.

This study was supported by VEGA 2/0046/12, 1/0032/14 and APVV-0348-12 grants.

The Influence of Omega-3 Fatty Acids on Permanent Light-induced Myocardial Alterations and Decrease of Ventricular Fibrillation Threshold in Hypertensive Rats

¹T. Benova, ²J. Radosinska, ¹C. Viczenczova, ¹B. Bacova, ³J. Zurmanova, ⁴V. Knezl, ⁵M. Zeman, ⁶B. Obsitnik, ¹N. Tribulova

¹Institute for Heart Research, SAS, Bratislava, Slovakia,

²Inst. Physiology, Med. Fac. Comenius Univ., Bratislava, Slovakia

³Dept. of Physiology, Faculty of Science, Charles University, Prague, Czech Republic

⁴Institute of Exper. Pharmacol. & Toxicol., SAS, Bratislava,

⁵Faculty of Natural Sciences of Comenius Univ., Bratislava

⁶Abbott Laboratories, Slovakia

Email: tamara.benova@savba.sk

Keywords: arrhythmias; Omacor; hypertension; connexin-43.

Introduction. Male spontaneously hypertensive (SHR) and age-matched normotensive Wistar rats were housed under standard 12h light/12h dark cycle or exposed to 24h continuous light/day for 6 weeks. Half of them received Omacor (omega-3 ethyl ester, 25g/kg diet). Left ventricular tissue was used to determine transcription of electrical cell-to-cell coupling protein, connexin-43 (Cx43), pro-inflammatory NFkB and iNOS using real-time PCR. Western blotting was used for protein expression of Cx43 and PKCε. Electrically induced ventricular fibrillation (VF) was examined using isolated perfused heart by Langendorff.

Results. Continuous light caused mild elevation of BP in normotensive and enhanced it in SHR as well as decreased threshold to induce VF in both groups comparing to rats under normal light cycle. Myocardial Cx43 mRNA level was not altered, but Cx43 protein and its functional phosphorylated forms (which affect electrical coupling) were decreased in SHR due to continuous light and partially restored by Omacor. Treatment with Omacor also attenuated of continuous light-induced increase of myocardial iNOS and NFkB that are known to down-regulate Cx43. In parallel, the intake of Omacor increased threshold to induce VF.

Conclusions. Findings indicate that continuous light itself affects Cx43 channels-mediated cardiac cell-to-cell communication and enhances propensity of hypertensive rats to malignant arrhythmias. These adverse effects can be, partially, eliminated by treatment with Omacor.

This work was supported by VEGA 2/0046/12, SK-CZ-0027-11 and SKS grants.

MODELING IN ELECTROCARDIOLOGY

Computer Modeling to Understand the Failing Heart

^{1,2,3}M. Potse

¹Center for Computational Medicine in Cardiology, Università della Svizzera italiana,
Lugano, Switzerland

²Carmen Team, Inria Bordeaux Sud-Ouest, Bordeaux, France

³LIRYC-Institute of Cardiac Rhythmology and Modeling, Bordeaux, France
Email: mark.potse@usi.ch

Keywords: Heart failure; left bundle branch block; ventricular conduction disorders; computer models.

Introduction. The best way to study a complex system is not by taking it apart and studying its components, but by attempting to put it together from components that are well understood. We are using this approach to improve our understanding of conduction disturbances in the failing heart. Heart-failure patients generally suffer from conduction disturbances that are often qualified as Left Bundle Branch Block. However, there is evidence that in some of these patients the left bundle itself is intact, and that in most patients conduction disturbances in the working myocardium play an important, if not a pivotal role. Detailed knowledge of the cause of the delayed conduction may be important to predict success or failure of treatments such as cardiac resynchronization therapy.

Methods and Materials. With ECG analysis alone, and even with electroanatomical mapping alone, it is not possible to characterize the problems in individual patients precisely. Therefore we are investigating the opposite approach. We use detailed, patient-tailored numerical models of individual patients with which we predict, based on hypothesized pathologies, the ECG, ventricular activation order, and morphologies of endocardial catheter electrograms. These predictions are compared with measured results to determine which hypothesis is the most likely in a given patient.

Results. Results in the first two patients show a correlation of 91% and 86%, respectively, between measured and simulated activation times. Visually matching ECG waveforms and a matching QRS duration were obtained. The results of parameter optimization suggest a wide variety of mechanisms, including early left-ventricular breakthroughs, scar-related block, and slow conduction suggestive of cardiomyopathy. In both patients, assuming re-entry in the left-ventricular Purkinje network worsened the match.

Conclusions. It is feasible, though presently still very time-consuming to parameterize a heart-torso model with patient-tailored geometry to the ECG and left-ventricular activation sequence of an individual patient. Initial results suggest that abnormal conductivity in the left-ventricular working myocardium plays a role in these patients.

The Impact of Action Potential and Conduction Velocity Distribution Changes on Markers of Repolarization Dispersion

¹G. Kozmann, ¹G. Tuboly, ²V. Szathmáry, ³J. Švehlíková, ³M. Tyšler

¹Department of Electrical Engineering and Information Systems, Faculty of Information Technology, University of Pannonia, Veszprém, Hungary,

²Institute of Normal and Pathological Physiology, Slovak Academy of Sciences, Bratislava, Slovakia,

³Institute of Measurement Science, Slovak Academy of Sciences, Bratislava, Slovakia
Email: kozmann.gyorgy@virt.uni-pannon.hu

Keywords: Repolarization dispersion; Action potential duration; Activation conduction velocity; Numerical heart model; Non-dipolarity index.

Introduction. A necessary prerequisite of malignant arrhythmias is the elevated repolarization dispersion (RD) of the ventricular myocardium. In this study, RD properties characterized by simulated QRST integral maps and by the non-dipolarity index (NDI) were analyzed as a function of action potential duration (APD) and activation conduction velocity (CV) distribution.

Methods and Materials. A five-layer numerical ventricular model was used with adjustable intramural APD and CV modulation features. In the simulations transmural gradient (TG) of epicardial and endocardial layers was defined as $APD_{\text{epi}} - APD_{\text{endo}}$. However, while keeping TG constant, different intramural APD profiles were allowed. Similarly, different CV values were allowed, expressed in the ratio of modelling distance unit and modelling time unit (mdu/mtu). Finally, realistically shaped inhomogeneous torso model was used to compute the QRST integral maps and NDIs.

Results. In our reference case the TG was -15 mtu, yielding an NDI of 0.16. The TG (i.e. APD profile) was systematically changed in the apical part of the ventricular model from -15 mtu up to +14 mtu in five steps, while the CV distribution was kept identical (i.e. CV was 3 mdu/mtu in the endocardial layer and 1 mdu/mtu in all the other layers) both in the apical part of the ventricle and in the rest of the model ventricle. APD modulation in this case increased NDI from 0.16 up to 0.76 in a non-linear way. In the second modelling phase APD modulations were repeated identically, but CV was set 2 mdu/mtu in the endocardial layer, and 0.5 mdu/mtu in the other apical layers. NDI maxima and minima due to the combined APD and CV modulations did not change, however the TG of the maximal NDI shifted in the direction of positive TGs.

Conclusions. NDI is primarily affected by the TG value. The impact of intramural APD maxima/minima on RD was negligible. The impact of decreasing CV on NDI was modest while TG was negative (i.e. close to the normal APD distribution), the maximal NDI was obtained when the TG was positive.

Constraints in the Inverse Problem of Electrocardiography

A. van Oosterom

Radboud University Nijmegen; Nijmegen, The Netherlands

Email: avo-linden@hom.nl

Keywords: inverse problem; constraints regularization; selecting regularization type and weight.

Introduction. The inverse problem of electrocardiography deals the estimation of the electric sources of the heart on the basis of voltage differences observed at some distance from the sources. The spatial nature of the observed signals may be viewed a maps, as can be the solutions of the inverse problem. Accordingly solving the inverse problem is known as electrocardiographic imaging. This report deals with demonstrating the effect of some different types of constraints that are essential in the imaging and finding their optimal weights.

Methods and Materials. The analyses was based on a set of 65 body surface potentials recorded on a healthy, young, male subject. The matching, MRI derived, geometry comprising the thorax, the lungs and the myocardium was used for setting up a numerical version of an inhomogeneous volume conductor. The transmural potential at the surface bounding the ventricles was estimated by means of dedicated software. This included the timing of local depolarization and repolarization. The resulting potential field on the epicardium and both endocardia was taken to serve as a gold standard, a reference that is not available in such detail from experimental data. The major different regularization methods tested were, zero- and second order Tikhonov and the truncated SVD based inverse, in the imaging of epicardial and endocardial potential fields.

Results. Second order Tikhonov regularization proved to be superior to both other variant tested. The location of the maximum curvature in the norm of the regularized solution as a function as a function of the norm of the residual difference was tested. It was found that, instead using the norm of the (regularized) solution, the size of downslope of the electrograms was a better indicator in setting the weight assigned to the regularization.

Conclusions. The main conclusion drawn from this analyse is that the quality of the development of imaging depends on the availability of electrophysiologically sound limits of the main features of the solution (like amplitude and slope).

Examples are the imaging of the potential field on the surface closely encompassing the heart (pericardium) on the basis of observed body surface potentials and the imaging the timing of activation and/or recovery of the myocardium. More invasive variants involve the imaging of the potential field and/or the activation timing on the endocardium on the basis of signals observed at up to 64 simultaneously recorded at electrode arrays (balloon or basket) introduced in intra-cavitary space. The methodology in all of these imaging applications rests on the same physical principles. At the same time they all suffer from the same fundamental limitations set by the nature of the diverging nature of the spreading out of the electric currents, i.e. the electric volume conduction effects in the electrically passive properties of the body tissues (or the blood inside the cavities) that link the observations to the electric sources of interest. As a consequence, generally the image quality is poor. Over the years, different methods for improving image quality have been proposed and tested. These amount to imposing prior constraints on the solutions, based on electrophysiological knowledge on the source properties as obtained in invasive studies. These constraints are combined with the expression formulating the transfer from source to observations (the forward problem). This leaves the inverse problem (imaging) to be solved by means of numerical techniques. In the field of linear algebra used to solve the ensuing expression the incorporation of the constraint is referred to as finding a regularized solution. The influence of the constraint can be influenced by weighing it numerically. Clearly, it too much weight is assigned to the constraint the solution found may agree well with the prior, but not to the true solution.

Inverse Localization of Pacing Sites on Heart Surface from 12 Lead Measurements and CT Imaging of Partial Torso

¹J. Coll-Font, ²B. Erem, ³P. Stovicek, ¹D.H. Brooks

¹B-SPIRAL group, ECE Dept., Northeastern University, Boston, USA, ²Boston Children's Hospital, Boston, USA,

³Charles University Hospital, Prague, Czech Republic
Email: jcollfont@ece.neu.edu

Keywords: inverse problem; cardiac imaging; electrophysiology.

Introduction. Cardiac electrical imaging from body surface potentials is a technology with great potential for pre-procedure planning in the context of ventricular ablation. Two clinically desirable features are localization of endocardial pacing sites and reduced dependence on anatomical imaging. We recently reported results which achieved those objectives using 120 body surface electrodes but with CT imaging of the thorax only at the level of the heart. Here we report on a study extending that method by only using measurements from the 12 lead configuration.

Methods and Materials. Prior to a pace mapping procedure, limited axial X-Ray CT images of the volume containing the subject's heart were acquired. These images were then used to fit a generic model of the torso and joint epicardial-endocardial ventricular "heart surface", from which a mathematical forward model relating heart and body surface potentials was obtained. Pacing sites were localized with the CARTO system and body surface potentials recorded with 120 electrodes. Our inverse technique was applied to reconstruct QRS potentials on that heart surface using only 9 electrodes chosen to mimic the 12 lead ECG, and pacing sites estimated from the reconstructed potentials were compared to CARTO locations.

Results. We will report results for 2 subjects in a total of 76 locations across both ventricles (results for one subject are shown in Table 1). For each pacing the cardiac potentials were reconstructed using the standard 12 configuration and compared to results using the full set of 120 leads. Mean and standard deviation of the localization errors at each pacing site are reported in the table for both the 120 lead and 12 lead measurements. For each pacing site, we also tested for significant differences between the two mean localization errors (12 vs 120 leads) using a two-tailed t-test.

Conclusions. The 12-lead localization results generally showed a statistically significant, but small, increase in error. Surprisingly, at some sites the error decreased on average, which we believe may be due to not using the leads located in regions with higher geometric errors (i.e., farther from the region where imaging was performed).

Table 1. Comparison of location errors for one subject. Columns indicate (#) number of beats, error for full lead set and error for 12 lead configuration.

	#	full	12	#	full	12
LV						
	33	38±3	39±7	35	28±4	23±6
	35	40±0	27±18	38	29±6	47±0
	15	24±13	33±4	38	33±11	52±10
	32	38±0	44±5	11	20±12	21±10
	34	38±1	38±2	34	39±9	49±15
	35	55±17	48±6	15	16±4	44±7
	23	35±6	51±6	22	31±16	45±15
RV						

Noninvasive Localization of Ectopic Activation Using BSPM and CT-Based Torso Model

^{1,2}M. Tysler, ¹J. Svehlikova, ^{2,3}O. Punshchykova, ²P. Kneppo, ³V. Maksymenko

¹Institute of Measurement Science SAS, Bratislava, Slovakia

²Faculty of Biomedical Engineering, CTU in Prague, Kladno, Czech Republic

³National Technical University of Ukraine “Kyiv Polytechnic Institute”, Faculty of Biomedical Engineering, Kyiv, Ukraine

Email: tysler@savba.sk

Keywords: inverse problem of electrocardiology; body surface potential mapping; torso model; ectopic activation.

Introduction. It has been shown elsewhere that cardiac imaging based on multichannel surface ECG and proper torso and heart model may be useful for non-invasive assessment of electrophysiological state of the heart by solving the inverse problem of electrocardiology. The accuracy of the solution may depend on the selected model of the cardiac sources, method used for assessment of its parameters, and fidelity of the ECG data and torso model. In this study accuracy of inverse localization of ventricular ectopic activity in dependence on the used heart and torso model was examined.

Methods and Materials. Two male patients (P1 57 years, P2 17 years) with premature ectopic activity in the ventricles causing ventricular tachycardia underwent 10 minutes of body surface potential mapping (BSPM) using the ProCardio 8 system with 62 electrodes placed according to the Amsterdam lead system. Then computed tomography (CT) scanning with slice thickness of 0.3 mm and a pixel size of 0.885 mm was performed on patients with applied ECG electrodes using the Toshiba Aquilion ONE™ system. Finally, intracardiac electrophysiological study (EPS) was performed using the St. Jude EnSite NavX™ cardiac mapping and navigation system and Bard LabSystem™ PRO EP Recording System to reveal the site of the premature ectopic activity. For non-invasive estimation of the site of the premature ectopic activity an inverse solution based on dipole model of the cardiac electric generator, measured BSPM data, and several torso models of different fidelity were employed: A - model with a common shape of torso with lungs adjusted to patient chest dimensions and simplified heart model located relatively to position of the ECG lead V2; B - the same torso and lungs model as in A, with heart model shape and position taken from the CT scan; C- realistic model of the torso, lungs and heart taken from the CT scan.

Results. Intracardiac EPS identified the initial ectopic activation in the posterior septum near heart base in P1 and in the left free ventricular wall near aortic sinus in P2. When the common torso model A was used, the noninvasively located sites were not in concordance with the EPS (in the free wall of the LV in P1, in LV near apex in P2). When torso models B or C were used, the sites were located within few millimetres from those found by the EPS (depending on the evaluated extrasystole), while the solution using model C was more accurate and more stable within the evaluated extrasystoles.

Conclusions. Fidelity of the torso and heart model strongly influences the inverse localization of the ectopic activity. Best results were achieved with a torso model based on full torso CT scan. However, if this is not available, an approximate torso shape adjusted to patient chest dimensions and properly positioned heart model based on CT-scan of the heart area can give acceptable accuracy of the inverse localization of an ectopic activity.

HEART RATE VARIABILITY

Circadian Variation of Holter-Based T-wave Alternans and Association with Autonomic Nerve System in Normal Heart Subjects

¹K. Hashimoto, ¹Y. Kasamaki, ²Y. Okumura, ²T. Nakai, ²S. Kunimoto, ²I. Watanabe, ²A. Hirayama, ³Y. Ozawa, ¹M. Soma

¹Division of General Internal Medicine, Department of Medicine, Nihon University School of Medicine, Tokyo, Japan,

²Division of Cardiovascular Medicine, Department of Medicine, Nihon University School of Medicine, Tokyo, Japan,

³MJG Cardiovascular Institute, Saitama, Japan

Email: Hashimoto.kenichi@nihon-u.ac.jp

Keywords: T wave alternans; Holter ECG; Autonomic Nerve System

Introduction. It has been reported that microvolt-level T wave Alternans (m-TWA) reflects repolarization abnormality, as useful identifying patients at high risk for sudden cardiac death. There have been several reports indicating the circadian variation of incidence for sudden cardiac death, which observed most frequent during afternoon. The purpose of this study was to examine the circadian variation of m-TWA in healthy subjects and association with autonomic nerve system for 24 hours in daily life.

Methods and Materials. m-TWA was recorded on 30 normal healthy subjects (men 19, women 11), aged 23 to 73 years (mean±SD, 46±7). m-TWA was analyzed by spectral methods using newly developed 24-hour Holter ambulatory ECG. The circadian variation of max magnitude of m-TWA was determined during 6 hours intervals (0-6h, 6-12h, 12-18h and 18-24h), respectively. We also measured the RR interval and analyzed the component of LnHF (Natural logarithm of High frequency), LF/HF (Low frequency/High frequency) for the heart rate variability (HRV) at the same time on 24-hour ambulatory ECG.

Results. Mean value of max m-TWA in each time interval were greater during 12-18h (21.44±13.96μV) than in those during 0-6h (10.43±7.8μV) and 18-24h (13.12±6.04μV) (P<0.0001 12-18 vs 0-6, 18-24, respectively). There was significant positive correlation between m-TWA magnitude and LF /HF (p<0.0001.R=0.466.) On the other hand, there was significant negative correlation between m-TWA magnitude and LnHF (p<0.0001.R=0.454).

Conclusions. In cardiac normal subject, m-TWA had the circadian variation through 24 hours which affected by autonomic nerve system. Our data suggests that the circadian variation of m-TWA may influence by autonomic tone when we assess the circadian variation of incidence for lethal ventricular arrhythmia in patients with cardiac disorder.

Extrapolation of the QT/RR Relation: Individualized vs Universal Formulae

^{1,2}V. Jacquemet, ²B. Dubé, ^{1,2}A. Vinet, ²M. Sturmer, ²G. Becker, ²T. Kus,
²R. Nadeau

¹Université de Montréal, Montréal (QC), Canada,

²Hôpital du Sacré-Coeur de Montréal, Montréal (QC), Canada

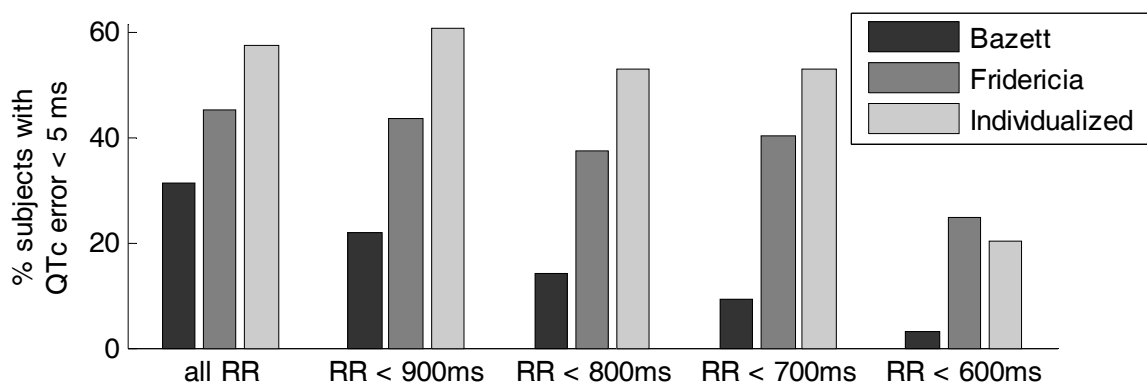
Email: vincent.jacquemet@umontreal.ca

Keywords: QT interval, QT rate-correction, QT/RR relation, subject-specific correction.

Introduction. The corrected QT (QTc) is assumed to represent the QT interval at 60 bpm. Since the hearts of most patients usually beat at higher rates, we compared the performance of extrapolating the QT/RR relation to predict the QT at 60 bpm using universal and individualized correction formulae.

Methods and Materials. QT and RR time series were extracted from 24-h Holter ECGs in 64 normal subjects (39 men) from the THEW database (University of Rochester). In all subjects, stable segments with RR intervals close to 1000 ms were identified. The average QT interval in these segments served as gold-standard value (QT₁₀₀₀) for the QTc. In the full recording and in the subsets of beats with RR intervals < 600, 700, 800 and 900 ms, the average Bazett and Fridericia QTc were computed, as well as the individualized QTc based on the optimization of 3-parameter QT/RR functions. Prior to QT correction, hysteresis reduction was performed using a universal formula (autoregressive filter with a memory of ~ 2 min). The extrapolation performance of each correction approach was quantified as the percentage of subjects in which the absolute difference between the QTc and QT₁₀₀₀ was smaller than 5 ms.

Results. The QT₁₀₀₀ was 373±13 ms in men and 400±16 ms in women (p<0.01). The quality of QT₁₀₀₀ prediction generally decreased when a narrower range of RR intervals was used for the extrapolation (see Figure). Bazett's performance was poorer for all ranges of RR intervals. Individualized correction outperformed universal formulae (the error was < 5 ms in 60% of the subjects), except when only data points with RR < 600 ms were included. In this case, Fridericia's correction was less sensitive to missing data.



Conclusions. Subject-specific QT correction was more accurate for predicting the QT₁₀₀₀, provided that a sufficient range of RR intervals was available.

Does Vagus Nerve Make Mistake ? Vasovagal Reaction in Young Healthy Persons - Benign or Severe

A. Stanczyk

Department of Cardiology and Internal Diseases, Military Institute of Medicine,
Warsaw, Poland

Email: astanczyk@wim.mil.pl

Keywords: vasovagal syncope; renin-aldosterone system; head-up tilt test.

Introduction. One of the most important reason of pathological vasovagal reflex activation is a short-term blood pressure dysregulation, caused by neuroendocrinological disturbances. Hand-grip test (HGT) and controlled breathing test (CBT) are noninvasive methods allowing to estimate the activity of autonomic nervous system.

The aim. Assessment of the relation between renin-aldosterone system activity in a response to autonomic modulation and benign ECG disturbances to the result of head-up tilt test in young healthy men without previous syncopal history.

Subjects and methods. 200 male volunteers without syncopal history were enrolled to the study. The examination was performed in a following order: 1/ 30 minutes of the horizontal rest 2/ CBT (5 minutes), 3/ 10 minutes of rest, 4/ HGT (5 minutes, 15 breaths per minute), 5/ 15 minutes of rest 6/ head-up tilt test (HUTT) according to Italian protocol. Concentration of active renin (R) and aldosterone (A) were measured at rest, after HGT, CBT and at the end of a passive phase of HUTT (during syncope or at the end of negative passive phase - HUTT passive). Positive results were interpreted according to VASIS classification. The day before a 24-hour Holter ECG monitoring were performed. Benign ECG disturbances were defined as a presence of: sinus inhibitions, paroxysmal PQ>200msek, paroxysmal nocturnal a-v block (Wenckebach type), nocturnal bradycardia.

Results. The results of R and A for all phases were achieved in 163 respondents. Positive HUTT (HUTT+) was observed in 89 persons (55%) (22 during passive phase – HUTT+passive; 67 after nitroglycerin provocation – HUTT+NTG). There were no differences in RAS activity between total group of patients with negative and positive HUTT. In HUTT+passive significant higher level of R at all stages were noted in comparison to HUTT+NTG. Relative increase of R and A in response to tilting was similar in all groups (independently of HUTT result). The results of logistic regression analysis showed, that presence of any benign ECG disturbances was significant predicting factor of positive HUTT.

Conclusions. Young men are predisposed to vasovagal syncope during HUTT, despite no previous syncopal history. A pathomechanism of individual types of syncope provoked during passive tilting seems to be different from similar observed after nitroglycerin provocation. The presence of benign ECG disturbances is a significant risk factor of positive HUTT.

Dynamic Beat-to-Beat Changes of the Cardiac Electric Field in Response to Situations with Increased Sympathetic Activity

¹E. Kellerová, ¹V. Szathmáry, ²G. Kozmann

¹Institute of Normal and Pathological Physiology, Slovak Academy of Sciences,
Bratislava, Slovak Republic

²Department of Electrical Engineering and Information Systems, Faculty of
Information Technology, University of Pannonia,
Veszprém, Hungary
Email: ekellerova@chello.sk

Keywords: integral ECG body surface maps; beat-to-beat dynamism; reactive changes; head-up tilting; psycho-emotional stress.

Introduction. Only a few studies – analyzing body surface potential maps (BSPMs) from a single, or from an average of some heart beats - have dealt with reactive changes of BSPMs and documented an increased sympathetic drive of the ventricular myocardium in response to different physiological conditions. The aim of the present study was to examine the previously unexplored dynamic beat-to-beat pattern of the reactive changes in the ventricular depolarization (QRS) and repolarization (QRST) parameters of the integral BSPMs, due to sympathetic activation.

Methods and Materials. Continual records of body surface ECG using 64 torso electrodes in 9 healthy men, were taken in supine rest, gradual head up tilting to 60° (TU) and back to supine (TD), sitting (SIT) and during a mental arithmetic test (MA). In each experimental situation the blood pressure (BP) was repetitively measured. To assess the dynamic pattern of the reactions, R-R intervals and selected QRS and QRST parameters from the respective integral BSPMs were evaluated for each heartbeat. In individual subjects depending on the heart rate from 906 – 1262 postural and/or 335-426 MA BSPMs.

Results. With changing position from supine to TU, there was a significant gradual decrease in the QRSTampl, in the average to 73% and to SIT to 83% of the resting supine value. Simultaneously the angle α significantly increased and the nondipolarity QRST BSPM indexes fell. The MA stress induced changes began in all subjects with a short latency after initiation of the mental task, usually peaked significantly at 30-60 seconds, returning to the control values to the end of the test, or some heart beats after. The main parameter of the integral repolarization BSPM – the QRSTampl fell to 81% of its control value. The pattern of both responses was inter-individually conformable, however variable in magnitude.

Conclusions. The results provided the first insight into the dynamism of reactive changes in ventricular activation and recovery, explained by pattern of the selective sympathetic drive of the ventricular myocardium in the complex cardiovascular response to postural or mental strain.

BODY SURFACE POTENTIAL MAPPING

Body Surface Potential Mapping in Rats with Experimental Pulmonary Hypertension

O. Suslonova, I. Roshchevskaya

Laboratory of Comparative Cardiology, Komi Science Centre, UD, RAS, Syktyvkar,
Russia

Email: compcard@mail.ru

Keywords: body surface potential mapping (BSPM); pulmonary hypertension; monocrotoline

Introduction. Pulmonary hypertension is known to lead to overload of the right side of the heart. The aim of this work was to analyze the change of amplitude-temporal characteristics of body surface potential maps (BSPMs) in rats with experimental pulmonary hypertension during ventricular depolarization.

Methods and Materials. BSPM was carried out in Wistar rats (n=17). Pulmonary hypertension was caused by a single subcutaneous injection of monocrotoline (60 mg/kg). Before and four weeks after an injection of the drug cardioelectrical potentials were recorded by a method of cardioelectrotopography from 64 subcutaneous needle electrodes uniformly distributed on the animal chest. Validity was defined by the Wilcoxon criterion for two dependent samples ($p < 0.05$).

Results. It was shown that in rats with experimentally induced pulmonary hypertension during ventricular depolarization the maximum amplitude of positive and negative extrema of BSPM significantly increased. The positive extremum was 1.39 ± 0.37 mV, the negative extremum – (-0.87 ± 0.41) mV in comparison with a control group (1.05 ± 0.38 mV; -0.61 ± 0.19 mV) respectively. In hypertensive rats, the first inversion finished on -3.18 ± 0.79 ms from the R_{II} - peak, that was significantly later than in a control group (-3.65 ± 0.47 ms). The second inversion finished during the ascending phase of the S_{II} -wave (6.08 ± 1.25 ms relative to the R_{II} -peak), that was significantly later than in a control group (5.33 ± 0.50 ms).

Conclusion. Pulmonary hypertension in Wistar rats leads to hypertrophy of the right ventricle that was histologically confirmed. It is reflected on BSPMs by a significant change of amplitudes of extrema and increase of the duration of the first and second inversions during ventricular depolarization.

The work is supported by the grant 09-0498814-a Russian Science Support Foundation.

The Extrema of Isopotential P-wave Maps in Young Adult Controls

K. Kozlíková, M. Trnka

Institute of Medical Physics, Biophysics, Informatics and Telemedicine,
Faculty of Medicine, Comenius University, Bratislava, Slovak Republic
Email: katarina.kozlikova@fmed.uniba.sk

Keywords: Body surface potential mapping; P wave; Time normalisation; Humans; Controls

Introduction. The electrical activity of the heart atria is represented by the P wave that can be recorded and analysed using different procedures. The aim of this retrospective study was to analyse the sequence of isopotential maps in young adult controls when using time normalisation of the P wave.

Methods and Materials. We constructed 21 isopotential maps from 24-lead system after Barr in 88 controls (40 men) without cardiovascular diseases, aged (18.5 ± 0.4) years. The first map corresponded to the P wave beginning, the last map to its end. We analysed values and the time course of extrema: maximum (MAX), minimum (MIN), peak-to-peak value (PEAK=MAX-MIN).

Results. The mean P wave duration was (84 ± 10) ms, significantly longer in men ((86 ± 9) ms versus (82 ± 10) ms, $p < 0.05$) measured in the root mean square signal. The potential values varied from $-187 \mu\text{V}$ to $193 \mu\text{V}$ in individual maps. We always found lower mean values of extrema (flatter maps) in women than in men, significantly different in 19/21 MAX comparisons, in 19/21 MIN comparisons, and in all PEAK comparisons ($p < 0.05$). The absolute maximum appeared in the middle of the P wave and preceded the absolute minimum in average by 1 or 2 maps (about 4 ms or 8 ms). The time courses of extrema (in μV) were fitted by polynomial curves against the sequential map number $x = 1, 2, \dots, 21$:

Regression curve	Correlation coefficient r
MAX = $-0.7 \cdot x^2 + 15.2 \cdot x + 3.3$	0.992
MIN = $-0.006 \cdot x^4 + 0.3 \cdot x^3 - 4.0 \cdot x^2 + 10.7 \cdot x - 22.8$	0.991
PEAK = $0.008 \cdot x^4 + 0.4 \cdot x^3 + 4.2 \cdot x^2 + x - 28.7$	0.999

Conclusions. The obtained values of extrema correspond to the published data from the standard 12-lead electrocardiograms (in average, lower values in women than in men), which, however, do not allow evaluating of the time course and cover only a small part of the chest.

This work was partially supported by the VEGA project 1/0727/14 from MESRS SR.

Impact of Heart Rate on Normal STT Integral Body Surface Potential Maps

¹J. Svehlikova, ²M.Kania, ²R. Maniewski, ¹M. Tysler

¹Institute of Measurement Science SAS, Bratislava, Slovakia,

²Nalecz Institute of Biocybernetics and Biomedical Engineering PAS, Warsaw, Poland

Email: jana.svehlikova@savba.sk

Keywords: STT integral body surface potential maps; stress test, heart rate; local repolarization changes.

Introduction. It was shown in simulation studies that local repolarization changes (ischemia) reflect in integral body surface potential maps (IBSPMs) of the STT interval. Therefore we suggested a method for identification and localization of local ischemic lesions from difference IBSPMs computed by subtraction of IBSPM without manifestation of ischemia from the IBSPM during ischemia. It was supposed that such data can be obtained in rest and during the stress test. However, during the stress test there is a considerable increase of the heart rate (HR) while in simulations no HR changes were considered. In this work the IBSPMs of healthy subjects were computed before and during the stress test and the changes in the IBSPMs as effect of increasing HR were studied.

Methods and Materials. BSPMs from 64 leads were measured during the stress test in 8 subjects with no cardiac disease history (age 30-77). Simultaneously the 12-lead ECG was measured to evaluate the test results in a standard way. During the test, the HR of each subject increased from the basal value at rest up to the value higher than 85% of the value (220-age) at the top of the exercise. The IBSPMs were computed for each subject at the basal and the highest HR as well as for three steps in between. The IBSPMs at each HR were computed from averaged signals (10 s intervals). The differences in IBSPMs in subsequent steps of the HR were evaluated for each subject.

Results. The increasing HR shortened the STT interval significantly. The correlation coefficient between the IBSPM at rest and IBSPM at the top HR was higher than 70%. To compare the root mean square (rms) values of the maps, the mapped integrals were normalized by dividing their values by the length of the corresponding STT interval. The rms value of the IBSPM at the top HR varied from 43% to 126 % of the rms value of the IBSPM at rest.

Conclusions. Remarkable differences in STT IBSPMs at rest and at stress were observed in healthy subjects. This fact should be considered when the differences in IBSPM during the stress test are evaluated for ischemic patients.

ATRIAL FIBRILLATIONS

Rate-Control Drugs Affect Variability and Irregularity Measures of RR Intervals in Permanent Atrial Fibrillation

¹V.D.A. Corino, ²S.R. Ulimoen, ²S. Enger, ²A. Tveit, ³P.G. Platonov.

¹Politecnico di Milano, Milano, Italy,

²Bærum Hospital, Rud, Norway,

³Lund University Hospital, Lund, Sweden

Email: valentina.corino@polimi.it

Keywords: beta-blocker; calcium-blocker; variability; irregularity.

Introduction. Reduced RR irregularity during atrial fibrillation (AF) has been associated with poor prognosis in prospective studies, however whether these measures are affected by the rate-control drugs is not fully explored. We assessed whether variability and irregularity of RR intervals are modified by rate-control drugs in permanent AF patients enrolled in the RATE Control in Atrial Fibrillation (RATAF) study.

Methods and Materials. This investigator-blind cross-over study included 60 pts (71 ± 9 years, 30% female) with permanent AF. Diltiazem 360 mg, verapamil 240 mg, metoprolol 100 mg, and carvedilol 25 mg were given once daily in the morning for 3 weeks in a randomized sequence. RR-variability (SDNN, pNN50, rMSSD) and irregularity (approximate entropy [AE] and R-index) measures were estimated from 20-min Holter ECG segments starting at 2PM.

Results. All drugs reduced heart rate (HR) and increased RR-variability. Both calcium antagonists achieved lower HR than either of beta-blockers. Carvedilol and metoprolol increased the irregularity parameters, whereas diltiazem and verapamil did not affect them. Figure shows mean HR, rMSSD and AE at baseline (B) and during carvedilol (C), diltiazem (D), verapamil (V) and metoprolol (M) administration.

Conclusion. Rate-control drugs affect variability of RR intervals during AF and should be accounted for when RR variability is assessed. Only beta-blockers influenced the irregularity of ventricular response during permanent AF.

Table 1: Mean \pm SD for all parameters during baseline and drug administration.

	Baseline	Carvedilol	Metoprolol	Diltiazem	Verapamil
HR	110 \pm 18	88 \pm 14*	89 \pm 16*	79 \pm 16* ° +	78 \pm 18* ° +
RMSSD	171 \pm 47	229 \pm 58*	226 \pm 66*	256 \pm 87* ° +	228 \pm 84* #
AE	2.06 \pm 0.15	2.12 \pm 0.09 *	2.14 \pm 0.10 *	2.08 \pm 0.18	2.07 \pm 0.23

* p<0.05 comparison with baseline, ° p<0.05 comparison with carvedilol, + p<0.05 comparison with metoprolol, ^ p<0.05 comparison with diltiazem

Analysis of Electrocardiographic Predictors of Atrial Fibrillation in Patients with Ischemic Stroke without Known History of Atrial Fibrillation

**¹M.A.Baturova, ²S.H.Sheldon, ¹J.Carlson, ²P.A.Brady, ²G.Lin, ³A.A.Rabinstein,
²P.A.Friedman, ¹P.G.Platonov**

¹Department of Cardiology, Lund University, Lund, Sweden

²Department of Cardiology, Mayo Clinic, Rochester, United States of America

³Department of Neurology, Mayo Clinic, Rochester, United States of America

Email: Maria.Baturova@med.lu.se

Keywords: atrial fibrillation; ischemic stroke; P wave duration; QT interval.

Introduction. Atrial fibrillation (AF) is a common cause of ischemic stroke, and its identification is essential to determine the role of anticoagulation in the therapy. Electrocardiographic (ECG) monitoring after cryptogenic stroke underdetects AF due to its paroxysmal nature. We hypothesized that the pathologic changes associated with AF would lead to abnormalities that can be detected by a digitally processed normal rhythm ECG obtained at the time of stroke presentation.

Methods. Ischemic stroke patients (n=110, age 67±10, 63% men) without AF history prospectively underwent continuous noninvasive ambulatory ECG monitoring for 3 weeks for AF detection and age- and gender-matched ischemic stroke patients with known AF history (n=55, HxAF) were studied. The standard 12-lead ECG with stroke admission was digitally processed and analyzed.

Results. During monitoring, brief paroxysms of asymptomatic AF (median duration 6 sec) were detected in 24 patients (PAF). Patients with PAF or HxAF (n=79, Any AF) did not differ from patients without detected AF (n=86) with regard to age (69±9 vs 66±10, p=0.078) but more often had heart failure (23% vs 5%, p=0.001). Patients without detected AF had shorter P-wave duration (136±15 vs 145±17 ms, p=0.001) as well as QTc interval (424±26 vs 440±33 ms, p=0.001) than patients with Any AF. After adjustment for clinical characteristics and antiarrhythmic drug use, P-wave duration (OR1.03: 95%CI 1.00-1.05, p=0.049) and QTc interval (OR1.02: 95%CI 1.01-1.03, p=0.013) were associated with AF. There was no difference in ECG-markers or clinical characteristics between patients with asymptomatic AF episodes and history of paroxysmal AF.

Conclusions. Analysis of a sinus rhythm ECG in patients with ischemic stroke assesses likelihood of AF in patients without known history of AF, and may inform intensity of follow up. P-wave prolongation likely reflects atrial remodeling predisposing to AF, whereas the association of AF ventricular repolarisation abnormalities may reflect a broader vascular process present in patients with AF and stroke.

Circadian Heart Rate Variability in Permanent Atrial Fibrillation Patients

I. Kurcalte, O. Kalejs, R. Erts, I. Konrade, A. Lejnieks

Riga Stradins University, Riga, Latvia

Email: irenakurcalte@gmail.com

Keywords: circadian heart rate variability; average day night heart rate ratio; average day night heart rate difference.

Introduction. Atrial Fibrillation (AF) is the most common sustained cardiac arrhythmia occurring in 1-2% of the general population. From 6 to 8 % of world population have diabetes mellitus (DM). The presence of DM in patients with AF is approximately 13%. Impairment of cardiovascular autonomic control is significantly associated with total mortality. The prevalence of cardiac autonomic neuropathy (CAN) varies from 2.5% to 50-90% and depends on used criteria and population studied. Current practical use of ECG-based risk predictors such as HRV, TWA, HRT, QT interval analysis is limited in permanent AF (PAF) patients due to absolute irregularity of ventricular contractions. We speculate that it is possible to use measurements of twenty-four hours (circadian) heart rate (HR) changes for cardiac autonomic control assessment and mortality risk prediction in PAF patients.

Methods and Materials. Study cohort - 331 symptomatic PAF patients (261 non diabetic (nonDM, mean age 74.4 (10), 121 male (46.4%)) and 70 diabetic (mean age 75.7 (8.5), 28 male (40%)), exposed to Holter monitoring in 2007-2010. Circadian HR indices (average day/night HR ratio (aveDNHRrat) and difference (aveDNHRdif)) and characteristics of ventricular arrhythmias (amount of ventricular ectopic beats (VEtotal) and presence of often VE (Lown class 2) were calculated and compared between (nonDM and diabetic) and within the groups (patients who died before or were alive after 01.01.2011), minimum follow-up - 36 month (39 (1-75)).

Results. During the follow-up 80 (30.7%) nonDM and 38 (54.3%) diabetic patients deceased (RR - 2.97 (1.73; 5.09 95% CI)). The circadian HR indices were significantly lower in dead patients compared with alive (aveDNHRrat, $p < .001$; aveDNHRdif, $p < .001$), in diabetics compared with nonDM patients (aveDNHRrat, $p = .003$; aveDNHRdif, $p = .003$). In dead diabetics group was higher total amount of VE ($p < .001$) and incidence of Lown class 2 VE ($p = .001$; RR - 6.31 (2.14; 18.59 95% CI). In diabetics with approved diabetic neuropathy diagnosis (n=12 (17.1%)) the aveDNHRrat was lower ($p = .036$). Circadian HR characteristics showed significant, but low negative correlation with BNP (brain natriuretic peptide) (aveHRDNrat, $r = -.42$, $p = .001$; aveDNHRdif, $r = -.39$, $p = .003$).

Conclusions. Decrease of circadian HR variability is associated with higher mortality risk in PAF patients. Diabetic PAF patients are at higher mortality risk than non-diabetic. Combination of decreased circadian HR variability with ventricular arrhythmias is associated with higher mortality risk in diabetic patients with PAF. Decrease of circadian HR variability in diabetic PAF patient can be associated with presence of cardiovascular autonomic neuropathy and heart failure. Evaluation of twenty four hours HR variability in PAF patients with and without DM can be tried for cardiac autonomic control investigation and risk assessment.

**POSTERS:
EXPERIMENTAL AND CLINICAL ELECTROCARDIOLOGY**

Alterations in Cardiac Cell-to-Cell Coupling Can Facilitate AF in Old Guinea Pig

**¹N. Tribulova, ²V. Nagibin, ¹T. Benova, ¹C. Viczenczova, ^{1,3}J. Radosinska,
⁴V. Knezl, ⁵I. Dovinova, ¹M. Barancik**

¹Institute for Heart Research, SAS, Bratislava, Slovakia,

²Bogomoletz Institute of Physiology, Kyiv, Ukraine,

³Institute of Physiology, Fac. Med., Comenius University, Bratislava, Slovakia,

⁴Institute of Experimental Pharmacology & Toxicology, SAS, Bratislava, Slovakia,

⁵Institute of Normal and Pathological Physiology, SAS, Bratislava, Slovakia

Email: narcisa.tribulova@savba.sk

Key words: aged heart; connexin-43; atrial fibrillation;

Introduction: Despite the progress in pathophysiology of atrial fibrillation (AF) the molecular mechanisms of this most common cardiac arrhythmia in aged population are still not fully elucidated. We have previously shown that unlike to young the aged guinea pig heart is much prone to develop AF upon repetitive burst stimulation. We hypothesize that in addition to atrial structural remodeling the alterations in cardiac cell-to-cell coupling due to the ageing may facilitate induction and persistence of AF.

Methods and Materials: Experiments were conducted on male and female 4-weeks-old and 24-weeks-old guinea pigs (GP). Heart atrial tissue was processed for ultrastructure examination using electron microscopy. Gap junction connexin-43 distribution was detected by in situ immunostaining while the level of Cx43 mRNA and expression of Cx43 protein were determined by real time PCR and western blotting. Expression of mRNA of extracellular matrix metalloproteinase-2 (MMP2) that is involved in myocardial remodeling was also analyzed.

Results: Subcellular examination revealed interstitial fibrosis, flattened adhesive junctions with widened extracellular spaces and lower number of gap junctions in old versus young GP heart atria. The density of Cx43-positive gap junctions was lower in atria of old comparing to young GPs. In parallel, the atrial tissue levels of Cx43 mRNA and Cx43 protein were decreased in old versus young GP. In contrast, mRNA expression of MMP2 was significantly higher in old versus young GP. The changes were more pronounced in old males comparing to females GP.

Conclusions: Findings indicate that age-related down-regulation of atrial Cx43, dehiscence of adhesive junctions and up-regulation of MMP-2 can facilitate development of AF in old heart.

This study was supported by VEGA 2/0046/12, 1/0032/14 and APVV-0348-12 grants.

Hyper- and Hypothyroidism Affect Myocardial Connexin-43 Expression and Susceptibility of the Rat Heart to Malignant Arrhythmias

¹B. Bacova, ¹C. Viczenczova, ¹T. Benova, ²J. Radosinska, ³J. Zurmanova, ⁴S. Pavelka, ⁴T. Soukup, ¹N. Tribulova

¹Institute for Heart Research, SAS, Bratislava, Slovakia,

² Institute of Physiology, Faculty of Medicine, Comenius University, Bratislava, Slovakia

³ Faculty of Science, Charles University in Prague, Prague, Czech Republic,

⁴ Institute of Physiology, v.v.i., AS CR, Prague, Czech Republic

Email: barbara.bacova@savba.sk

Keywords: Connexin-43, Hypo/hyperthyroidism, Ventricular fibrillation, Red palm oil.

Introduction: The heart muscle is modulated by thyroid hormones and their deficiency or excess in hypo- (HY) or hyperthyroid (TH) status, which is accompanied by oxidative stress, may affect both cardiac function and arrhythmogenesis. We hypothesized that intercellular connexin-43 (Cx43) channels might be implicated. The goal of this study was to explore the expression of myocardial Cx43 and its functional phosphorylated forms in rats with altered thyroid status as well as the effects of antioxidant-rich red palm oil (RPO) intake in these conditions.

Methods and Materials: Male adult euthyroid rats (EU); HY rats (methimazole-treated); TH rats (T3/T4-treated) were fed RPO (100 microL/100g b.w./day) for six weeks and compared with untreated rats. Left ventricular tissue was taken especially for Cx43 and PKC-epsilon mRNA and protein analysis using real-time PCR and immunoblotting. Inducible ventricular fibrillation (VF) was examined using Langendorff-mode perfused heart.

Results: Heart and left ventricular weight was increased in TH but decreased in HY compared to EU rats. Susceptibility of the heart to VF was significantly increased in TH rats while decreased in HY compared to EU rats. Cx43 mRNA levels were higher in TH but lower in HY rats. In contrast, Cx43 protein and its functional phosphorylated forms as well as corresponding PKC-epsilon expression were decreased in TH but increased in HY rats. RPO intake reduced heart and left ventricular weight in TH rats; partially normalized Cx43 mRNA, Cx43 protein, its phosphorylated forms and PKC-epsilon expression in TH rats and protected them from VF.

In conclusion, down-regulation of myocardial Cx43 in TH is associated with higher incidence of malignant arrhythmias while its up-regulation in HY with decreased susceptibility of the heart to VF. Antiarrhythmic effect of RPO in TH rats can be in part attributed to attenuation of Cx43 abnormalities most likely due to prevention of its degradation by free radicals.

Study supported by VEGA 0046/12, APVV-SK-CZ-0027-11 and MSCT-CR 7AMB12SK158.

The Effect of Single-Dose Chest Irradiation on the Expression of Connexin-43 and PKC Signaling Pathway in the Heart of Rats

¹C. Viczenczova, ¹B. Bacova, ^{1,2}J. Radosinska, ¹T. Benova, ³C. Yin, ³R. Kukreja, ¹J. Slezak, ¹N. Tribulova

¹Institute for Heart Research, SAS, Bratislava

²Institute of Physiology, Medical Faculty of Comenius University, Bratislava

³Division of Cardiology, Medical College of Virginia, Virginia Commonwealth University, Richmond, Virginia, USA

Email: csilla.viczenczova@savba.sk

Keywords: connexin-43; PKC; miRNA-1; radiation; rat heart.

Introduction. Intercellular coupling protein, connexin-43 (Cx43) ensures direct electrical and metabolic communication that is essential for synchronized myocardial function. Expression of Cx43 in mammalian cells is highly sensitive to ionizing radiation and other stressful conditions. The purpose of this study was to explore the effect of a single dosage irradiation on myocardial Cx43 as well as PKC signaling and whether miRNA-1, which affects GJA1 gene transcription for Cx43, is implicated.

Methods and Materials. Adult, male Wistar rats were subjected to single chest irradiation at 25 Gy. After six weeks the hearts were excised from anaesthetized animals. Left ventricular tissue (LV) was taken for in situ Cx43 immunolabelling as well as immunoblotting of Cx43 and PKC. Level of miRNA-1 was quantified by RT-PCR.

Results. Results showed that the body and heart mass were decreased in irradiated rats compared to controls. Disordered cardiomyocyte distribution of Cx43 positive gap junctions was found in the hearts after irradiation. Compared to the controls, total Cx43 expression and its functional phosphorylated forms were significantly increased in LV due to irradiation. In contrast, miRNA-1 expression was significantly decreased in those animals. Furthermore, expression of both PKC-epsilon and PKC-delta was increased in left ventricle of rats exposed to irradiation. The former is involved in Cx43 phosphorylation and both PKC in oxidative stress-induced cardioprotection.

Conclusions. Our findings indicate that single dose irradiation leads to a compensatory up-regulation of myocardial Cx43 via suppressed expression of miRNA-1 as well as enhancement of pro-surviving PKC signalling.

This study was supported by APVV 0241/11 and VEGA /0046/12 grants.

Borderline and Spontaneously Hypertensive Male and Female Rats Exhibit Different Tolerance to Ischemia/Reperfusion

¹V. Ledvényiová, ¹D. Pancza, ¹S. Čarnická, ¹M. Nemčeková, ²I. Bernátová, ¹T. Ravingerová

¹Institute for Heart Research, Slovak Academy of Sciences, Centre of Excellence SAS NOREG, Bratislava, Slovakia

²Institute of Normal and Pathological Physiology, Slovak Academy of Sciences, Centre of Excellence SAS NOREG, Bratislava, Slovakia

Email: weroro@gmail.com

Keywords: hypertension; sex differences; social stress; ischemia/reperfusion injury.

Introduction. Genetic predisposition and social stress represent important risk factors in etiology of hypertension associated with impaired myocardial response to ischemia and reperfusion (I/R), which can differ in male and female heart as sex is an important determinant of cardiovascular morbidity and mortality in human population. Tolerance to I/R injury persists even in the hearts of animals with predisposition to hypertension and may be modified by cardiac adaptation to stressful conditions.

The study aimed to examine the impact of chronic stress on response to I/R in borderline/spontaneously hypertensive male and female rats (BHR/SHR) in comparison with its effects in normotensive (WKY) counterparts.

Methods and Materials. Male and female 5-week-old BHR, SHR and WKY were exposed to 2-week crowding stress (CS; livingspace 200cm²/rat). Unstressed animals had livingspace 480cm²/rat. Langendorff-perfused hearts of all experimental rats were exposed to 30-min global ischemia and 2-h reperfusion for the evaluation of reperfusion-induced ventricular arrhythmias, infarct size (IS) and recovery of contractile function.

Results. CS impaired postischemic recovery of contractile function with stronger effect in WKY males. CS exaggerated total number of premature ventricular complexes (PVC) in WKY males, but not females. On the other hand, the total duration of more severe forms of ventricular arrhythmias (ventricular tachycardia-VT) was decreased only in stressed WKY females. BHR rats were markedly more susceptible to VT than SHR rats of both sexes. We observed a dramatic decline in occurrence of VT in BHR-CS but not in SHR-CS males and females. Interestingly, IS was not affected by CS in normotensives as well as in stressed BHR and SHR hearts.

Conclusions. CS modifies parameters of I/R injury in a distinct way. Inherited predisposition to hypertension may be responsible for differences in arrhythmogenesis and adaptive potential in animals exposed to social stress, which appear to be sex-dependent.

Grants APVV-0523-10, APVV-0102-11.

Evaluation of Repeated Global Ischemia in Isolated Rabbit Heart

^{1,2}M. Ronzhina, ³V. Olejníčková, ³T. Stračina, ¹T. Potočňák, ^{1,2}O. Janoušek,
^{1,2}P. Veselý, ^{1,2}J. Kolářová, ^{2,4}M. Nováková, ^{1,2}I. Provazník

¹Department of Biomedical Engineering, Brno University of Technology,
Brno, Czech Republic,

²International Clinical Research Center – Center of Biomedical Engineering,
St. Anne's University Hospital Brno, Brno, Czech Republic,

³Department of Physiology, Faculty of Medicine, Masaryk University,
Brno, Czech Republic,

⁴International Clinical Research Center – Animal Center, St. Anne's University
Hospital Brno, Brno, Czech Republic

Email: ronzhina@feec.vutbr.cz

Keywords: Isolated rabbit heart; global ischemia; orthogonal electrograms.

Introduction. Animal models are often used to study the changes of heart electrical activity caused by myocardial ischemia. Rabbit model is very powerful tool because of the similarity of rabbit cardiac physiology to that of human. In experimental cardiology, voltage-sensitive dye (VSD) can be applied for action potential recording. In this study, the time course of changes in EGs recorded from isolated rabbit hearts without chemical intervention and undergoing VSD loading has been evaluated.

Methods and Materials. The orthogonal EGs recorded in isolated hearts of twelve New Zealand rabbits by touch-less method were used in this study. Four indexes (duration of QRS complex, T wave amplitude, ST30 level, and distance between maxima of QRS and T wave) were calculated from EGs recorded according to two protocols (with and without application of VSD di-4-ANEPPS). The ischemic changes sensor previously introduced by García et al. was used to describe the indexes changes caused by repeated short-term global ischemia (three ischemic episodes lasting 10 minutes).

Results. The most significant changes are characteristic for ST30 level and QRS duration. In most of experiments, ST30 level and T wave amplitude changes occur as the earliest during the fourth minute of ischemic episode. The values of changes sensor calculated for different ischemic periods are quite similar. The changes in EG morphology during ischemic periods are more slowly than the return of indexes to their control values at the beginning of reperfusion.

Conclusions. The ischemic changes of all indexes are reversible. Values of indexes at the end of the last reperfusion period are quite similar to control values. The time course of EG morphology changes is not affected significantly by application of VSD.

Electrocardiographic Predictors of Response to Vasoreactivity Testing in Patients with Pulmonary Arterial Hypertension

¹E. Blinova, ¹T. Sakhnova, ¹O. Arkhipova, ¹N. Danilov, ¹T. Martynyuk,
¹I. Chazova, ²V. Trunov, ²E. Aidu

¹Cardiology Research Complex, Moscow, Russia,

²Institute for Information Transmission Problems RAS, Moscow, Russia

Email: blinova2009.73@gmail.com

Keywords: pulmonary arterial hypertension; electrocardiography; acute pulmonary vasodilator testing

Introduction. Vasoreactivity testing (VT) in patients with pulmonary arterial hypertension (PAH) is important for the optimization of the treatment and evaluation of prognosis. The aim of the study was to assess the possibilities of electrocardiographic parameters for prediction of response to VT in patients with PAH.

Methods and Materials. 65 patients (mean age 41.4±12.4 years; 81% women) with PAH who underwent right-heart catheterization and VT were evaluated. 12-lead digital ECG were recorded. ECG parameters under investigation were: P wave amplitude in lead II (PII), QRS axis, QRS duration, R and S waves amplitudes in leads V1 and V5, spatial QRS-T angle, magnitude G and spatial components G_x, G_y, G_z of the “recovery acceleration” vector.

Results. There were 23 responders (35%) to VT. Responders had lower mean pulmonary artery pressure (46.6±11.0 mm Hg versus 61.3±19.0 mm Hg, p <0.01), pulmonary vascular resistance (837±447 dyn·s/cm⁵ versus 1386±741 dyn·s/cm⁵, p <0.01), heart rate (69.6±10.8 bpm versus 81.3±13.7 bpm, p <0.01), PII (1.70±0.79 mm versus 2.34±0.97 mm, p <0.01), QRS-T angle (61.3±27.3 dgr versus 104.5±39.9 dgr, p <0.01), RV1+SV5 (8.98±5.04 mm versus 15.7±8.0 mm, p <0.01) and higher values of G_x (22.6±15.1 ms versus 5.3±17.9 ms, p <0.001) and G_y (22.6±11.2 ms versus 8.8±8.4 ms, p <0.001) as compared with non-responders. At receiver operating characteristic curve analysis the most informative variables were G_x (the area under the ROC curve 0.77, SE 0.07), G_y (0.84±0.06), QRS-T angle (0.81±0.05) and RV1+SV5 (0.76±0.06). On multivariate logistic regression analysis after correction for age, sex, heart rate, WHO class, and echocardiographic systolic pulmonary artery pressure, G_y emerged as an independent predictor of response (odds ratio, 1.17; 95% confidence interval 1.06-1.30; p = 0.01).

Conclusions. The use of repolarization process mapping by DECARTO technique may be helpful for predicting the results of VT in patients with PAH.

QRS Complex Changes after Pulmonary Endarterectomy in Patients with Chronic Thromboembolic Pulmonary Hypertension

¹M. Boháčková, ¹T. Valkovičová, ²L. Bachárová, ³M. Kaldarárová, ¹I. Šimková

¹NÚSCH a.s., Bratislava, Slovak Republic

²International Laser Center, Bratislava, Slovak Republic

³NÚSCH a.s. Children Cardiocenter, Bratislava, Slovak Republic

Email: marcela.bohacekova@gmail.com

Keywords: CTEPH; ECG; right ventricular hypertrophy.

Introduction. Chronic thromboembolic pulmonary hypertension (CTEPH) is a progressive disease with persistent thrombotic occlusion of pulmonary bed leading to vascular remodeling and resulting in pulmonary hypertension. If left untreated, condition is fatal due to increased right ventricular afterload and right heart failure. Right ventricular dilation and hypertrophy occurs from either volume overload or hypertrophy from pressure overload, and it can affect ECG findings. The aim of the study was to study ECG signs of right ventricular hypertrophy (RVH) in patients with CTEPH and their changes due to treatment.

Methods and Materials. Study population consisted of 33 patients with CTEPH divided in two groups: 21 operable patients (6F/15M, age: average 64.1 years (42-74)) treated surgically and 12 non-operable patients (9F/3M, age: average 68.9 years (52-81)) treated conservatively (anticoagulation therapy). The following ECG parameters were analyzed: maximum spatial QRS vector magnitude (QRS max), Butler-Leggett formula for RVH (BL), Sokolow-Lyon criteria for RVH (SL). Right ventricular diameter (RVD) was measured by echocardiography.

Results. A significant difference in SL values between the groups before treatment (12.9 ± 6.2 mm vs 8.9 ± 4.5 mm) was found. Values of SL and BL in patients treated surgically decreased significantly after operation (13.7 ± 7.6 mm vs 7.4 ± 5.4 mm and 12.9 ± 6.2 mm vs 6.4 ± 3.3 mm). In patients treated conservatively no significant difference was observed. No significant changes were observed in QRSmax in either of the groups. There was a significant difference in RVD between groups at the beginning of the study (57 ± 6.8 mm and 38.5 ± 4.3 mm). The RVD values decreased significantly in patients after surgical treatment (57 ± 6.8 mm vs 32.7 ± 3.3 mm). Changes in ECG parameters and RVD did not correlate significantly.

Conclusion. Study results showed that ECG indices for RVH as well as RVD in patients with CTEPH treated surgically decreased significantly. However, these changes were not interrelated.

Application of SFHAM Model for Diagnostics of Ischemic Heart Disease

¹J. S. Janicki, ²A. Teresińska, ³W. Leoński, ¹M. Chapiński, ⁴M. Sobieszcańska, ⁵R. Piotrowicz

¹Physico-Medical Research Institute, Puszczykowo, Poland

²Department of Nuclear Medicine, Institute of Cardiology in Warsaw, Poland

³Institute of Physics, University of Zielona Góra, Zielona Góra, Poland

⁴Department of Pathophysiology, Wrocław Medical University, Wrocław, Poland

⁵Department and Clinic of Cardiac Rehabilitation, Institute of Cardiology,

Warsaw, Poland

Email: prezes@ibf.com.pl

Keywords: ECG; QRS complex; SATRO ECG; SFHAM; CHD.

Introduction. The ECG examination allows obtaining information about the electrical processes occurring in the heart, the course of which may depend on a number of pathological changes occurring in it. However, the both, currently used criteria and issues in interpretation of the results, lead to limited diagnostic value of this method. Any improvement in ECG examination requires considerable extension of currently applied electric signals analysis. To achieve this, we have used a new model of the electrical activity of the heart – SFHAM – describing the morphology of the QRS complex, and the SATRO ECG diagnostic method which is based on the SFHAM model. Our main aim was to assess the effectiveness of SATRO ECG method in CHD diagnosis, and compare it with myocardial perfusion scintigraphy Tc99m SPECT.

Methods and Materials. For a group of 243 subjects (75 females and 168 males, average age: 56±9 years) supposed to have CHD, standard resting and stress ECG (ECG-R and ECG-S, respectively), and SPECT examinations were performed. Then, with use of SATRO ECG method, parameters describing electric activity of various segments of the left ventricle were calculated on basis of ECG-R results.

Results. Sensitivity of SATRO ECG in CHD diagnosing was 100% and specificity 70%, whereas predictive values of the positive and negative results were 98% and 100%, respectively. Moreover, statistical kappa Cohen test showed that statistical correlation between SATRO ECG and SPECT methods ($k=0.800$, $p<0.0001$) exists. Such correlations are not detected when SPECT was compared with ECG-R ($k = 0.055$, $p = 0.031$) and ECG-S ($k = 0.018$, $p = 0.294$).

Conclusions. 1. SATRO ECG examination seems to be more useful in detecting perfusion defects recognized with use of SPECT method, as compared with resting and stress ECG. 2. The positive results of the diagnosis of CHD indicate a relationship between the obtained parameters and the actual processes occurring in the heart and suggest the possibility of applying them for the diagnosis of other disorders of the heart..

Comparative Assessment of ECG Dynamics in Myocardial Infarction According to Reperfusion Therapy (Primary or Facilitated Coronary Angioplasty) and Timing of the Procedure

G.V. Ryabykina, A.V. Sozykin, E.N. Dyuzheva

Russian Cardiology Research and Production Complex, Moscow, Russia
Email: ecg.newtekh@gmail.com

Keywords: ECG-12 dynamics; acute coronary syndrome; angioplasty.

Introduction. The aim of this study was to compare ECG-12 dynamics depending on the methods of facilitated and primary angioplasty in acute coronary syndrome (ACS).

Methods and Materials. We study 81 patients with ACS (73- acute myocardial infarction, 8- unstable angina) who underwent PTCA with or without preliminary thrombolysis. Group 1 - 50 patients with primary PTCA (pPTCA), Group 2- 31 patients with facilitated PTCA (fPTCA). The ECG analysis before and after reperfusion included dynamics of summary ST elevation (Σ ST+) and depression (Σ ST-), changes of summary R waves amplitude (Σ R) in 12 leads. The results were estimated depending on the time till treatment of the infarction-related artery.

Results. In the pPTCA group there are no reliable differences in Σ R before and after treatment, in fPTCA significant Σ R reduction after treatment was observed. Significant Σ R reduction appeared when reperfusion started (RS) 2-6 hours of pain onset (PO). If RS in first 6 hours after PO, Σ ST+ and Σ ST- dynamics was positively reliable in both groups. The most pronounced Σ ST+ fall was observed during 2 hours of PO with pPTCA - 3 times and fPTCA – 2.5 times lower. If RS 2-6 hours later Σ ST+ decreases twice. When RS later than 6 hours the ST indices did not change substantially, being even higher. Total Σ ST+ after treatment in fPTCA group was higher than in pPTCA (Tab.1).

Conclusions. The facilitated PTCA results in a more pronounced reduction of the summary R wave amplitude compared with primary angioplasty. Significant decrease of ST elevation was observed if PTCA performed in 6 hours after heart attack onset.

ECG changes with pPTCA (Group 1) and fPTCA (Group 2)

	Group 1			Group 2		
	Σ R	Σ ST+	Σ ST-	Σ R	Σ ST+	Σ ST-
Total before treatment	63.8	11.5	5.3	55.2	16.3	6.5
Total after treatment	61.5*	6.0*	2.0*	46.5	7.8	2.8
Up 2 hr after PO						
Before	68.0	12.9	4.5	76.5	17.4	8.4
After treatment	65.7	4.1**	1.4**	62.5	6.6**	0.9**
Up to 2-6 hr after						
Before	59.4	11.7	6.1	52.8	18.0	6.1
After treatment	59.8	5.5**	1.8**	43.6**	8.0**	2.3**
More than 6 hr after						
Before	68.0	8.6	4.3	47.7	5.4	7.0
After treatment	59.4	9.8	3.3	47.0	7.6	7.3
*p<0.05 – differences are significant between Group 1 and 2						
**p<0.05 – before and after treatment						

Myocardial Ischemia in Genesis of Microvolt T-wave Alternans

E.N. Dyuzheva, G.V. Ryabikina, A.V. Sobolev, A.E. Vlasova

Russian Cardiology Research and Production Complex, Moscow, Russia

Email: ecgnewtekh@gmail.com

Keywords: T-wave alternans; silent ischemia; left main stenosis; CABG.

Introduction. To study the influence of myocardial ischemia (MI) on MTWA measured by the holter monitoring (HM).

Methods and Materials. 47 patients underwent HM: 35 multiple vessel disease patients (15-without silent ischemia (SI), 20-without SI), 12 controls -without ischemic heart disease (IHD). Using a modified moving average method, we determined MTWA average daily level (ADL), maximum daily level (MDL), episodes of high level ($> 80 \mu\text{V}$) (EHL). HM was repeated (n=29) in 7-14 days after coronary bypass grafting (CABG).

Results. IHD group compared with controls had: higher ADL on MC5 lead (10.2 vs 7.5 μV , $p<0.05$), on MC1 lead (8.8 vs 6.0 μV , $p<0.05$), more EHL (3.6 vs 0.4, $p<0.01$), higher MDL 108 vs 65, $p<0.05$). ADL on MC5 in presence of SI was substantially higher than in controls (11.6 vs 8.7 μV , $p<0.01$), IHD without SI didn't differ from controls (8.7 vs 7.4, NS). Patients with SI and left main stenosis (LMS) more significantly differ from controls in the number of EHL (4.4 and 3.7 vs 0.4, $p<0.01$) than patients without SI (2.2 vs 0.4, $p<0.05$). LMS patients had higher MDL compared to control (122 vs 65 μV , $p < 0.001$). After CABG: for LMS MDL decreased to 78.6 μV ($p<0.05$), for all IHD ADL decreased to 7.3 μV on MC1 ($p<0.05$), to 6.9 μV on MC4 ($p<0.01$), EHL decreased to 2.7 ($p<0.05$), was a trend to MDL reduction to 83 ($p < 0.06$).

Conclusions. MTWA may reflect the severity of MI, because patients with multiple vessel disease (especially with SI and LMS) have higher MTWA level, which reduces after CABG.

Does Synthesized Lead V9 Reflect Left Atrial Activity During Atrial Fibrillation?

¹X. Zhu, ¹Y. Yoshida, ²D. Wei, ²K. Fukuda and ²H. Shimokawa

¹Biomedical Information Technology Lab, Aizu-Wakamatsu, Japan,

² School of Medicine, Tohoku University, Sendai, Japan

Email: zhuxin@u-aizu.ac.jp

Keywords: Atrial fibrillation, dominant frequency, frequency analysis, intracardiac electrogram, and posterior lead.

Introduction. It is reported that left-to-right atrial gradient in atrial fibrillation (AF) subjects could be useful to identify the culprit chamber (left or right atrium) for AF maintenance. Previous studies have demonstrated right-sided precordial leads could reflect mostly right atrial (RA) activity, while posterior lead V9 could do mostly left atrial (LA) activity. We established 18 synthesized lead ECG which enabled us to extrapolate posterior leads V7-9 and right-sided precordial leads (V3R-V5R) through standard 12-lead ECG. We conducted a preliminary study on whether synthesized leads are able to evaluate both atrial activities during atrial fibrillation.

Methods and Materials. We recorded the standard 12-lead ECG, posterior leads V7–V9, right-sided precordial leads V3R–V5R and intracardiac electrograms (EGM) in the RA, LA and coronary sinus (CS) simultaneously from 1 male subject with paroxysmal AF before pulmonary vein isolation. In order to perform frequency analysis of fibrillatory waves, AF activities in surface ECGs were obtained in a QT-based method, which does not require QRS and T wave subtractions. Furthermore, intracardiac EGMs were rectified for frequency analysis. Finally, the corresponding dominant frequency (DF) was estimated from the peak frequency in 4-9 Hz of each lead's fibrillatory wave or EGM's FFT. Then, we confirmed the correlativity among DFs in intracardiac leads, 18 recorded leads, and synthesized additional leads

Results. The DFs in LA from intracardiac ECGs in CS and LA (5.1 and 5.0 Hz) were consistent with that in lead V9 (5.1 Hz). Furthermore, that in synthesized lead V9 showed the close value (5.0 Hz). Furthermore, the DF in intracardiac RA (4.8 Hz) was close to that in V1 (4.8 Hz), compared to those in V3R-V5R.

Conclusions. Synthesize lead V9 could evaluate the LA activity, and help in monitoring AF and identifying ablation sites through combining with the standard 12-lead ECG.

Acute Effect of Caffeine on Heart Rate Variability in Young Healthy Subjects

¹T. Princi, ²K. Cankar, ²V. Starc, ¹V. Grill

¹Department of Life Sciences, University of Trieste, Trieste, Italy

² Insitute of Physiology, Faculty of Medicine, University of Ljubljana,
Ljubljana, Slovenia
Email: tprinci@units.it

Keywords: Caffeine; heart rate variability; healthy volunteers.

Introduction. The caffeine is one of the most widely used pharmacologically active substances. It has many different physiological effects on the cardiovascular function. Also the cardiac autonomic control could be altered by caffeine consumption. However, findings regarding the effect of caffeine consumption on cardiac autonomic nervous system (ANS) activity are controversial. The aim of the present study was to assess the effects of caffeine on cardiac ANS in young healthy subjects.

Methods and Materials. In sixteen healthy volunteers (7 women), age 24-35, the electrocardiogram (ECG) was recorded continuously at rest before as well as 30 min and 60 min after caffeine ingestion (200 mg of caffeine in 50 ml of water). Before each the beginning of ECG registration the arterial blood pressure was measured. As assessment of cardiac ANS activity the power spectral analysis (autoregressive spectra) and the Poincaré plot analysis of the heart rate variability (HRV) were used. Autoregressive spectra were evaluated on intervals of 512 points. The powers of low (LF: 0.04-0.15 Hz) and high (HF: 0.15–0.40 Hz) spectral bands were determined. In Poincaré plot analysis SD_1 and SD_2 indexes were used as marker of vagal and sympathetic activities, respectively.

Results. The heart rate did not change significantly after caffeine ingestion. The Poincaré plot SD_1 index significantly increased ($p < 0.05$) 30 min after caffeine consumption, whereas SD_2 significantly increased ($p < 0.05$) after 60 min. No significant modification of LF and HF spectral parameters was detected. The total spectral power significantly augmented after 30 min. The systolic and diastolic blood pressure significantly increased 30 and 60 min compared to values before ingestion.

Conclusions. These results indicate an effect of caffeine on the cardiac ANS activity. It is likely that single moderate caffeine dose can increase vagal and sympathetic function as well as total vago-sympathetic activity in the myocardium.

Electrocardiographic Abnormalities in the Elderly: A Study in a Large in Primary Care Database

**¹M.S. Marcolino, ¹B.C.A. Marino, ¹A.M. Ribeiro, ¹T.G.P. Assis, ²M.B.M. Alkmim,
¹A.L. Ribeiro**

¹Medical School and Telehealth Center, University Hospital Universidade Federal de Minas Gerais, Belo Horizonte, Brazil; Telehealth Network of Minas Gerais, Brazil

²Telehealth Center, University Hospital Universidade Federal de Minas Gerais, Belo Horizonte, Brazil; Telehealth Network of Minas Gerais, Brazil

Email: milenamarc@gmail.com

Keywords: electrocardiography; primary health care; telemedicine; elderly.

Introduction. The proportion of elderly people continues to grow worldwide, especially in the developing countries. This poses a challenge to health policy makers, as disease patterns have been changing. Cardiovascular diseases are the leading cause of disability and mortality worldwide. The electrocardiogram (ECG) is a useful tool to assess the impact of cardiovascular disease in the population context and to guide preventive actions. The objective of this study is to analyse the prevalence of electrocardiographic abnormalities in elderly patients in primary care.

Methods and Materials. In this observational and retrospective study, all 12-lead standard digital ECGs analysed by cardiologists of the Telehealth Network of Minas Gerais, a public telemedicine service in Brazil, from January to December 2011, were assessed. This service attends primary care of 660 cities in the state of Minas Gerais. ECGs were sent by remote healthcare professionals through internet to be analysed by cardiologists who are trained and experienced in the analysis and interpretation of ECG. The prevalence of ECG abnormalities in elderly patients was assessed.

Results. During the study period, 264,324 exams were performed; 33.2% (87,804) of them in elderly patients (median age of 69.9 years, interquartile range 64.6-76.4; 57% women). Hypertension was observed in 48.7% of the patients, diabetes in 9.1%, smoking in 6.4%, and Chagas disease in 3.5%. Only 41.6% of the exams had no abnormalities, and this proportion was significantly lower in octogenarians (27.7%, $p < 0.01$). The mean number of abnormalities was 1.13 ± 1.29 . Atrial fibrillation or flutter was observed in 4.2% of the ECGs; 8.4% in octogenarians. Supraventricular premature beats were observed in 3.8% and ventricular in 4.7%; left bundle branch block in 3.6% and right bundle branch block in 5.5%; left anterior fascicular block in 11.7%, left ventricular hypertrophy in 6.2%; and non-specific repolarization abnormalities in 30.4%. The reason for performing the exam was investigation of chest pain in 63,322 patients (73.2%). Of these, 8.9% had abnormalities related to ischemia, 3.0% of acute ischemia.

Conclusions. This study in a large sample of elderly patients in primary care revealed that electrocardiographic abnormalities are common in this population. The prevalence of atrial fibrillation, which is important to guide the implementation of anticoagulation strategies, is noteworthy.

QRS Complex Patterns in Patients with Obstructive Sleep Apnea

^{1,2}L. Bacharova, ¹E. Triantafyllou, ¹Ch. Vazaios, ³R. Tisko, ³I. Paranicova,
³R. Tkacova

¹Institute of Pathological Physiology, Medical Faculty, Comenius University,
Bratislava, Slovakia

²International Laser Center, Bratislava, Slovakia

³Dept. Respiratory Medicine, Faculty of Medicine, P.J. Safarik University, Kosice,
Slovakia

Email: bacharova@ilc.sk

Background and Objectives. An increased rate of ventricular arrhythmias and conduction disturbances is documented in patients with obstructive sleep apnea (OSA), being related to altered electrical properties of myocardium and altered sequence of depolarization creating a substrate for triggering arrhythmias. We aimed to evaluate the QRS complex morphology in patients with OSA that could be potentially linked to arrhythmias..

Methods. The study population consisted of 199 consecutive patients examined in the sleep laboratory, divided into quartiles according to the apnea/hypopnea index (AHI): Group Q1: AHI 0.7-1.9 #/h; Group Q2: AHI 11.0-32.3 #/h; Group Q3: AHI 32.3-63.0 #/h; Group Q4: AHI 65.1-157.8 #/h. Resting 12-lead ECG was recorded, the QRS parameters analyzed included QRS amplitude in individual leads, the QRS spatial vector magnitude (QRSmax), electrical axis (EA), three ECG criteria for left ventricular hypertrophy (ECG-LVH): Sokolow-Lyon index, Cornell voltage and Gubner criterion, and two ECG criteria for right ventricular hypertrophy (ECG-RVH): Sokolow-Lyon index for RVH and Butler-Leggett formula.

Results. There were no significant differences in QRSmax values between the groups. The occurrence of ECG-LVH was low (total 7%), on the other hand 96 % of patients showed signs of ECG-RVH. The values of EA were significantly shifted gradually to the left (Q1: 40.1±19.8°; Q2: 34.5±18.0°; Q3: 27.6±15.3°; Q4: 31.6±16.2°). Additionally, QRS morphology showed a variety of intraventricular conduction defects, including QRS notching, non-specific conduction defects and patterns of left/ or right bundle branch blocks.

Conclusions. The OSA patients displayed significant changes in QRS complex morphology suggestive of depolarization sequence deterioration indicative of considerable electrical remodeling that could be potentially linked to the arrhythmia occurrence.

Support: Grants VEGA 1/0111/12 and APVV 0134-11.

QRS Complex Characteristics in Patients with Eisenmenger Syndrome with Pre- and Post-Tricuspid Defects

^{1,2}T. Valkovičová, ³M. Kaldararová, ^{1,2}M. Boháčková, ⁴L. Bachárová,
^{1,2}I. Šimková

¹Dept. of Cardiology and Angiology, Slovak Medical University, Bratislava, Slovakia

²National Institute of Cardiovascular Diseases, Bratislava, Slovakia

³National Institute of Cardiovascular Diseases – Children's Cardiac Center, Bratislava, Slovakia

⁴ International Laser Center, Bratislava, Slovakia

Email: valkovicova.tatiana@gmail.com

Keywords: Eisenmenger syndrome; right ventricular hypertrophy; ECG; echocardiography; brain natriuretic peptide.

Introduction. Eisenmenger syndrome (extreme pulmonary arterial hypertension due to congenital shunt lesion) results in severe right ventricular (RV) pressure overload. The prognosis of patients depends on changes in RV morphology and function resulting from the shunt location. In this study we analyzed ECG in relation to echocardiographic parameters (ECHO) and serum N-terminal brain natriuretic peptide concentration (BNP) in patients with pre-tricuspid (pre-TD) and post-tricuspid defects (post-TD).

Methods and Materials. 19 patients with pre-TD defect (14 F/ 5M, median age 57 years) and 24 patients with post-TD defect (16 F/ 8M, median age 41 years) were included in the study. The following ECG parameters were analyzed: the Sokolow-Lyon criterion for RV hypertrophy (SL-RVH), the Butler-Leggett formula (BL), and the maximum QRS spatial vector magnitude (QRSmax). The RV diameter (RVd), RV wall thickness (RVWT), the tricuspid annular plane systolic excursion (TAPSE) and RV ventricular fractional area change (FAC) were measured echocardiographically. The serum BNP concentration was determined by an electrochemiluminescence method.

Results. The SL-RVH and BL exceeded the upper normal limits; there was no significant difference between the groups. Significant difference was found in QRSmax between the pre-TD and post-TD groups (16.6±6.8 mm and 25.2±8.9 mm, respectively). The RVWT showed signs of RVH being significantly higher in the post-TD group (8.7±2.1 mm and 10.4±2.9 mm, respectively). RVd was significantly bigger in the pre-TD group, showing signs of dilatation (42.9±10.05 mm and 28.5±6.9 mm). The TAPSE and FAC values were within normal limits. The BNP concentrations were highly above the upper normal limits in both groups, no significant difference was observed.

Conclusion. While echocardiography showed significant difference in the anatomical configuration of RV between groups, the functional echocardiographic parameters and the classical ECG criteria for RVH did not differ. The QRSmax values were associated inversely with RV dilatation in the pre-TD group.

Holter ECG Findings in Patients with Medial Arterial Calcinosi

¹L. Gaspar, ²I. Gasparova, ¹M. Makovnik, ¹P. Gavornik, ¹A. Dukat

¹2nd Department of Internal Medicine, Comenius University, Bratislava, Slovakia

²Institute of Medical Biology, Genetics and Clinical Genetics, Comenius University,
Bratislava, Slovakia

Email: ludovitgaspar@email.com

Keywords: medial calcinosis; Holter ECG; cardiac arrhythmia; ischemia.

Introduction: Medial arterial calcinosis (Mönckeberg's sclerosis) is common in patients with diabetes mellitus and chronic kidney disease. It is an independent risk factor for cardiovascular and all-cause mortality.

Aim of the study: To determine the incidence of cardiac arrhythmia and ischemia with the use of Holter ECG monitoring in a group of patients with medial calcinosis.

Patients and Methods: 22 individuals (10 men and 12 women) with the mean age of 59 years were examined. The age range was 50 – 85 years. Sixteen patients had diabetes mellitus. Nine patients had chronic renal disease, five of them were in the 4th stage according to K/DOQI classification. Holter ECG monitoring with an average duration of 22.16 hours was carried out using Marquette-Hellige General Electric (USA) devices. Medial calcinosis was defined as ankle-brachial pressure index (ABI) with a value of 1.3 and more.

Results: Only 2 patients (9 %) from our group had normal Holter ECG records, without arrhythmia or ischemia. Complex form of arrhythmia Lown IIIB or IVA was in 11 patients (50 %), atrial fibrillation in 6 (27 %), 2nd degree A-V block Mobitz type I in 1 patient (4.5 %) and myocardial ischemia in 6 persons (27 %).

Conclusions: In our study we found significant cardiac arrhythmia and/or ischemia in 91 % of investigated patients with medial arterial calcinosis. Our results confirm the importance of Holter ECG monitoring in this patients, because of increased cardiovascular risk, including sudden cardiac death.

Repolarization in Chronic Kidney Disease: Experimental Study

¹S. Kharin, ¹M. Strelkova, ¹V. Krandycheva, ¹A. Tsvetkova, ²K. Shumikhin, ¹D. Shmakov

¹Lab. of Cardiac Physiology, Institute of Physiology of the Komi Science Centre of the Ural Branch of the Russian Academy of Sciences, Syktyvkar, Russian Federation,

²Department of Biomedical Disciplines, Komi Branch of Kirov State Medical Academy, Syktyvkar, Russian Federation

Email: s.kharin@physiol.komisc.ru

Keywords: repolarization; heart failure; subtotal nephrectomy; chronic kidney disease; animal model.

Introduction. Chronic kidney disease in humans is associated with a risk of fatal ventricular arrhythmias. Ventricular arrhythmias are triggered by altered cardiac repolarization. The most commonly used model of chronic kidney disease is subtotal nephrectomy (SNx). In this study, we aimed to investigate ventricular repolarization in SNx rats compared with sham-operated controls using a multi-channel mapping system.

Methods and Materials. Adult female Wistar rats underwent two-stage SNx or sham operation. Eight weeks after surgery, ventricular epicardial electrograms and hemodynamic parameters were recorded in situ. Hearts were examined histologically.

Results. Histologic examination showed inflammatory cell infiltration, degeneration of myocytes, fibrosis, and clusters of hypertrophied myocytes in hearts from SNx but not sham-operated control rats. Systolic and diastolic dysfunction was developed in the SNx rats. The SNx rats had a significantly longer QT interval compared with sham-operated controls. Activation–recovery intervals (ARIs) were longer in hearts from the SNx rats compared with controls. After SNx, ARI prolongation at the ventricular base was greater than that at the ventricular apex; ARIs in the right ventricle were prolonged to a greater extent than ARIs in the left ventricle. The global ARI dispersion was greater in the SNx rats compared with controls. After SNx, local ARI dispersions were found to increase non-uniformly; the greatest increase was observed at the apex of the right ventricle; interregional differences in the local ARI dispersion were reduced.

Conclusions. Increased heterogeneity of ventricular repolarization due to inhomogeneous prolongation of ventricular repolarization was demonstrated in the rat SNx model of chronic kidney disease. This may account for a high risk of fatal ventricular arrhythmias in patients with renal failure. This study was supported by the Ural Branch of the Russian Academy of Sciences ('Basic Sciences to Medicine' program, project No. 12-P-4-1003).

**POSTERS:
NEW METHODS AND TECHNOLOGIES
IN ELECTROCARDIOLOGY**

The Lead Fields of the Standard 12-Lead ECG

^{1,2,3}M. Potse

¹Carmen Team, Inria Bordeaux Sud-Ouest, Bordeaux, France

²LIRYC-Institute of Cardiac Rhythmology and Modeling, Bordeaux, France

³Center for Computational Medicine in Cardiology, Università della Svizzera italiana,
Lugano, Switzerland

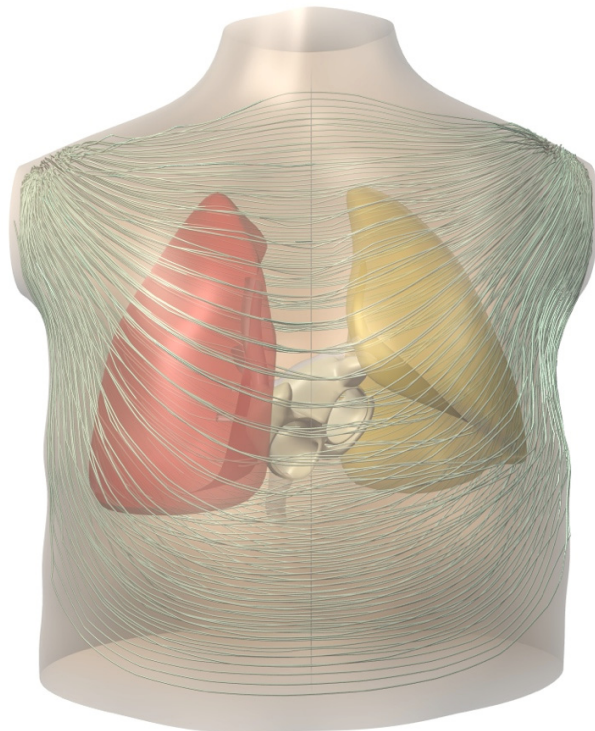
E-mail: mark.potse@inria.fr

Keywords: Electrocardiogram; lead field; lead vector; teaching; visualization.

Introduction. Lead fields are a generalization of the classical concept of lead vectors, and can be used to understand how cardiac sources translate into deflections in a given ECG lead. Whereas lead vectors are gross approximations, lead fields are mathematically precise and take the shape and inhomogeneities of the torso into account. Over 60 years ago, lead fields have been studied using fluid mappers. These devices work in 2 dimensions and have limitations with respect to the representation of tissue anisotropy and inhomogeneity of electrical resistance. Using modern computational tools, lead fields can be studied in more detail and in three dimensions.

Methods and Materials. The lead fields of the standard 12 leads were computed in a complete and realistic model of the human heart and torso at 1 mm resolution. The fields were visualized as streamlines using 3D rendering techniques.

Results. As might be expected, the lead fields were similar to what has been found previously. *The figure shows the lead field of lead I in a truncated torso model with the electrodes attached to the shoulders.* A surprisingly small difference was found between the fields of leads II and III. In addition, the 3D renderings demonstrated in an intuitive way how the three limb electrodes that form Wilson's Central Terminal (WCT) create a virtual negative terminal which changes location depending on which positive terminal is used. This virtual electrode was located behind the heart in case the positive electrode was one of Wilson's precordial electrodes, V1 to V6. When the positive electrode was on the back of the torso, the lead field diverged strongly inside the ventricles.



Conclusions. More than half a century after their inception lead fields are not only a powerful means to illustrate some well-known electrocardiographic concepts, but continue to provide new insights. In particular the asymmetry in the behaviour of anterior and posterior leads referenced to WCT has not been shown in this way before.

Assesment of AF Capture during Antitachycardia Pacing by Using Largest Lyapunov Exponent. Insights from a Biophysical Model

^{1,2}A. Luca, ¹J-M. Vesin, ²A. Vlad

¹Applied Signal Processing Group, Swiss Federal Institute of Technology, Lausanne, Switzerland

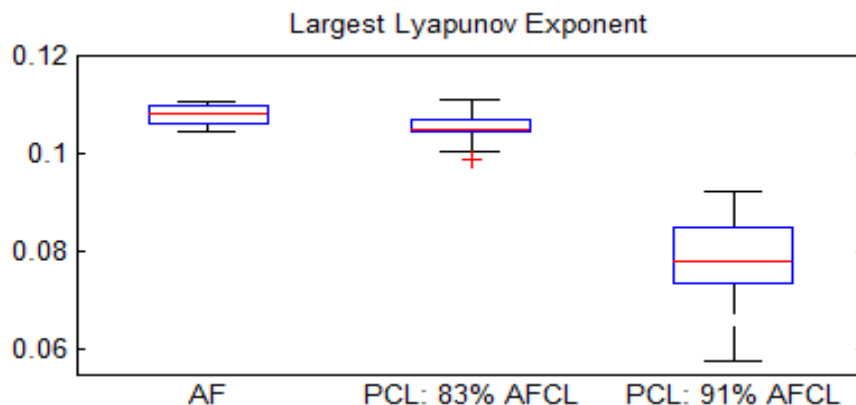
²Applied Electronics and Engineering Information Department, University POLITEHNICA of Bucharest, Bucharest, Romania
Email: adrian.luca@epfl.ch

Keywords: atrial fibrillation; largest Lyapunov exponent; time series analysis; atrial biophysical computer model.

Introduction. During atrial fibrillation (AF), the typical organized electrical activity of the heart is replaced by disorganized, chaotic electrical activity. This led to an interest in investigating the potential of chaos theory for the quantification of AF complexity as a marker of pacing effectiveness. By means of the Largest Lyapunov Exponent (LLE) and a biophysical computer model, we analysed the complexity level of the electrical activity during AF and during antitachycardia pacing (ATP). The biophysical model was based on a homogenous tissue in which the Luo-Rudy I model was adjusted to mimic electrical remodelling as observed in patients suffering from permanent AF.

Methods and Materials. A database of simulated AF (SAF) initial conditions was created by selecting instantaneous transmembrane potentials during ongoing SAF and keeping them as initial conditions (IC) for the subsequent simulation of ATP. For each IC, 60 seconds of rapid pacing from the septum area (at different pacing cycle lengths - PCL as a percentage of the AF cycle length - AFCL) were applied and transmembrane potentials time series in the right atrial anterior wall were recorded. The LLE was separately computed during AF and ATP using Rosenstein's algorithm.

Results. The figure shows that the LLE decreased during ATP relative to AF ($p < 10^{-5}$, Kruskal-Wallis test). Also, the significant differences for different PCLs (0.105 ± 0.003 vs 0.078 ± 0.009 , $p < 10^{-7}$, K-S test) indicate that LLE can guide the choice of PCL for ATP (a smaller LLE means a more regular atrial activity, *i.e.* here a good AF capture by ATP).



Conclusions. These results suggest that LLE may serve as indicator of the AF complexity and also as a useful discriminating metric in automatic assessment of AF capture during ATP.

Derivation of McFee-Parungao Orthogonal Leads from Standard Electrocardiogram

¹V. Trunov, ¹E. Aidu, ²V. Fedorova, ³E. Blinova, ³T. Sakhnova

¹Institute for Information Transmission Problems RAS, Moscow, Russia

²Ates Medica Soft, Moscow, Russia

³Cardiology Research Complex, Moscow, Russia,

Email: trunov@iitp.ru

Keywords: derived orthogonal ECG; McFee-Parungao lead system; VCG; DECARTO.

Introduction. Numerical methods of deriving orthogonal vectorcardiogram (VCG) from the standard 12-lead electrocardiogram and vice versa are widely used in clinical practice. In the Cardiology Research Complex (Moscow), a great deal of ECG recordings were made in the McFee-Parungao lead system. These data were archived and now form a large and potentially helpful database. Adequate instruments to perform mutual transformations of ECG records obtained in the Frank, McFee-Parungao or conventional lead systems are required. The aim of this study was to develop and evaluate linear transformations for deriving the McFee-Parungao VCG from standard 12-lead or Frank ECG.

Methods and Materials. Sequentially recorded 12-lead ECGs and orthogonal McFee-Parungao ECGs of 195 patients were analyzed. VCG and respective 12-lead ECG were aligned to synchronize the signals. Then correcting linear transformations (CLT) were found for the best approximation of measured signals on the learning part of data sample. The accuracy of the VCG derivation was evaluated on the test sample that was not used to estimate transformation parameters. The mean squared distance between spatial-temporal curves of the derived and true VCGs and mean squared errors of the derived VCG parameters were used as accuracy measures of transformations.

Results. Mean squared distances between the derived and true VCG components demonstrated the advantage of CLT for derivation of McFee-Parungao VCG over Frank-based transformations (Kors, Bemmel, and Dower). Similar results were obtained for derivation of some integral parameters of VCG, including QRS-T angle and ventricular gradient.

Conclusions. Frank-based transformations usually underestimate the amplitude characteristics of VCGs recorded in the McFee-Parungao system. Correcting linear transformations can significantly reduce the distance between derived and true measured VCG presented as spatial-temporal curves and improve the accuracy of diagnostic parameters derived from vectorcardiographic and decartographic data.

Prognostic Value of the QRS-T Angle Measured during Exercise Test

¹M. Kania, ²R. Zaczek, ³M. Kobylecka, ¹R. Maniewski

¹Nalecz Institute of Biocybernetics and Biomedical Engineering, Warsaw, Poland,

²Department of Cardiology, Medical University of Warsaw, Warsaw, Poland

³Department of Nuclear Medicine, Medical University of Warsaw, Warsaw, Poland

Email: mkania@ibib.waw.pl

Keywords: body surface potential mapping; TCRT; exercise test; coronary artery disease; risk factor, ejection fraction.

Introduction. The total cosine R-to-T (TCRT) is a vectorcardiographic measure of differences in propagation directions of depolarization and repolarization wavefronts in the heart. The high value of QRS-T angle reflects increased heterogeneity of repolarization process. The aim of study was to assess the prognostic value of the TCRT parameter measured during exercise stress test in cardiac insufficiency.

Methods and Materials. The high-resolution body surface potential maps (HRBSPM) were measured during exercise test on supine ergometer in the group of 107 patients. The TCRT was computed from averaged ECG signals at maximal workload. The prognostic value of TCRT parameter was determined based on the results of SPECT and echocardiography. The diagnostic criterion was calculated as a maximal value of the product of the specificity and the sensitivity.

Results. The significant difference ($p=0.0001$) in TCRT parameter was obtained for HRBSPM measured at peak exercise for low ejection fraction (LVEF \leq 45%, TCRT=114 \pm 27°) and high EF (LVEF $>$ 45%, TCRT=92 \pm 25°). The sensitivity and specificity in detection of patients with low EF was 69% for an optimal threshold value of TCRT \geq 102°. The differences in TCRT between patients with positive and negative SPECT results were not significant (100 \pm 28° vs. 95 \pm 28°; $p=0.53$). This result is also reflected in poor values of sensitivity and specificity in recognition of patients with ischemic heart disease (c.a. 50%).

Conclusions. Increased QRS-T angle was associated with low left-ventricular ejection fraction. The statistically significant difference of TCRT values in patients with low EF and high EF may suggest high prognostic value of TCRT parameter in risk assessment of cardiac arrhythmia. Unfortunately no discrimination power of TCRT parameter to separate patients with and without myocardial ischemia was found.

Comparison of Dubois and Base-Apex Lead Methods to Calculate QRS Angle (Mean Electrical Axis) in Thoroughbreds

C. Fré da Costa, N. Samesima, C. A. Pastore

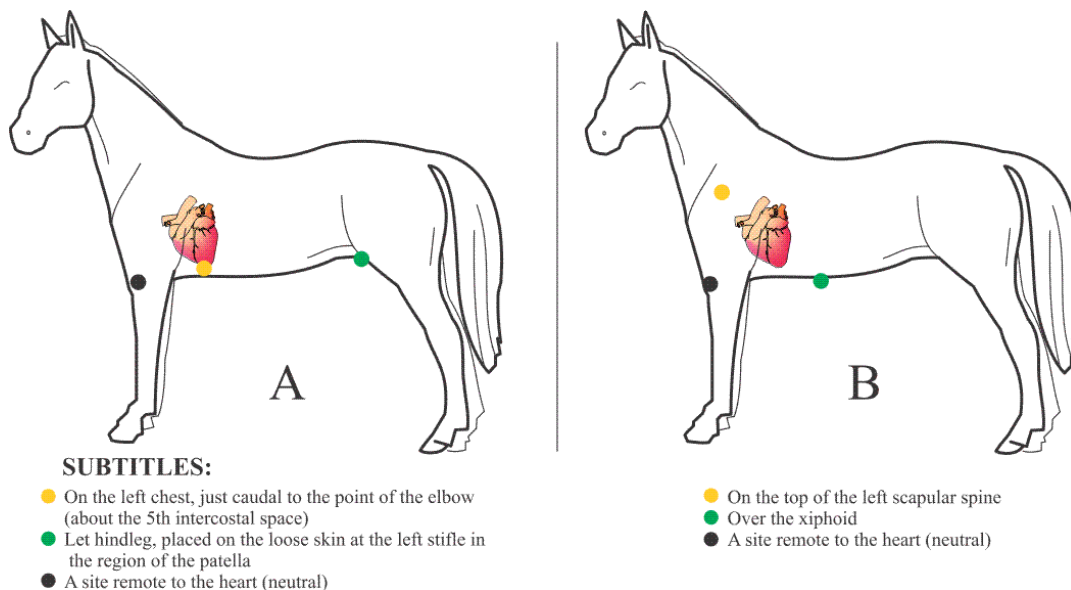
Heart Institute (InCor) –HCFMUSP, São Paulo, Brazil

Email: ecg_pastore@incor.usp.br

Keywords: Electrocardiogram; QRS angle measurement; Equines.

Introduction. Methods to evaluate the cardiac mean electrical axis in equines are controversially used in veterinary literature. Studies describe two distinct lead positioning systems, with different results and no standardization of technique. Our study compared results of QRS complex angles obtained by the base-apex and the Dubois lead systems.

Methods and Materials. Fifty-three Thoroughbred racehorses kept at the São Paulo Jockey Club underwent rest ECG with ten leads (DI, DII, DII, aVR, aVL, aVF, RV2, V2, V4 and V10) placed according to Figure 1 (Part A - base-apex, Part B - Dubois lead system), in normal quadruped position. All ECG measurements were performed by a sole observer (CFC). Leads DI and aVF were used to calculate $\hat{S}\hat{A}\hat{Q}\hat{R}\hat{S}$ (α tangent). Also compared were the results obtained by the classic table developed for dogs and cats by Tilley, using leads DI and DIII. Paired T test (Wilcoxon) was used to compare results, with $p \leq 0.05$.



Results. Thoroughbreds' mean age was 4.0 ± 1.3 y.o., mean weight 474 ± 32 kg, and mean height 1.62 ± 0.04 m. Mean QRS angles found in leads DI and aVF were (base-apex and Dubois, respectively) $-15.0 \pm 11.3^\circ$ vs $-79.9 \pm 7.4^\circ$ ($p < 0.0001$). $\hat{S}\hat{A}\hat{Q}\hat{R}\hat{S}$ obtained by DI/DIII were (base-apex and Dubois, respectively) $+135.1 \pm 90.9^\circ$ vs $-81.1 \pm 3.6^\circ$ ($p < 0.0001$). The base-apex method showed statistically significant difference between $\hat{S}\hat{A}\hat{Q}\hat{R}\hat{S}$ measured in DI/aVF and DI/DIII ($p < 0.0001$), while Dubois did not ($p = 0.9$).

Conclusion. Lead positioning by the Dubois method improves centralization of the equine heart. Results obtained by this method are more consistent with the equine anatomy. Provided the use of Dubois, the dog and cat Table can be used for equines as well.

Heart Rate Variability Expressed by Poincaré Plot in Metabolic Syndrome

A. Drkošová, J. Kozumplík

Department of Biomedical Engineering BUT, Brno, Czech Republic

Email: drkosova@phd.feec.vutbr.cz

Keywords: heart rate variability; metabolic syndrome; Poincaré plot;

Introduction. Heart rate variability, considered as an indicator of autonomic nervous function shows differences between healthy persons and patients with metabolic syndrome.

Methods and Materials. Data from 40 patients with metabolic syndrome and 48 healthy subjects were obtained in the 1. Internal Cardioangiology unit of the University Hospital sv. Anna in Brno during 5 min in horizontal position, followed by 8 min tilt (75°) and again 5 min horizontal position. The controlled breathing of the subjects was 6 times per minute (tilt6) and 20 times per minute (tilt20) respectively. Poincaré plots and calculated indexes SD1 and SD2 were used to evaluate the differences between heart rate variability in these two groups.

Results. The SD1 and SD2 showed lower values during rest in patients with the metabolic syndrome and a smaller decrease of these parameters occurred also during the tilt with respect to values obtained in the control group. This change can be expressed by the difference Δ SD1 and Δ SD2 before and during the tilt. In average Δ SD1 and Δ SD2 show higher values in healthy subjects as compared to patients with metabolic syndrome. The most important difference was observed in Δ SD1 obtained from the tilt20 signals. Further on, calculating SD1 changes in subsequent 1 min intervals showed that the short-term variability decreases faster and more in healthy subjects than in the metabolic syndrome group after tilting and increases again faster after resuming the horizontal position.

Conclusions. The results show that the average value of the decrease of short- (Δ SD1) and long-term (Δ SD2) variability is greater in healthy subjects than in subjects with metabolic syndrome. In conclusion, the Δ SD1 obtained from a signal measured in tilt in controlled breathing of 20 times per minute may perhaps be able to distinguish between healthy persons and patients with metabolic syndrome if it is correctly used.

Assessment of the Number of Ischemic Lesions from Body Surface Potential Maps

M. Teplan, J. Švehlíková, M. Tyšler

Institute of Measurement Science, Slovak Academy of Sciences, Bratislava, Slovakia,
Email: michal.teplan@savba.sk

Keywords: body surface potential maps; discriminant analysis; geometrical and statistical map properties; number of lesions.

Introduction. Patients with ischemic heart disease and atherosclerosis may suffer from one or more simultaneously occluded coronary arteries. It would be helpful to have preliminary information about the number of ischemic lesions without an invasive examination. As multiple-lead ECG measurements on the thorax can provide more information than the standard 12-lead ECG, difference STT integral body surface potential maps (DI BSPMs) were employed to assess the information about possible number of lesions. In this study various characteristics of simulated DI BSPMs were employed to discriminate cases with single and double modelled lesions with changed repolarization.

Methods and Materials. One or two lesions in different positions in the ventricular myocardium were modelled and corresponding BSPMs were calculated on the surface of an inhomogeneous torso model using the multiple dipole cardiac generator DI BSPMs were computed by subtracting the normal integral BSPM from an integral BSPM computed from the heart with one or two modelled lesions. In the numerical ventricular model 96 pairs and 48 single lesions were modelled and corresponding BSPMs were computed. Various geometrical and statistical properties of DI BSPM were used as features for discriminant analysis. Feature selection was realized by greedy forward selection algorithm. Quadratic Fisher discriminant analysis with cross-validation was then used for determining the number of lesions in each case.

Results. Taking into account just one best performing feature, the overall error rate for distinguishing number of lesions was as high as 25.2 %. More than 100 features were specified and tested. Their dimensionality was reduced by a feature selection algorithm resulting in 12 features as the optimal number for distinguishing DI BSPM representing two lesions from maps representing a single lesion. The overall error rate was 4.1 %, with partial errors 9.6 % for misclassification of single lesions and 1.2 % for misclassification of double lesions.

Conclusions. Discriminant analysis based on exploitation of geometrical and statistical properties of integral BSPMs may be helpful in successful identification of the number of ischemic lesions.

**BSPM Band Patterns
for Diagnosing Intraventricular Conduction Disturbances
in Young Adults with Chronic Kidney Disease Treated with Hemodialysis**

¹K. Laszki-Szcząchor, ¹M. Sobieszcańska, ²D. Zwolińska, ¹H. Filipowski,
¹M. Tabin, ²D. Polak-Jonkisz

¹Department of Pathophysiology, Wrocław Medical University, Wrocław, Poland

²Department of Paediatric Nephrology, Wrocław Medical University, Wrocław,
Poland

Email: malsobie@poczta.onet.pl

Keywords: BSPM; VAT; bundle branch block; chronic kidney disease; hemodialysis.

Introduction. Chronic kidney disease is inevitably connected with a risk of cardiovascular complications. Non-invasive methods for detecting initial stage of those conditions are of great clinical importance. Goal of the present study was to create from BSPM recordings the simplified ‘band patterns’ useful in searching discrete intraventricular conduction disturbances in young adult patients with CKD subjected to hemodialysis treatment.

Methods and Materials. The study group consisted of 10 young patients (the mean age: 16.8 ± 2 yrs) with CKD on hemodialysis therapy. A 87-lead HPM-7100 Fukuda Denshi system for BSPM recordings was used. Based on values of ventricular activation time (VAT) registered at the all body surface electrodes, colorful patterns, in which the particular colorful bands corresponded to various VAT values, were created. Application of those VAT patterns yields a spatial display of distribution of the ventricular activation progression in the examined CKD patients.

Results. Using the data obtained in our previous investigations from the young adults with CKD, the VAT based band patterns for various kinds of blocks of His bundles were established. As a reference, the colorful band patterns for intraventricular conduction were obtained from the control normal subjects. The concept enables to compare the VAT values colorful bands taken from the individual examined CKD patient with the band patterns available both for normals and for various types of intraventricular conduction disturbances. In such manner, it is easy to match the new case with the given patterns and detect quickly some impairments.

Conclusions. VAT based band patterns make it possible to perform a quick and non-invasive screening of intraventricular conduction disturbances in hemodialyzed young patients with chronic kidney disease.

Analysis of the Ventricular Depolarisation Using Autocorrelation Maps

M. Trnka, K. Kozlíková

Institute of Medical Physics, Biophysics, Informatics and Telemedicine, Faculty of
Medicine, Comenius University, Bratislava, Slovak Republic
Email: michal.trnka@fmed.uniba.sk

Keywords: body surface potential mapping; QRS complex; autocorrelation maps; controls.

Introduction. Voltage distributions over the whole chest surface can be displayed in form of a set of isopotential maps (IPMs) that can be analysed quantitatively using the Pearson's correlation coefficient allowing the construction of autocorrelation maps (ACMs). The aim of this retrospective study was to analyse the ACMs in young adults in time normalised QRS complex.

Methods and Materials. The QRS complex duration of each subjects was divided into 20 equidistant parts. We constructed 21 isopotential maps from 24-lead system after Barr in 90 controls (42 men) without cardiovascular diseases, aged (18.6 ± 0.4) years. For each QRS complex, every IPM was compared with every IPM using Pearson's correlation coefficient r . These values were displayed in form of ACMs, squared graphs with values $r = 1.000$ on the main diagonal and symmetrical according to it.

Results. The mean QRS complex duration was (92 ± 12) ms. The mean correlation coefficients of single ACMs were 0.087 ± 0.044 (range 0.011 – 0.207). The high positive correlation $r \geq 0.900$ covered in average (26 ± 5) % of the whole ACM (mean 0.970 ± 0.004 ; 15 % – 40 %). Negative correlations occurred mainly parallel to the main axis with the mean value -0.543 ± 0.054 (down to $r = -0.994$). We identified three basic types of ACMs according to the form of regions with positive and negative correlations. In the type I, high positive correlation at beginning of the QRS complex and along the main diagonal changed into a negative correlation reaching the borders of the ACM (15 men, 12 women; 30% of all maps). In the type II, the negativity was followed by positivity at the borders of the ACM (23 men, 32 women; 61%). In the type III, the positivity was followed by a second negativity in the corners of the ACMs (4 men, 4 women; 9%).

Conclusions. These ACMs display the large normal variability in ventricular depolarisation by eliminating the influence of the torso.

This work was partially supported by the VEGA project 1/0727/14 from MESRS SR.

Quantitative VCG and BSPM Repolarization Parameters Evidence Increased Sympathetic Activation of the Ventricular Myocardium in Different Adrenergic Situations

V. Regecová, E. Kellerová

Institute of Normal and Pathological Physiology, Slovak Academy of Sciences,
Bratislava, Slovak Republic
Email: valeria.regecova@savba.sk

Keywords: Ventricular repolarization; VCG and BSPM; Sympathetic activation; Stress; Prehypertension; Obesity.

Introduction. Participation of the sympathetic nervous system (SNS) in normal or pathological cardiovascular regulations is documented mainly by blood pressure (BP) and heart rate (HR). However, these measures do not pick-up the site-specific sympathetic drive of the ventricular myocardium. The aim of our experiments was to find out whether previously proposed parameters characterizing ventricular repolarization will be sensitive enough to detect the presumptive effect of SNS hyperactivity on the ventricular myocardium in different situation.

Methods and Materials. PC based electrocardiographic system was used to record the VCG and BSPM. From a selected single beat the maximal spatial vector of ventricular depolarization(sQRSmax) and repolarization(sTmax), their spatial angle, the peak-to-trough amplitudes of the respective BSPM (QRS, STT, QRST)ampl, the RR and QTc intervals were evaluated. Simultaneously the BP was measured. A total of 100 young men (median age 18 y.) with no cardiovascular symptomatology, participated in the study, divided in subgroups, to investigate the effect of different sympathergic situations (psychoemotional stress, head-up tilting, high normal BP, obesity).

Results. The cardiovascular response to the forced MA was in 67 % of subjects accompanied by negativization of the integral repolarization BSPM and diminution of sTmax. Head-up tilting provoked an increased HR and BPdiast with an evident decline of sTmax and highly significant STT and QRST BSPMampl decrement. In prehypertensive ss. compared to the sub-group with optimal BP, decreased magnitudes of the repolarization parameters sTmax and QRST BSPMampl (by more than 20%) were found, at rest, as well as during the MA. Analogical differences were evident in overweight and obese subjects.

Conclusions. The discriminative power of the VCG and BSPM repolarization parameters was strong enough to distinguish the psychoemotional and postural changes in the cardiac electric field. Over the dividing value of the optimal casual BP, already in the class defined as normal and high normal and in the obese, the repolarization parameters, point to an increased sympathetic drive of ventricles, similar to that, observed under mental or physical strain. This finding is in coincidence with the concept of an increased cardiac output and enhancement of myocardial contractility in the initial stage of hypertension in adolescents.

Comparison of Propagation of Atrial Excitation with the Cardiopotential Distribution on the Body Surface of Fish

S. Smirnova, I. Roshchevskaya, M. Roshchevsky

Laboratory of Comparative Cardiology, Komi Science Centre UD RAS, Syktyvkar,
Russia

Email: smirnova.sl@mail.ru

Keywords: atrial depolarization, body surface potential map, epicardium, Atlantic cod *Gadus morchua*.

Introduction. This research was aimed at studying the sequence of depolarization along the atrial epicardium and formation of the cardioelectric field on the body surface of Atlantic cod *Gadus morchua*.

Methods. The study was carried out on nine Atlantic cod *Gadus morchua*. We analyzed spatial-temporal characteristics of the body surface potential map (BSPM) and sequence of atrial epicardial depolarization of fish.

Results. The initial zone of depolarization appeared on the atrial epicardium of fish before the occurrence of the P-wave in the ECG II. During the ascending phase of the P-wave the excitation wave evenly spread from the caudal part of the dorsal side to the cranial part in the right-lateral area. At the peak of the P-wave and during the first half of the descending phase of the P-wave the dorsal side and the caudal part of the ventral side in the right-lateral area were depolarized.

Conclusions. Initial phases of atrial depolarization are projected on BSPM by the distribution of zones of positive and negative cardiopotentials before the beginning of the P-wave in the ECG. The location of zones of positive and negative cardiopotentials and the movement of extrema on the body surface reflect the movement of the excitation wave along the atrium from the venous sinus to the heart ventricle of fish.

The work is supported by the grant 09-0498814-a Russian Science Support Foundation.

First *In Vivo* Application of Tungsten Dotted Tubing in Cardiac Cryoablation

¹M. Stöger, ²G. Fischer, ²C.N. Nowak, ¹F. Hintringer

¹Division of Internal Medicine III / Cardiology, Medical University Innsbruck, Innsbruck, Austria

²AFreeze GmbH, Innsbruck, Austria
Email: markus.stoeger@i-med.ac.at

Keywords: arrhythmia; cryoablation; intracardiac electrograms.

Introduction. Cryoablation catheters have gained increasing interest for the treatment of arrhythmia, especially atrial fibrillation. Cryo-tip catheters for treatment of other types of supraventricular tachycardia display a limited spatial ECG resolution as they contain a large metallic boiling chamber at their tip. This drawback might be overcome by the use of Tungsten dotted polyurethane.

Methods and Materials. Tungsten particles (size <10 µm) were added to a polyurethane tubing (outer diameter 7 Fr) for increasing its thermal conductivity while preserving the electrical isolation properties of a plastic tubing. This tube was mounted on a steerable 7 Fr cryocatheter with a cooling power of approximately 15 W (refrigerant: nitrous oxide). On the distal end the tube was closed by a metallic distal electrode and two additional proximal electrode rings were mounted on the tubing (3 mm spacing). Electrodes were electrically separated between each other. Three cryoablations (4 minutes duration) were performed in the right atrium of a pig. Intracardiac electrograms were recorded prior to ablation at each site. Lesions were studied histologically one week after ablation.

Results. A temperature of about -85°C was achieved within the boiling chamber of the catheter. Electrograms were comparable as recorded by standard electrophysiology catheters. One week after the intervention lesions were visible macroscopically. Lesion diameter was about 4 mm. In addition, the formation of electrically non-conducting lesions could be confirmed histologically by Azan staining (**Chyba! Nenašiel sa žiaden zdroj odkazov.**)

Conclusions. It could be confirmed that thermal conductivity of a standard medical tubing can be improved by adding metallic particles. Electrodes mounted on such a tubing may allow accurate mapping of focal tachycardias due to their high spatial resolution, without limiting the size of the boiling chamber and therefore maintaining the cooling power of a cryo-tip catheter with a metallic boiling chamber.

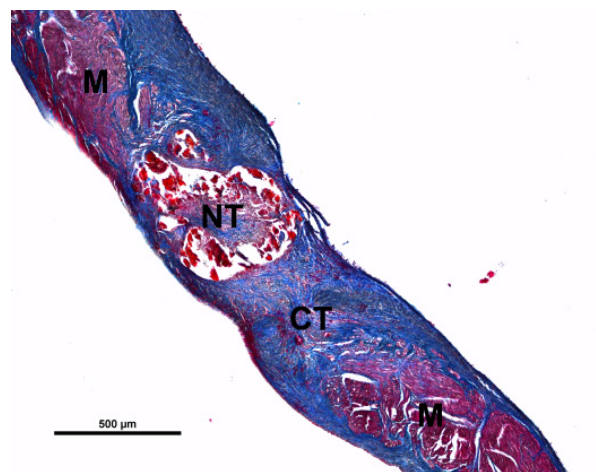


Fig. 1. The histological section (Azan staining) shows ends with intact myocardium (M, purple) and a necrotic area (NT) with remnants of tissue surrounded by connective tissue (CT, blue).

Tpeak-Tend Interval and Arteriography Variables

¹I. Mozos, ²S. Gligor

¹”Victor Babes” University of Medicine and Pharmacy, Department of Functional Sciences, Timisoara, Romania

²Vest University, Department of Physical Therapy and Special Motion, Timisoara, Romania

Email: ioanamozos@yahoo.de

Keywords: Tpeak-Tend interval; QT interval; arterial stiffness; endothelial dysfunction; arterial age

Introduction. The Tpeak-Tend interval (Tpe), an index of transmural dispersion of repolarization, predisposes, if prolonged, to life-threatening ventricular arrhythmias. Arterial stiffness and endothelial dysfunction are markers of subclinical atherosclerosis. The aim of the present study was to assess the relationship between Tpe and arterial function.

Methods and Materials. A total of 54 healthy participants, aged 33±10 years, underwent arteriography and standard 12-lead ECG. Brachial augmentation index (Aix Brach), aortic augmentation index (Aix Ao), pulse wave velocity, ejection duration, systolic blood pressure in the aorta, arterial age, diastolic reflection area, diastolic area index and Tpeak-Tend, QT interval (QT) and heart rate corrected QT interval (QTc) were assessed.

Results. Brachial augmentation index, aortic augmentation index, pulse wave velocity, ejection duration and arterial age were: -46±23%, 14±12%, 8±1.4 m/s, 294±21 ms, 41±14 years, respectively. Significant correlations and associations were found between Tpe and Aix Brach ($r=0.295$), Aix Ao ($r=0.295$), ejection duration, systolic blood pressure in the aorta (multiple $R=0.936$, $R\text{ square}=0.876$, adjusted $R=0.855$, significance $F<0.01$), pulse wave velocity (multiple $R=0.919$, $R\text{ square}=0.845$, adjusted $R=0.826$, significance $F<0.01$), diastolic reflection area, diastolic area index (multiple $R=0.937$, $R\text{ square}=0.879$, adjusted $R=0.855$, significance $F<0.01$) and arterial age (multiple $R=0.871$, $R\text{ square}=0.76$, adjusted $R=0.741$, $F<0.01$). A $Tpe>100\text{ms}$ was significantly associated with accelerated arterial aging ($p<0.01$) and impaired coronary perfusion ($p=0.031$) (multiple $R=0.867$, $R\text{ square}=0.751$, adjusted $R=0.723$, $F<0.01$). Accelerated arterial aging was also significantly associated with increased Tpe/QT and Tpe/QTc .

Conclusions. A prolonged Tpe is associated with endothelial dysfunction, arterial stiffness, impaired coronary perfusion and accelerated arterial aging. Ventricular arrhythmia risk is related to subclinical atherosclerosis, impaired coronary perfusion and accelerated arterial aging.

Decartographic and Echocardiographic Correlations in Patients with Pulmonary Arterial Hypertension

**T. Sakhnova, E. Blinova, M. Saidova, A. Loskutova, O. Arkhipova, E. Yurasova,
T. Martynyuk, I. Chazova**

Cardiology Research Complex, Moscow, Russia,
Email: tamara-sahnova@mail.ru

Keywords: pulmonary arterial hypertension; right ventricular overload; repolarization; echocardiography.

Introduction. In patients with pulmonary arterial hypertension (PAH) ventricular gradient and decartographic parameters of “recovery acceleration” were shown to be helpful for the detection of right ventricular overload and for the assessment of its severity; ventricular gradient was shown to predict mortality. The aim of the work was to study the interrelations of “recovery acceleration” and echocardiographic parameters in patients with PAH.

Methods and Materials. We examined 30 PAH patients (87% females; age (mean±SE) 38.0±2.0 years). Systolic pulmonary artery pressure (SPAP), right ventricular (RV) dimensions and function were assessed using comprehensive echocardiographic examination, including Tissue Doppler Imaging. We studied magnitude G and spatial components G_x, G_y, G_z of the “recovery acceleration” vector calculated using the derived orthogonal-lead ECG.

Results. All patients had severe PAH (SPAP>50 mm Hg, mean SPAP 98.6±4.8 mm Hg). Correlation coefficients of decartographic and echocardiographic parameters are presented in the table. Echocardiographic parameters include: RV anterior wall thickness (AWT); anterior-posterior (APD) and middle (MD) RV dimensions; parameters of RV systolic function: tricuspid annular plane systolic excursion (TAPSE), RV fractional area change (FAC), RV and interventricular septum systolic velocities (TVI-S); parameters of RV diastolic function: RV and interventricular septum diastolic velocities (TVI-E); longitudinal strain (LS). For all presented correlation coefficients p<0.05.

	SPAP	AWT	APD	MD	TAPSE	FAC	TVI-S	TVI-E	LS
G	-0.6			-0.5	0.4	0.4	0.4	-0.6	
G _x	-0.6	-0.6	-0.5	-0.6		0.6	0.4	-0.4	-0.4
G _y		-0.4	-0.5	-0.6		0.4	0.6	-0.4	-0.6

Conclusions. In patients with severe PAH decartographic parameters of “recovery acceleration” correlate with RV dimensions and parameters of RV systolic and diastolic function.

Synthesized Posterior Right Sided Chest Lead Electrocardiograms Are Useful for Detecting Right Ventricular Myocardial Infarction

S. Fukunaga, T. Kinoshita, K. Akitsu, H. Koike, A. Abe, H. Yuzawa, T. Suzuki, H. Sato, T. Fujino, K. Kobayashi, Y. Okano, T. Ikeda

Department of Cardiovascular Medicine, Toho University Faculty of Medicine,
Tokyo, Japan

Email: s-fuku@med.toho-u.ac.jp

Keywords: Synthesized 18-lead Digital ECG; Right Ventricular Myocardial infarction; Right Sided Chest Lead Electrocardiogram

Background: It has been reported that synthesized 18-lead digital electrocardiograms (ECGs) are useful in detecting area of myocardial ischemia. The ECGs are composed of the standard ECG leads (6 limb leads and 6 left chest leads, V₁ to V₆) and additionally the right chest leads (V_{3R}, V_{4R}, V_{5R}) and back leads (V₇, V₈, V₉), which are mathematically derived from the standard 12-lead ECG waveforms. In the present study, we tested whether synthesized 18-lead ECGs can precisely detect right ventricular myocardial infarctions.

Methods and Results: This study enrolled 93 consecutive patients (76 men, average 66 ± 14 years) who were diagnosed as acute posterior MI by coronary angiography in our institution. All patients sequentially underwent synthesized 18-lead digital ECG recordings (1550 Nihon Kohden, Co. Ltd., Tokyo) in the coronary care unit. Diagnosis of right ventricular MIs was done using echocardiography, Swan-Gantz catheter measurements, and so on. We evaluated ECG complexes of synthesized posterior right sided chest lead (V_{3R}, V_{4R}, V_{5R}). When the ST-segment elevation > 0.1 mV of the ECG leads was detected, it was determined as positive ST-segment elevation. We finally evaluated how many positive ST-segment elevation synthesized 18-lead digital ECGs could detect in patients with right ventricular MIs and diagnostic value is useful or not to detect right ventricular MIs. Of the 93 patients, 5 (5.4%) had right ventricular MIs. Of these 5 patients, 3 (60%) had positive ST-segment elevation in synthesized posterior right sided chest lead ECGs.

Conclusion: This study reveals that synthesized posterior right sided chest lead ECGs can highly detect right ventricular MIs. It could be a useful device without recording real posterior right sided chest lead ECG.

Relation of Sex and ECG Variables on Cardiovascular Mortality Risk in 10 Years Follow-Up

G. Muromtseva, A. Deev, S. Shalnova

¹National Research Centre for Preventive Medicine, Moscow, Russia

Email: gmuromtseva@yahoo.com

Keywords: relative mortality risk; Minnesota code; gender effect.

Introduction. Prediction of cardiovascular mortality (CVM) determined by various factors: gender, age, ECG-variables and others. The goal of this work is to evaluate the effect of the gender on CVM prognosis with ECG variables.

Methods and Materials. Follow up of randomly selected cohort from Moscow population (17821 subjects aged 25-64, mean age 47±11 years), examined in 1975-2001 years, was carried out for 21 years on average. There were 1153 cases of CVM in 10 years. We used Cox regression model to determine the relationship between 10-year CVM. A relative mortality risk (RR) was estimated using multivariate age-, sex-adjusted Cox model. ECG variables included atria fibrillation (AF), left ventricular hypertrophy (LVH), QQS codes (QQS) and ischemic codes (ISCH). Males were coded 1, females – 2.

Results. For women AF and LVH have higher impact, while QQS and ISCH have lower impact on CVM prediction as compared of men.

Variables	Minnesota code variables	$\beta \pm \text{st.error } \beta$	RR (95%CI)	p
AF	8-3	1.46±0.21	4.32 (2.88-6.48)	0.0001
LVH	3-1 or 3-3	0.63±0.11	1.89 (1.53-2.32)	0.0001
QQS	1-1-1 to 1-2-7	1.11±0.16	3.05 (2.24-4.14)	0.0001
ISCH	4-1, 4-2, 5-1, 5-2 without 3-1 or 3-3	1.46±0.13	4.32 (3.33-5.61)	0.0001
sAF	(sex-1)*AF	1.07±0.36	2.93 (1.44-5.94)	0.003
sLVH	(sex-1)*LVH	0.60±0.25	1.82 (1.11-3.00)	0.02
sQQS	(sex-1)*QQS	-0.67±0.47	0.51 (0.20-1.27)	0.15
sISCH	(sex-1)*ISCH	-0.55±0.25	0.83 (0.54-1.29)	0.03

Conclusions. The influence of the gender to predict CVM with ECG variables was as follows: QQS – women RR is 0.51 of men RR; ISCH – women RR is 0.83 of men RR; AF – women RR is 2.93 of men RR; LVH – women RR is 1.82 of men RR.

Automated ECG Delineation Using Machine Learning Algorithms

¹I. Saini, ²D. Singh, ¹A. Khosla

¹Dept. of Electronics & Communication Engineering, Dr B R Ambedkar National Institute of Technology Jalandhar, India

²Dept. of Instrumentation & Control Engineering, Dr B R Ambedkar National Institute of Technology Jalandhar, India
Email: drdilbag@gmail.com

Keywords: KNN; SVM; gradient; classifier; durations; intervals.

Introduction. The aim of automated Electrocardiogram (ECG) delineation system is the reliable detection of fundamental ECG components and from these fundamental measurements, the parameters of diagnostic significance, namely, P-duration, PR-interval, QRS-duration, QT-interval, are to be identified and extracted. In this work, two supervised machine learning algorithms, K-Nearest Neighbor (KNN) and Support Vector Machine (SVM) have been applied for accurate and efficient delineation of ECG signals.

Methods and Materials. The algorithms were evaluated on a standard database 12-lead CSE DS-3 database ($f_s = 500\text{Hz}$). The mean (m) and standard deviation (std) of P-duration, PR-interval, QRS-duration and QT-interval were calculated as the average of the errors, taken as the time difference between the algorithmic results and the referee cardiologist annotations.

Results. The mean and standard deviations of the basic intervals (P-duration, PR-interval, QRS-duration and QT-interval) obtained by KNN and SVM algorithms and three 12-lead programs used in the CSE study from the combined program median is given in Table 1. The results of the proposed algorithms are comparable with the other evaluation programs of CSE.

Table 1. Comparison of mean and standard deviation of ECG wave intervals using KNN and SVM algorithms on CSE database

Method	P-duration m±std(ms)	PR-interval m±std(ms)	QRS-duration m±std(ms)	QT-interval m±std(ms)
KNN	-2.5±9.3	5.4±9.9	-2.3±7.2	5.0±13.4
SVM	-0.1±7.9	2.3±7.1	-1.1±7.0	3.9±11.8
CSE Prog. 2 (Marquette)	-12.0±17.6	-8.7±12.1	-0.8±7.2	6.2±15.4
CSE Prog. 11 (Glasgow)	-2.4±12.6	5.1±12.5	-1.4±7.1	3.9±14.8
CSE Prog. 13 (Padova)	2.8±10.1	-2.8±8.3	1.8±7.3	-1.1±9.2

Conclusions. Both presented algorithms of delineation may be capable of enhancing specific rhythms in ECG signals, which may in turn, proves helpful in accurately detecting the P, QRS and T-wave components. Mean and standard deviation has also been calculated and compared with the results of referees and tolerance limits accepted by cardiologists for CSE.

Heart Asynchrony in Time-Frequency Interpretation Up to 1000 Hz

^{1,2}P. Jurak, ^{1,2}J Halamek, ²P. Leinveber, ²T. Reichlova, ¹F. Plesinger, ²P. Vesely,
¹V. Vondra, ¹P. Klimes, ²J. Sumbera, ²K. Zeman, ²M. Novak

¹Institute of Scientific Instruments of the ASCR, v.v.i., Brno, Czech Republic

²St. Anne's University Hospital, ICRC, Brno, Czech Republic

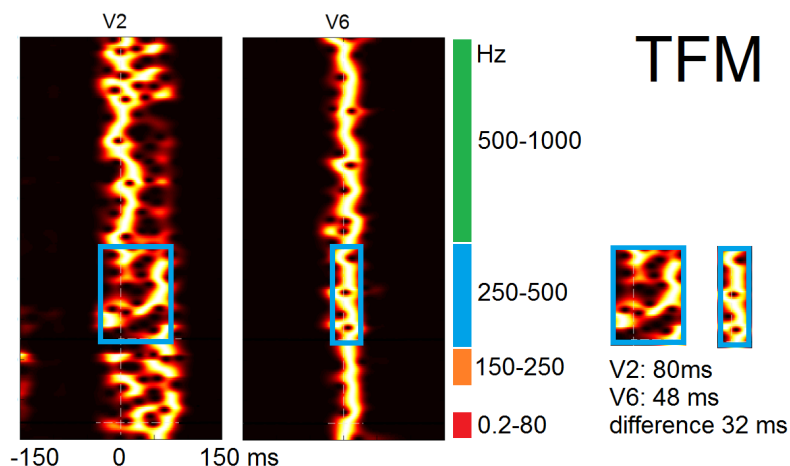
Email: jurak@isibrno.cz

Keywords: ultra-high-frequency ECG; time frequency maps; QRS complex.

Introduction. Here we present the normalised time-frequency mapping (TFM) of ultra-high-frequency components in the QRS complex from ECG. The width, intensity and latency of power are possible numerical parameters of TFM. The width and latency measured in different leads reflects the asynchrony in activation of right and left ventricle.

Methods and Materials. The 10-minute resting 12-lead ECG with a sample rate at 25 kHz and dynamic range of 24 bits was recorded. The TFM was used to determine signal oscillation power in the ultra-high-frequency range from 0.2 to 1000 Hz with the time window 150 ms before and 150 ms after the QRS complex position. The TFM matrix for each lead was obtained by averaging TFMs (artefact free) from over 500 QRS complexes. The mean width of 10% power peak in four frequency ranges 0.2-80, 150-250, 250-500 and 500-1000 Hz – (see Figure) was computed from averaged TFMs. The results from combined V1-V3 and V4-V6 leads in 10 healthy subjects and 10 heart transplant patients in the same age category were compared.

Results. The figure shows the example of TFM in single leads V2 and V6 in heart transplant subject with identification of power width in frequency band 250-500 Hz (blue colour). The difference between mean power width V1-V3 vs. V4-V6 over two groups was 23±11, 15±14, 8±7, 8±6 ms in healthy subjects and 35±30, 31±19, 24±20, 31±19 ms in heart transplant subjects for four frequency bands 0.2-80, 150-250, 250-500* and 500-1000** Hz, * p<0.05, ** p<0.005.



Conclusions. The TFM interpretation of ultra-high-frequency oscillations up to 1000 Hz provides additional information about the electrical asynchrony of right and left ventricle. The ability to distinguish between groups of healthy and transplanted hearts increases with frequencies over 250 Hz. Weak ultra-high frequency oscillations provide new spatiotemporal representation of heart contractile cell depolarization activation.

QRS Power in Frequency Ranges up to 1000 Hz

¹P. Leinveber, ^{1,2}P. Jurak, ^{1,2}J Halamek, ¹T. Reichlova, ²F. Plesinger, ¹P. Vesely,
^{1,2}V. Vondra, ^{1,2}P. Klimes, ¹J. Sumbera, ¹K. Zeman, ¹M. Novak

¹St. Anne's University Hospital, ICRC, Brno, Czech Republic

²Institute of Scientific Instruments of the ASCR, v.v.i., Brno, Czech Republic

Email: pavel.leinveber@fnusa.cz

Keywords: ultra-high-frequency ECG; QRS power; QRS complex.

Introduction. Valid information in ECG signal is situated also above known frequency 250 Hz. The power of QRS complexes in various frequency ranges can provide valuable information in diagnostics of cardiac diseases using the ultra-high-frequency ECG.

Methods and Materials. The 12-lead ECG (sampling rate 25 kHz, resolution 24 bits) in supine resting position was acquired in 11 healthy and 17 ischemic heart disease (IHD) subjects with similar age and normal QRS width. The power envelopes over all ECG leads were calculated from 500 averaged QRS complexes in 5 frequency ranges – 0,2-1000, 80-150, 150-250, 250-500, 500-1000 Hz. The QRS power and peak power were determined from the power envelopes and compared between two groups in different frequency ranges. The power ratio of each band to basic band (0,2-1000 Hz) was also assessed in both groups and statistically compared.

Results. No significant differences in QRS power were found through all frequency ranges. The peak power was significantly lower in IHD group on frequency range 500-1000 Hz ($p < 0,05$). When comparing power ratio against basic frequency range (0,2-1000 Hz), the QRS power was significantly lower in IHD group in 80-150 Hz ($p < 0,05$) and 500-1000 Hz ($p < 0,01$), and the peak power was significantly lower in IHD group in 500-1000 Hz ($p < 0,005$).

Conclusions. The power in frequencies over 500 Hz decreases more in IHD then healthy subjects against their basic frequency range. The power of QRS components up to 1000 Hz provides clear information which can be used for better and possibly early diagnostics of heart diseases such as IHD. This method could help distinguish between healthy and diseased heart.

Detection of Time Intervals in Biomedical Signals Using Template Matched Filter

¹A. Sarwan Kumar, ²B. Sneha Anand, ²C. Amit Sengupta

¹National Institute of Technology, Jalandhar, India,

²Indian Institute of Technology, Delhi, India

Email: pahujas@nitj.ac.in

Keywords: FHRV; FECG; uterine contractions; fetal movements; R-R interval.

Introduction. Fetal Heart Rate Variability (FHRV) is a reliable quantitative marker of autonomic nervous system (ANS) activity of the fetus and its analysis has gained importance in medical research and clinical applications. Fetal Electrocardiograph (FECG) is clinically used to help doctors diagnose various diseases. Worldwide, the standard method of monitoring the fetus during labor is the display of continuous fetal heart rate (FHR) and the uterine activity with the help of cardiotocogram (CTG). By analysis and appropriate interpretation of changes in the CTG obstetricians hope to prevent the delivery of dead or impound babies who had suffered as a result of a lack of oxygen during labor and delivery. These signals are analyzed using an automatic PC-based virtual instrument in LabVIEW. A template matching technique works well in the calculation of R-R interval of the ECG/FECG data and peaks of the biomedical signals.

Methods and Materials. Various techniques are used to detect QRS complex like linear digital filters, nonlinear transformations, decision processes, and template matching. Typically, two or more of these techniques are combined together in a detector algorithm. The most common approach for QRS detection is based on template matching. A model of the normal QRS complex, called a template, is extracted from the filtered ECG. This template is compared with the subsequent incoming real-time ECG to look for a possible match, using a mathematical criterion. A close enough match to the template represents a detected QRS complex. If a waveform comes along that does not match but is a suspected abnormal QRS complex, it is treated as a separate template, and future suspected QRS complexes are compared with it. From the QRS detector, the RR intervals and heart rate are determined. The same way the peaks are identified from the fetal movements and uterine contractions for finding their intervals. Signals were recorded non-invasively using BIOPAC, sampling frequency was 1000 samples per seconds while the ECG and FECG were recorded by Ag-Ag/Cl electrodes on the thoracic region and abdomen region. Uterine and fetus movements were recorded non-invasively by pressure sensors placed in various positions on the abdomen of the subjects while some phantom data was also recorded to depict fetal movements with the help of an IPG instrument.

Results. The algorithm discussed here is designed in LabVIEW. The unfiltered ECG and pulse signals are passed through the band pass or notch filter. The reference signal is compared with the subsequent incoming ECG samples for a possible match, using a mathematical criterion. A close match to the template represents an impulse of unity gain.

Conclusions. In this paper we have tested a template matching algorithm for QRS complex detection on the different signals, i.e. ECG, FECG, and Fetal Movements. Future research will concentrate on the diagnosis of disease using the system designed and in various fetomaternal well being studies.

Electrocardiographic Diagnosis of Emergency Conditions in Rural Areas by the System of Remote ECG Transmission and Analysis

¹N.A. Vishnyakova, ²G.V. Ryabykina, ²V.E. Volkov, ²E.N. Dyuzheva,
²E.V. Blinova

¹Uryupinsk central district hospital, Uryupinsk, Russia,

²Russian Cardiology Research and Production Complex, Moscow, Russia

Email: Ecg.newtekh@gmail.com

Keywords: telecardiology; system of ECG transmission; rural area.

Introduction. System for remote ECG transmission (RET) and analysis allows to explore population of rural areas (RA) and to receive ECG interpretation by qualified experts at the distance. The RET is particularly important for the diagnosis of emergency conditions (EC) in difficult to access for qualified medical examination RA. The aim of this study was diagnosis of EC in patients of RA by the system RET and analysis (Easy ECG) .

Methods and Materials. Easy ECG used in the Uryupinsk district RA. This system linked through the Internet 4 rural ambulances and Uryupinsk hospital with Institute of Clinical Cardiology RCRPC in Moscow. 56,991 people live in Uryupinsk district. ECG analysis was performed automatically and than specialists in Uryupinsk with the help of experts in Moscow clarified the diagnosis. If necessary, experts performed analysis of vectorcardiogram derived from 12-lead and DECARTO.

Results. 3728 ECG have been registered and transferred to the Advisory Center. 39 EC was first identified on the basis of ECG analysis from 25.03.13. till 11.11.13. Previous ECGs in these cases were not registered or they showed no changes. The most significant ECG findings were 2 acute myocardial infarctions from 7 cases of chest pain. 11 ECG had signs of old myocardial infarctions (28,2%), including 2 - in the presence of left bundle branch block (LBBB) and 1- ischemic cardiomyopathy. Frequent findings were intraventricular blocks (46,1%): including 4- LBBB, 1-RBBB (12,8%), 12 cases of an isolated left ventricular hypertrophy(LVH) and 2 cases LVH in the presence of LBBB(35.8%). Only 1 ECG was normal.

Conclusions. Study shows the importance of ECG registration at the bedside with remote transmission and expert analysis regardless of availability local qualified medical diagnostic services.

Design of Very Precise and Miniature Low Power ECG Holter

¹E. Vavrinsky, ^{1,2}M. Daricek, ^{1,2}M. Donoval, ^{1,2}F. Horinek, ³D. Moskalova

¹Institute of Electronics and Photonics, Slovak University of Technology,
Bratislava, Slovakia,

²NanoDesign ltd., Bratislava, Slovakia,

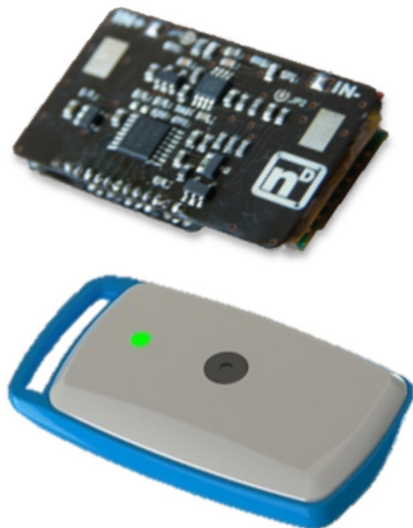
³Department of Psychology, Comenius University, Bratislava, Slovakia
Email: erik.vavrinsky@stuba.sk

Keywords: ECG Holter; miniature; low power; low noise, 24-bit.

Introduction. The most effective healthcare is based on precise prevention and diagnostics. R&D in this field finally provides new methods and systems with potential of broad use in practice. This paper introduced design of ECG monitoring system which uses latest advances in high-tech electronics.

Methods and Materials. The system is designed for 24- hour daily monitoring of health in rehabilitation centres as well as for remote healthcare at home. Except for very precise measurement features, which characterize this device (high gain, low noise, multi-probe measuring), some special features as low voltage and ultra-low power consumption were reached. The system is based on 24-bit analog front-end ADS1292R and 32-bit, 16 MHz Jennic processor. In this system data are stored on built-in micro SD card, but wireless data transmission to PC is also offered. The data are saved in EDF+ format. System allows also simultaneousness measurement of acceleration and respiration.

ECG HOLTER DESIGN



TECHNICAL PARAMETERS OF SENSOR SYSTEM

Number of Channels	2
Programmable Gain	1, 2, 3, 4, 6, 8 or 12, Low-noise
ADC resolution	2x 24-bit, no data missing
Sample rate	125 SPS - 8 kSPS
MCU	32 bit, 16 MHz
Built-In	- Right Leg Drive Amplifier - Lead-Off Detection - Oscillator and Reference
Integrated	Respiration Impedance Measurement
Acceleration sensor	3D, 10/12/14 bit, 100 SPS
Supply voltage	1x Li-Pol 120 mAh, over 24h stamina charging time: 20min
Temperature range	0 – 70 °C
Electrodes	10 x 20 mm, Gold plated on copper or 10 x 1 mm, Silver wire or Disposable Silver-Silver Chloride
Connector	Micro USB
Data storage	Integrated 2 GB microSD card
Output data format	EDF+
Weight	20 g
Dimensions	37 x 25x 15 mm

Next features: RGB LED signalization, magnetometer, trigger button, automatic switch on/off

Results. Designed sensor system was tested on a wide range of experiments, where ECG parameters like: P, Q, R, S, T amplitudes, RR, PR, JT, QT, QTc time intervals, T wave symmetry, HRV spectrum and EDR algorithm were in detail analysed.

Conclusions. High quality and scientific potential of designed smart system was experimentally proven. Obtained results clearly proved high stability and well noise cancellation of dedicated sensing system with better measurement results in comparison to other conventionally used devices.

Mechanical Chest Compressions and Quality of CPR in Out-of-Hospital Cardiac Arrest Evaluated by Trans-Thoracic Impedance Measurements

¹T. Tranberg, ²C.J. Terkelsen

Department of Cardiology, Aarhus University Hospital, Denmark^{1,2}

Email: tinne_tranberg@hotmail.com

Keywords: LUCAS chest compression system; high-quality CPR; out-of-hospital cardiac arrest; trans-thoracic impedance measurements.

Introduction. Mechanical chest compression devices have been proposed to provide high-quality CPR; however, research in the prehospital setting is limited.

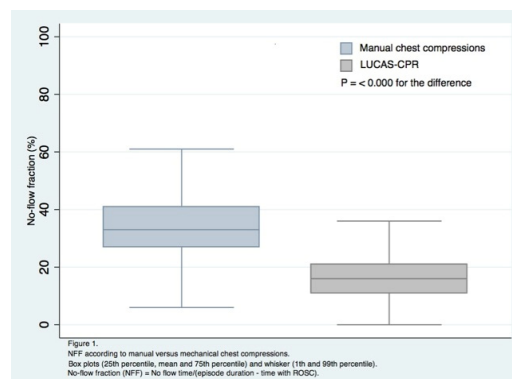
This study aims to evaluate mechanical chest compressions provided by the LUCAS (Lund University Cardiac Arrest System) device compared to manual chest compression in a cohort of out-of-hospital cardiac arrest (OHCA) cases.

Methods and Materials. In a prospective study conducted in the Central Denmark Region, the Emergency Medical Service and the physician-manned ambulances treated 196 non-traumatic OHCA cases occurring from April 1st 2011 to February 1st 2013. The 196 OHCA cases were treated with LUCAS-CPR after an episode with manual chest compressions. 41 OHCA cases were excluded due to missing trans-thoracic impedance measurements and the remaining 155 OHCA cases comprised the study population. The CPR quality was evaluated using trans-thoracic impedance measurements collected from the Life-pack 12 connected to the OHCA patient, and the effect was assessed in terms of no-flow fraction.

Results. The median total episode duration was 21 minutes (interquartile range 13 to 34 minutes). The episode with LUCAS-CPR was significantly longer compared to the duration of the episode with manual chest compressions (12 minutes vs. 5 minutes, $P < 0.001$).

The no-flow fraction was significantly lower during LUCAS-CPR (16%) compared to manual compressions (35%) with a difference of 19% (95% CI: 16% to 21%; $P < 0.001$).

Compared to manual chest compressions the average compression rate during LUCAS-CPR was performed according to the recommendation from Guidelines for Resuscitation (102/minute vs. 124/minute, $P < 0.001$). The average number of chest compressions delivered pr. minute were significantly higher during LUCAS-CPR compared to manual compressions (94/minute vs. 74/minute, $P = 0.012$).



Conclusion. LUCAS-CPR is associated with a significant reduction in no-flow fraction compared to manual chest compressions during OHCA resuscitation.

AUTHORS INDEX

A		Cotet I.	24, 53	Gottshalk B.	60
Abdollah H.	51	Couderc J.P.	36	Green C.	19
Abe A.	120	Čarnická S.	63, 91	Grill V.	99
Adameová A.	63				
Aidu E.	93, 108	D		H	
Akitsu K.	120	Danilov N.	93	Haláček J.	23, 48, 123, 124
Alkmim M.B.M.	18, 100	Daricek M.	127	Hashimoto K.	74
Anand S.B.	125	De Ambroggi. L.	14	Hatala R.	31, 59
Anselm D.D.	60	Deev A.	121	Hegland D.	19
Arkhipova O.	93, 119	Donoval M.	127	Hintringer F.	117
Assis T.G.P.	100	Dorostkar P.	30, 57	Hirayama A.	74
Atwater B.	19	Dossel O.	42	Hlivák P.	59
Avram R.	24, 53	Dovinová I.	88	Hopman W.	51, 52
Azarov J.E	39	Drkošová A.	111	Horinek F.	127
		Dubé B.	75		
B		Dukát A.	103	CH	
Bacová B.	61, 65, 89, 90	Dyuzheva E.N.	96, 97	Chapiński M.	95
Bachárová L.	10, 94, 101, 102			Chazova I.	93, 119
Balážová E.	59	E			
Barancik M.	88	Engels E.B.	32	I	
Baranchuk A.	51, 52, 60	Enger S.	83	Ikeda T.	120
Barlaka E.	63	Enriquez A.	51, 52	Illíková V.	59
Baturova M.A.	85	Erem B.	22, 70		
Bayés de Luna A.	51, 52	Erts R.	86	J	
Becker G.	75			Jacquemet V.	75
Beňová T.	64, 65, 88, 89, 90	F		Janicki J.S.	95
Bernikova O.G.	39, 62	Fedorova V.	108	Janoušek O.	25, 48, 92
Blinova E.V.	93, 108, 119, 126	Femenia F.	52	Jansová H.	33
Boháčeková M.	94, 102	Filipowski H.	113	Jaruševičius G.	46
Botker H.E.	17	Fischer G.	117	Jurák P.	23, 123, 124
Brady P.A.	85	Franco B.G.	35		
Brooks D.H.	22, 70	Fré da Costa C.	110	K	
		Friedman P.A.	85	Kaiser E.	56
C		Fujino T.	120	Kaldararova M.	94, 102
Caldwell J.	51	Fukuda K.	98	Kalejs O.	86
Cankar K.	99	Fukunaga S.	120	Kania M.	82, 109
Carlson J.	85			Karma A.	22
Cerny M.	45	G		Kasamaki Y.	74
Clark E.	35	Gablovský I.	63	Kautzner J.	33
Coll-Font J.	22, 70	Galizio N.	52	Kay J.	50
Collins K.	50	Gašpar L.	103	Kellerová E.	77, 115
Conde D.	51, 52	Gašparová I.	103	Kharin S.	62, 104
Corino V.D.A.	83	Gavorník P.	103	Khosla A.	122
Cortez D.	50	Gligor S.	118	Kinoshita T.	120
		Gogolinskaité D.	46	Klimeš P.	123, 124
		Gorenek. B	29	Kneppo P.	72

Knezl V.	64, 65, 88	Moga M.	24, 54	R	
Kobayashi K.	120	Moga V.D.	24, 54	Rabinstein A.A.	85
Kobylecka M.	109	Moskalova D.	127	Radošinská J.	64, 65, 88, 89, 90
Kochilas L.	30	Mozos I.	38, 118	Rajtík T.	63
Koike H.	120	Muratore C.	52	Rasmussen A.M.B.	40
Kolářová J.	25, 48, 92	Muromtseva G.	121	Rasputina A.	47
Konrade I.	86			Ravingerová T.	63, 91
Kozlíková K.	80, 114	N		Redfearn D.P.	51
Kozmann G.	68, 77	Nadeau R.	75	Rees C.	22
Kozumplík J.	111	Nagibin V.	88	Regecová V.	115
Krandycheva V.	104	Nakai T.	74	Reichlová T.	123, 124
Krucoff M.	19	Nemčeková M.	63, 91	Retyk E.	52
Kuijt W.	19	Nguyen D.	50	Rezus C.	24, 54
Kukreja R.	90	Novák M.	123, 124	Ribeiro A.L.	18, 52, 100
Kumar S.A.	125	Nováková M.	25, 48, 92	Ribeiro A.M.	100
Kunimoto S.	74	Nowak C.N.	117	Rodriguez J.F.	55
Kurcalte I.	24, 53, 86			Ronzhina M.	25, 48, 92
Kus T.	75	O		Roshchevskaya I.	47, 79, 116
L		Obšitník B.	65	Roshchevsky M.	116
Laszki-Szczachor K.	113	Oesterlein T.G.	42	Roukoz H.	57
Lazou A.	63	Okano Y.	120	Ruckdeschel E.	50
Ledvényiová V.	63, 91	Okumura Y.	74	Ryabykina G.V.	96, 97, 126
Leinveber P.	23, 123, 124	Olejníčková V.	25, 92		
Lejniaks A.	86	Ovechkin A.O.	39	S	
Lenis G.	42	Ozawa Y.	74	Sadig Ali F.	51
Leoński W.	95			Saidova M.	119
Lin G.	85	P		Saini I.	122
Lloyd S.	35	Pancza D.	91	Sakhnova T.	93, 108, 119
Loskutova A.	119	Paranicova I.	101	Samesima N.	56, 110
Luca A.	107	Pastore C.A.	56, 110	Sato H.	120
Luik A.	42	Pavelka S.	89	Sauer W.	50
M		Pereira Filho H.G.	56	Sedláček K.	33
Macfarlane P.W.	35	Peterek T.	45	Sedova K.A.	39, 62
MacLeod R.S.	22	Petrenas A.	46	Sengupta A.C.	125
Makovník M.	103	Piotrowicz K.	36	Shalnova S.	121
Maksymenko V.	72	Piotrowicz R.	95	Sheldon S.H.	85
Maniewski R.	82, 109	Platonov P.G.	83, 85	Shepard Ch.W.	57
Marcolino M.S.	18, 100	Plešinger F.	123, 124	Shimokawa H.	98
Marino B.C.A.	18, 100	Polak-Jonkisz D.	113	Shmakov D.	62, 104
Martynyuk T.	93, 119	Potočňák T.	92	Shumikhin K.	104
Mazoras V.	46	Potse M.	12, 67, 106	Schmitt C.	42
McCanta A.C.	50	Princi T.	99	Simpson Ch.	51
Michael K.	51	Printzen F.W.	32	Singh D.	122
Mirmohamadsadeghi L.	44	Provazník I.	25, 92	Singh J.P.	32
		Punshchikova O.	72		

Sivanandam S.	30	Thuesen L.	17		89, 90
Slezák J.	64, 90	Thygesen K.	17	Vidu F.	24, 53
Smirnova S.	116	Tisko R.	101	Vinet A.	75
Sobieszczańska M.	95, 113	Tkáčová R.	101	Vishnyakova N.A.	126
Sobolev A.V.	97	Tranberg T.	128	Vlad A.	107
Soma M.	74	Triantafyllou E.	101	Vlasova A.E.	97
Sorensen Ch.A.	17	Tribulová N.	64, 65, 88, 89, 90	Volkov V.E.	126
Sorensen J.T.	17	Trnka M.	80, 114	Vondra V.	123, 124
Sornmo L.	46	Trunov V.	93, 108	Vozda M.	45
Soukup T.	89	Tsvetkova A.	104		
Sozykin A.V.	96	Tuboly G.	68	W	
Stanczyk A.	76	Tveit A.	83	Watanabe I.	74
Starc V.	99	Tyšler M.	68, 72, 82, 112	Wei D.	98
Stengaard C.	16			Wichterle D.	33
Stoger M.	117				
Stračina T.	25, 92	U		X	
Strelkova M.	104	Ulimoen S.R.	83	Xio J.	36
Sturmer M.	75				
Suslonova O.	79	V		Y	
Suzuki T.	120	Vaglio M.	36	Yin C.	90
Szathmáry V.	68, 77	Valentino M.	52	Yoshida Y.	98
Szekely A.	53	Valkovičová T.	94, 102	Yurasova E.	119
Šimková I.	94, 102	van Deursen C.J.M.	32	Yuzawa H.	120
Šťovíček P.	70	van Oosterom A.	69		
Šumbera J.	123, 124	Vančura V.	33	Z	
Švehlíková J.	68, 72, 82,112	Vavrinský E.	127	Zaczek R.	109
		Vaykshnorayte M.A.	39	Zareba W.	11, 27, 36
		Vazaios Ch.	101	Zeman K.	123, 124
T		Vegh E.M.	32	Zeman M.	65
Tabin M.	113	Verma B.	42	Zemzemi N.	43
Teplan M.	112	Veselý P.	23, 48, 92, 123, 124	Zhu X.	98
Teresińska A.	95	Vesin J.M.	44, 107	Zurmanová J.	65, 89
Terkelsen Ch.J.	16, 40, 128	Viczenczová C.	64, 65, 88,	Zwolińska D.	113

ISBN 978-80-969672-6-1



9 788096 967261 >